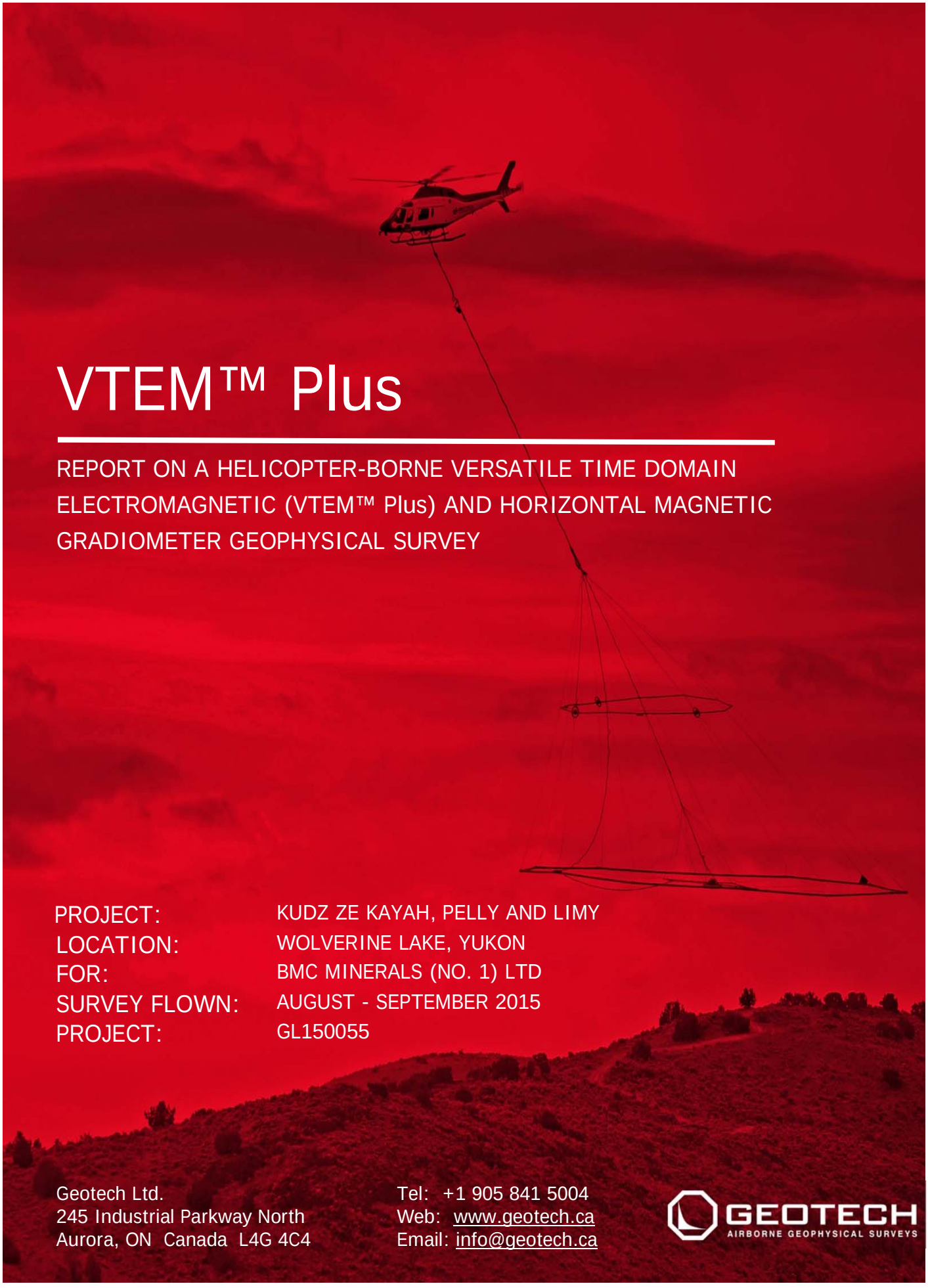

VTEM™ Plus

REPORT ON A HELICOPTER-BORNE VERSATILE TIME DOMAIN ELECTROMAGNETIC (VTEM™ Plus) AND HORIZONTAL MAGNETIC GRADIOMETER GEOPHYSICAL SURVEY

PROJECT:	KUDZ ZE KAYAH, PELLY AND LIMY
LOCATION:	WOLVERINE LAKE, YUKON
FOR:	BMC MINERALS (NO. 1) LTD
SURVEY FLOWN:	AUGUST - SEPTEMBER 2015
PROJECT:	GL150055

Geotech Ltd.
245 Industrial Parkway North
Aurora, ON Canada L4G 4C4

Tel: +1 905 841 5004
Web: www.geotech.ca
Email: info@geotech.ca

GEOTECH
AIRBORNE GEOPHYSICAL SURVEYS

TABLE OF CONTENTS

LIST OF FIGURES

LIST OF TABLES

APPENDICES

EXECUTIVE SUMMARY

KUDZ ZE KAYAH, PELLY AND LIMY - WOLVERINE LAKE, YUKON

During August 28th to September 7th 2015 Geotech Ltd. carried out a helicopter-borne geophysical survey over Kudz Ze Kayah, Pelly and Limy situated near Wolverine Lake, Yukon.

Principal geophysical sensors included a versatile time domain electromagnetic (VTEMplus) system and horizontal magnetic gradiometer with two caesium sensors. Ancillary equipment included a GPS navigation system and a radar altimeter. A total of 557 line-kilometres of geophysical data were acquired during the survey.

In-field data quality assurance and preliminary processing were carried out on a daily basis during the acquisition phase. Preliminary and final data processing, including generation of final digital data and map products were undertaken from the office of Geotech Ltd. in Aurora, Ontario.

The processed survey results are presented as the following maps:

- Electromagnetic stacked profiles of the B-field Z Component,
- Electromagnetic stacked profiles of dB/dt Z Component,
- B-Field Z Component Channel grids,
- dB/dt X Component Fraser Filtered Channel grid,
- Total Magnetic Intensity (TMI),
- Magnetic Total Horizontal Gradient,
- Magnetic Tilt-Angle Derivative of TMI,
- Calculated Time Constant (Tau) with Calculated Vertical Derivative contours and
- Resistivity Depth Images (RDI) sections are presented.

Digital data includes all electromagnetic and magnetic products, plus ancillary data including the waveform.

The survey report describes the procedures for data acquisition, processing, final image presentation and the specifications for the digital data set.

1. INTRODUCTION

1.1 GENERAL CONSIDERATIONS

Geotech Ltd. performed a helicopter-borne geophysical survey over Kudz Ze Kayah, Pelly and Limy situated near Wolverine Lake, Yukon (Figure 1 & Figure 2).

Robin Black represented BMC Minerals (No. 1) Ltd during the data acquisition and data processing phases of this project.

The geophysical surveys consisted of helicopter borne EM using the versatile time-domain electromagnetic (VTEMplus) system with Full-Waveform processing. Measurements consisted of Vertical (Z) and In-line Horizontal (X) components of the EM fields using induction coils and the aeromagnetic total field using a magnetic gradiometer. A total of 557 line-km of geophysical data were acquired during the survey.

The crew was based out of Inconnu Lodge (Figure 2) in Yukon for the acquisition phase of the survey. Survey flying started on August 28th and was completed on September 7th, 2015.

Data quality control and quality assurance, and preliminary data processing were carried out on a daily basis during the acquisition phase of the project. Final data processing followed immediately after the end of the survey. Final reporting, data presentation and archiving were completed from the Aurora office of Geotech Ltd. in November, 2015.

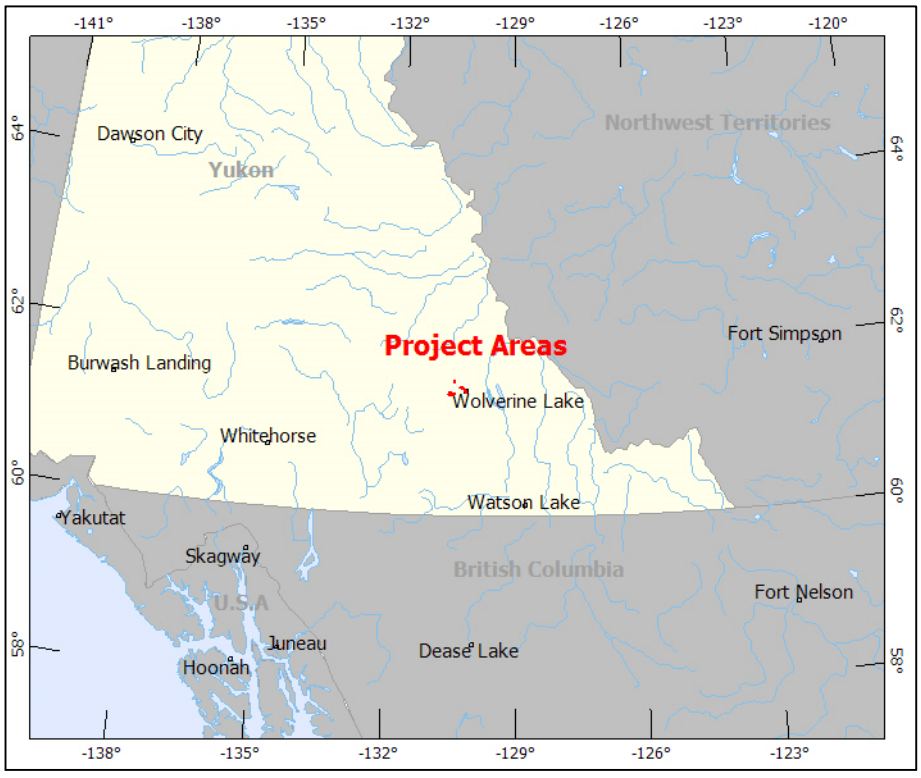

Figure 1: Survey location

1.2 SURVEY AND SYSTEM SPECIFICATIONS

The survey areas, Kudz Ze Kayah, Pelly and Limy are located approximately 13 kilometres west, 1.5 kilometres north and 19 kilometres northwest of Wolverine Lake, Yukon respectively (Figure 2).

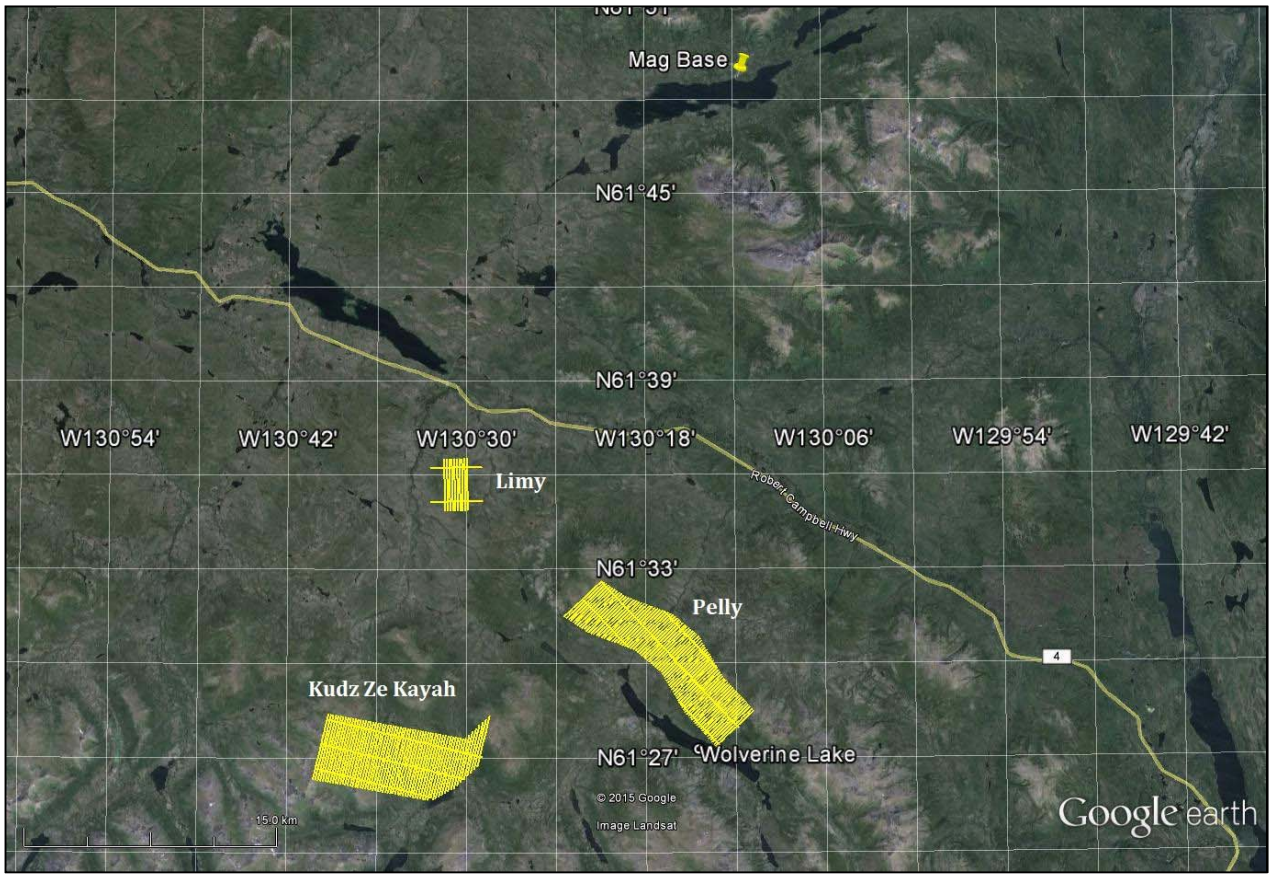

Figure 2: Survey area location on Google Earth.

The block, Kudz Ze Kayah was flown in a northeast to southwest (N 15° E azimuth) direction, Pelly was flown in a southwest to northeast (N48° E azimuth) direction, and Limy were flown in a north to south (N 0° E azimuth) with traverse line spacing of 150 metres as depicted in Figure 3 to 5. Tie lines were flown perpendicular to the traverse lines at a spacing of 1500 and 2000 metres respectively. For more detailed information on the flight spacing and direction see Table 1.

1.3 TOPOGRAPHIC RELIEF AND CULTURAL FEATURES

Topographically, the survey areas exhibits a highly rugged relief with an elevation ranging from 1091 to 2038 metres above mean sea level over an area of 73 square kilometres (Figure 3 to 5).

There are various rivers and streams running through the survey areas which connect various lakes. There are no visible signs of culture such as roads, transmission lines, mining areas and settlements located in the survey areas (Figure 3 to 5).

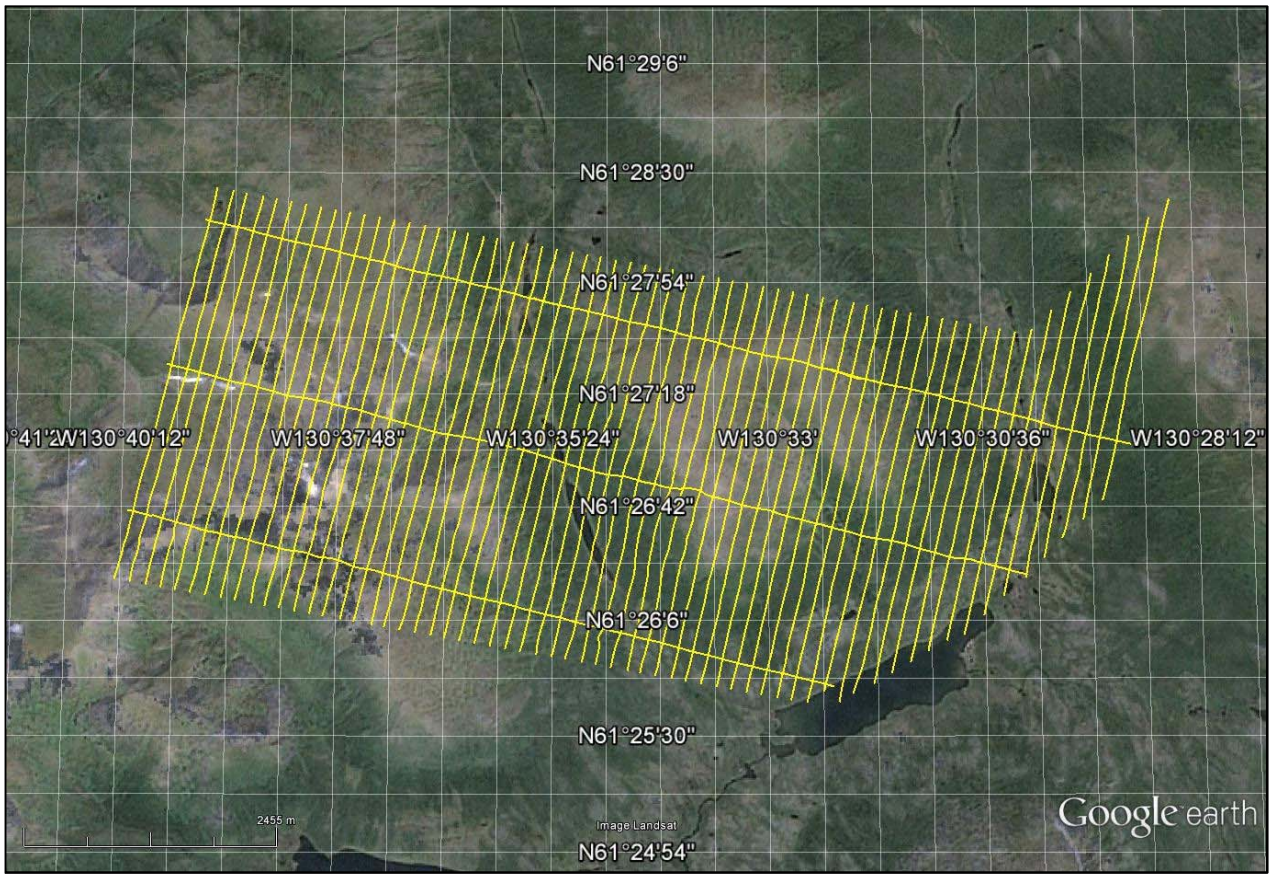

Figure 3: Flight path of Kudz Ze Kayah over a Google Earth Image.

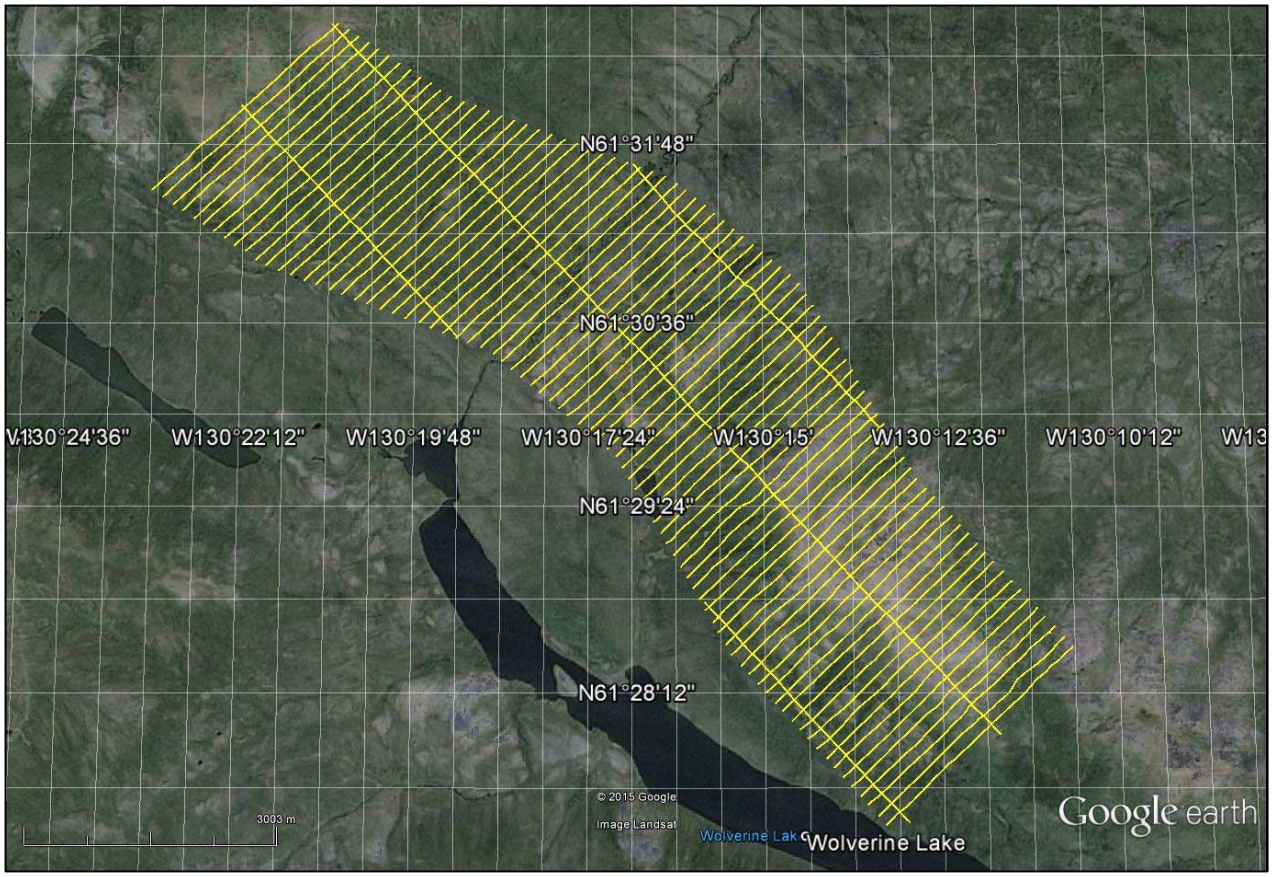

Figure 4: Flight path of Pelly over a Google Earth Image.

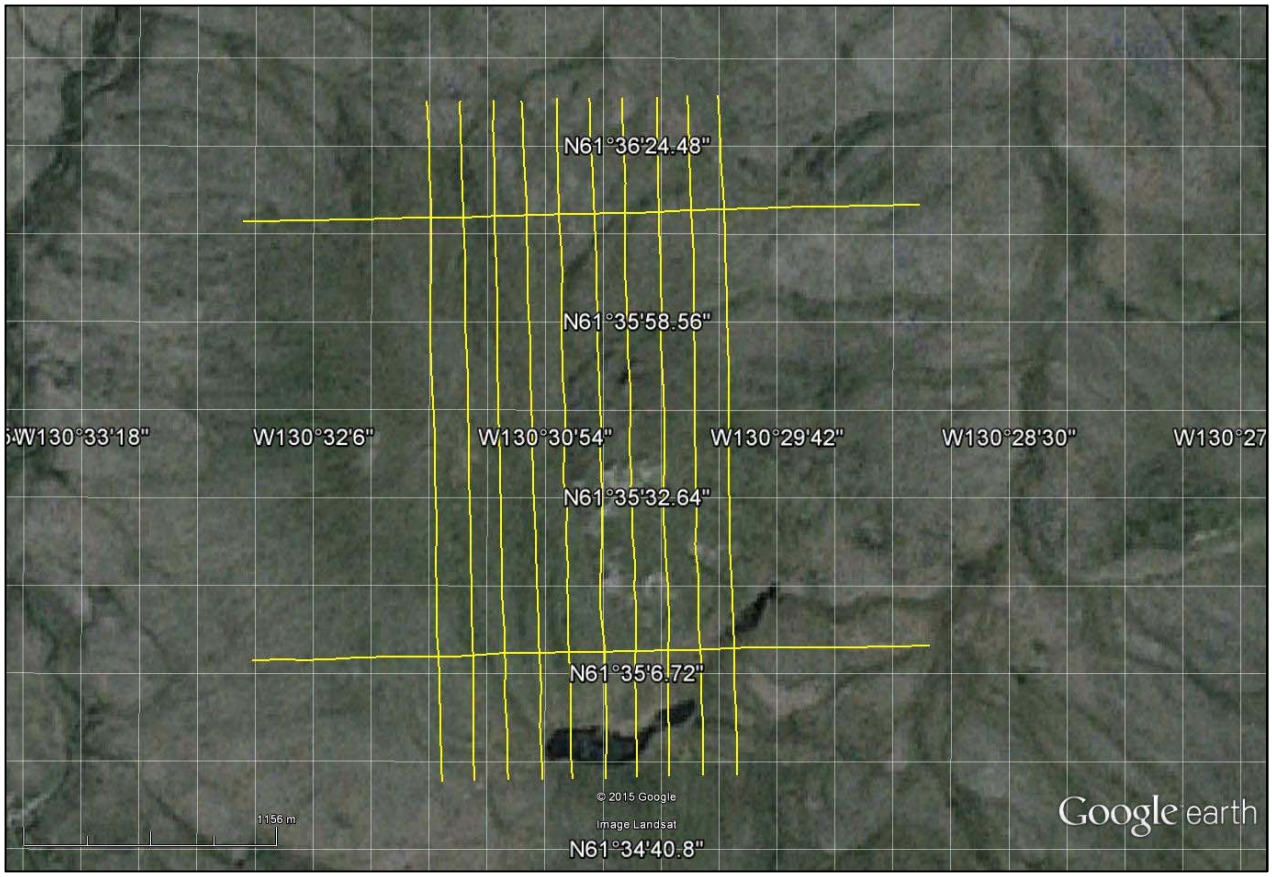

Figure 5: Flight path of Limy over a Google Earth Image.

2. DATA ACQUISITION

2.1 SURVEY AREA

The survey areas (see Figure 3, Figure 4, Figure 5, and Appendix A) and general flight specifications are as follows:

Table 1: Survey Specifications

Survey block	Line spacing (m)	Area (Km^2)	Planned[1] Line-km	Actual Line-km	Flight direction	Line numbers
Kudz Ze Kayah	Traverse: 150	35	260	241.1	N 15° E / N 195° E	L1000 - L1620
	Tie: 1500			26.3	N 105° E / N 285° E	T2001 - T2020
Pelly	Traverse: 150	36	261	245.3	N 48° E / N 228° E	L3000 - L3780
	Tie: 1500			24.1	N 138° E / N 318° E	T4000 - T4021
Limy	Traverse: 150	2	36	31.0	N 0° E / N 180° E	L5000 - L5090
	Tie: 2000			6.2	N 90° E / N 270° E	T6000 - T6010
TOTAL		73	557	574		

Survey area boundaries co-ordinates are provided in Appendix B.

2.2 SURVEY OPERATIONS

Survey operations were based out of Inconnu Lodge in Yukon from August 22nd until September 7th 2015. The following table shows the timing of the flying.

Table 2: Survey schedule

Date	Flight #	Flown km	Block	Crew location	Comments
22-Aug-2015				Watson Lake, Yukon	Crew arrived
23-Aug-2015				Watson Lake, Yukon	System Assembly
24-Aug-2015				Watson Lake, Yukon	System Assembly
25-Aug-2015				Watson Lake, Yukon	System testing
26-Aug-2015				Watson Lake, Yukon	Test completed
27-Aug-2015				Inconnu Lodge, Yukon	System ferry - no production due to weather
28-Aug-2015	1,2,3	103	Kudz Ze Kayah	Inconnu Lodge, Yukon	103km flown
29-Aug-2015	4	9	Pelly	Inconnu Lodge, Yukon	9km flown - limited due to weather
30-Aug-2015	5,6	144	Kudz Ze Kayah, Pelly	Inconnu Lodge, Yukon	144km flown
31-Aug-2015				Inconnu Lodge, Yukon	No production due to weather
1-Sep-2015				Inconnu Lodge, Yukon	No production due to weather
2-Sep-2015	7	69	Limy, Pelly	Inconnu Lodge, Yukon	69km flown limited due to weather
3-Sep-2015	8,9,10	139	Pelly	Inconnu Lodge, Yukon	139km flown
4-Sep-2015	11,12	84	Kudz Ze Kayah, Pelly	Inconnu Lodge, Yukon	84km flown
5-Sep-2015	13	16	Kudz Ze	Inconnu Lodge, Yukon	reflights

[1] Note: Actual Line kilometres represent the total line kilometres in the final database. These line-km normally exceed the Planned Line-km, as indicated in the survey NAV files.

Date	Flight #	Flown km	Block	Crew location	Comments
			Kayah		
6-Sep-2015				Inconnu Lodge, Yukon	Reflights not done due to weather
7-Sep-2015	14	15	Kudz Ze Kayah, Pelly	Inconnu Lodge, Yukon	Remaining kms were flown – flying complete

2.3 FLIGHT SPECIFICATIONS

During the survey the helicopter was maintained at a mean altitude of 77 metres above the ground with an average survey speed of 80 km/hour. This allowed for an actual average Transmitter-receiver loop terrain clearance of 44 metres and a magnetic sensor clearance of 54 metres.

The on board operator was responsible for monitoring the system integrity. He also maintained a detailed flight log during the survey, tracking the times of the flight as well as any unusual geophysical or topographic features.

On return of the aircrew to the base camp the survey data was transferred from a compact flash card (PCMCIA) to the data processing computer. The data were then uploaded via ftp to the Geotech office in Aurora for daily quality assurance and quality control by qualified personnel.

2.4 AIRCRAFT AND EQUIPMENT

2.4.1 SURVEY AIRCRAFT

The survey was flown using a Eurocopter Aerospatiale (Astar) 350 B3 helicopter, registration C-GAKF. The helicopter is owned and operated by Access Helicopters. Installation of the geophysical and ancillary equipment was carried out by a Geotech Ltd crew.

2.4.2 ELECTROMAGNETIC SYSTEM

The electromagnetic system was a Geotech Time Domain EM (VTEM™Plus) full receiver-waveform streamed data recorded system. The "full waveform VTEM system" uses the streamed half-cycle recording of transmitter and receiver waveforms to obtain a complete system response calibration throughout the entire survey flight. The VTEM™ transmitter current waveform is shown diagrammatically in Figure 6. VTEM with the Serial number 19 had been used for the survey.

The VTEM™ Receiver and transmitter coils were in concentric-coplanar and Z-direction oriented configuration. The receiver system for the project also included a coincident-coaxial X-direction coil to measure the in-line dB/dt and calculate B-Field responses. The Transmitter-receiver loop was towed at a mean distance of 31 metres below the aircraft as shown in Figure 7.

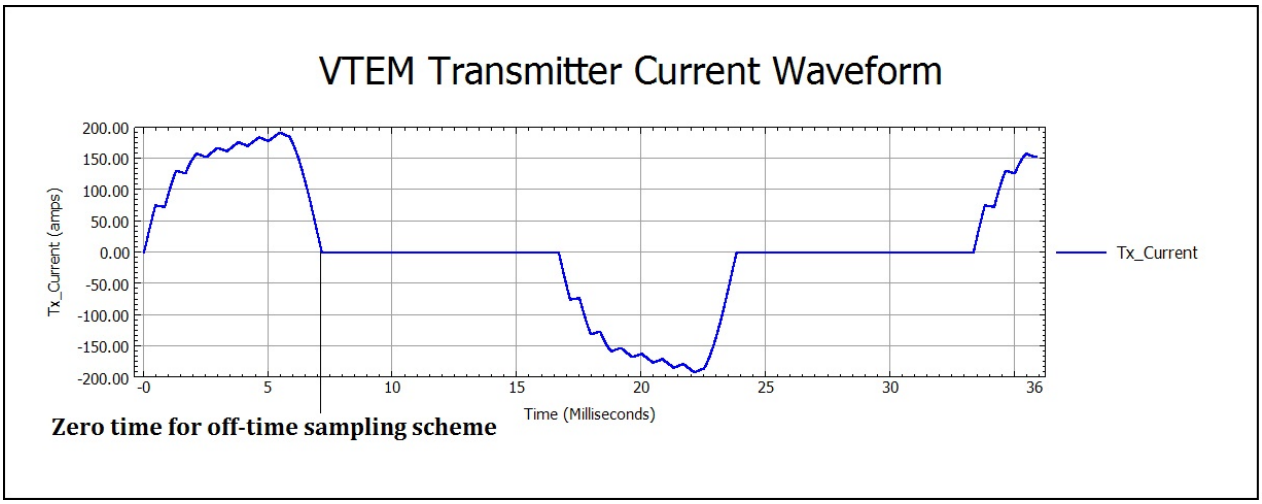

Figure 6: VTEM™ Transmitter Current Waveform

The VTEM™ decay sampling scheme is shown in Table 3 below. Forty-three time measurement gates were used for the final data processing in the range from 0.021 to 8.083 msec. Zero time for the off-time sampling scheme is equal to the current pulse width and is defined as the time near the end of the turn-off ramp where the dI/dt waveform falls to 1/2 of its peak value.

Table 3: Off-Time Decay Sampling Scheme

VTEM™ Decay Sampling Scheme				
Index	Start	End	Middle	Width
Milliseconds				
4	0.018	0.023	0.021	0.005
5	0.023	0.029	0.026	0.005
6	0.029	0.034	0.031	0.005
7	0.034	0.039	0.036	0.005
8	0.039	0.045	0.042	0.006
9	0.045	0.051	0.048	0.007
10	0.051	0.059	0.055	0.008
11	0.059	0.068	0.063	0.009
12	0.068	0.078	0.073	0.010
13	0.078	0.090	0.083	0.012
14	0.090	0.103	0.096	0.013
15	0.103	0.118	0.110	0.015
16	0.118	0.136	0.126	0.018
17	0.136	0.156	0.145	0.020
18	0.156	0.179	0.167	0.023
19	0.179	0.206	0.192	0.027
20	0.206	0.236	0.220	0.030
21	0.236	0.271	0.253	0.035
22	0.271	0.312	0.290	0.040
23	0.312	0.358	0.333	0.046

VTEM™ Decay Sampling Scheme				
Index	Start	End	Middle	Width
Milliseconds				
24	0.358	0.411	0.383	0.053
25	0.411	0.472	0.440	0.061
26	0.472	0.543	0.505	0.070
27	0.543	0.623	0.580	0.081
28	0.623	0.716	0.667	0.093
29	0.716	0.823	0.766	0.107
30	0.823	0.945	0.880	0.122
31	0.945	1.086	1.010	0.141
32	1.086	1.247	1.161	0.161
33	1.247	1.432	1.333	0.185
34	1.432	1.646	1.531	0.214
35	1.646	1.891	1.760	0.245
36	1.891	2.172	2.021	0.281
37	2.172	2.495	2.323	0.323
38	2.495	2.865	2.667	0.370
39	2.865	3.292	3.063	0.427
40	3.292	3.781	3.521	0.490
41	3.781	4.341	4.042	0.560
42	4.341	4.987	4.641	0.646
43	4.987	5.729	5.333	0.742
44	5.729	6.581	6.125	0.852
45	6.581	7.560	7.036	0.979
46	7.560	8.685	8.083	1.125

Z Component: 4 - 46 time gates
X Component: 20 - 46 time gates

VTEM™ system specifications:

Transmitter	Receiver
• Transmitter loop diameter: 26 m • Number of turns: 4 • Effective Transmitter loop area: 2123.7 m^2 • Transmitter base frequency: 30 Hz • Peak current: 191 A • Pulse width: 7.17 ms • Waveform shape: Bi-polar trapezoid • Peak dipole moment: 405,630 nIA • Actual average Transmitter-receiver loop terrain clearance: 44 metres above the ground	• X Coil diameter: 0.32 m • Number of turns: 245 • Effective coil area: 19.69 m^2 • Z-Coil diameter: 1.2 m • Number of turns: 100 • Effective coil area: 113.04 m^2

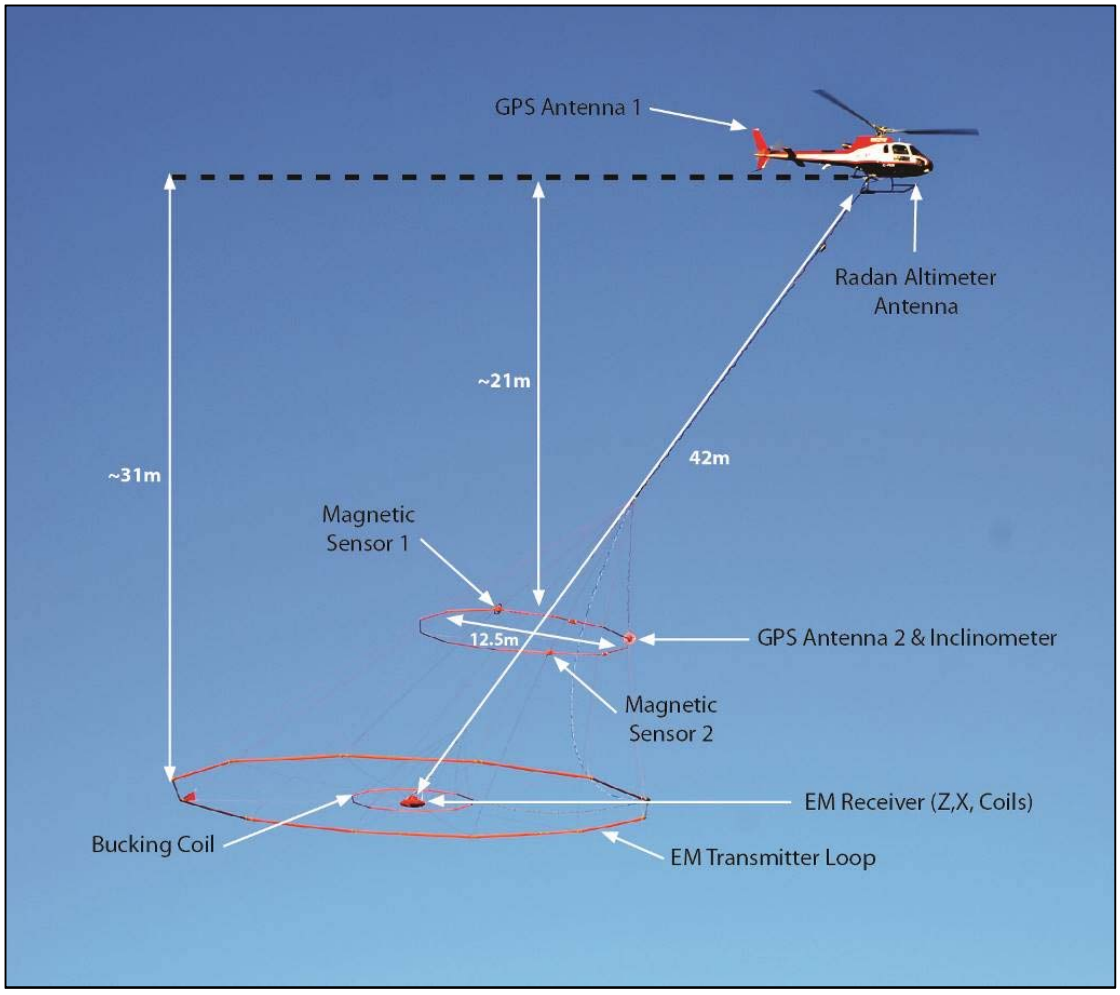

Figure 7: VTEM™Plus System Configuration.

2.4.3 FULL WAVEFORM VTEM™ SENSOR CALIBRATION

The calibration is performed on the complete VTEM™ system installed in and connected to the helicopter, using special calibration equipment.

The procedure takes half-cycle files acquired and calculates a calibration file consisting of a single stacked half-cycle waveform. The purpose of the stacking is to attenuate natural and man-made magnetic signals, leaving only the response to the calibration signal.

2.4.4 HORIZONTAL MAGNETIC GRADIOMETER

The horizontal magnetic gradiometer consists of two Geometrics split-beam field magnetic sensors with a sampling interval of 0.1 seconds. These sensors are mounted 12.5 metres apart on a separate loop, 10 metres above the Transmitter-receiver loop. A GPS antenna and Gyro Inclinometer is installed on the separate loop to accurately record the tilt and position of the magnetic gradiomag bird.

2.4.5 RADAR ALTIMETER

A Terra TRA 3000/TRI 40 radar altimeter was used to record terrain clearance. The antenna was mounted beneath the bubble of the helicopter cockpit (Figure 7).

2.4.6 GPS NAVIGATION SYSTEM

The navigation system used was a Geotech PC104 based navigation system utilizing a NovAtel's WAAS (Wide Area Augmentation System) enabled GPS receiver, Geotech navigate software, a full screen display with controls in front of the pilot to direct the flight and a NovAtel GPS antenna mounted on the helicopter tail (Figure 7). As many as 11 GPS and two WAAS satellites may be monitored at any one time. The positional accuracy or circular error probability (CEP) is 1.8 m, with WAAS active, it is 1.0 m. The co-ordinates of the survey area were set-up prior to the survey and the information was fed into the airborne navigation system. The second GPS antenna is installed on the additional magnetic loop together with Gyro Inclinometer.

2.4.7 DIGITAL ACQUISITION SYSTEM

A Geotech data acquisition system recorded the digital survey data on an internal compact flash card. Data is displayed on an LCD screen as traces to allow the operator to monitor the integrity of the system. The data type and sampling interval as provided in Table 4.

Table 4: Acquisition Sampling Rates

Data Type	Sampling
TDEM	0.1 sec
Magnetometer	0.1 sec
GPS Position	0.2 sec
Radar Altimeter	0.2 sec
Inclinometer	0.1 sec

2.5 BASE STATION

A combined magnetometer/GPS base station was utilized on this project. A Geometrics Caesium vapour magnetometer was used as a magnetic sensor with a sensitivity of 0.001 nT. The base station was recording the magnetic field together with the GPS time at 1 Hz on a base station computer.

The base station magnetometer sensor was installed at 130° 11.6730' W, 61° 48.7029' N; away from electric transmission lines and moving ferrous objects such as motor vehicles. The base station data were backed-up to the data processing computer at the end of each survey day.

3. PERSONNEL

The following Geotech Ltd. personnel were involved in the project.

FIELD:

Project Manager:	Darren Tuck (Office)
Data QC:	Neil Fiset (Office)
Crew chief:	Roger Leblanc
Operator:	n/a

The survey pilot and the mechanical engineer were employed directly by the helicopter operator – Access Helicopters.

Pilot:	Michael Holcroft
Mechanical Engineer:	n/a

OFFICE:

Preliminary Data Processing:	Neil Fiset
Final Data Processing:	TaiChyi Shei
Final Data QA/QC:	Geoffrey Plastow
Reporting/Mapping:	Liz Mathew

Data acquisition phase was carried out under the supervision of Andrei Bagrianski, P. Geo, and Chief Operating Officer. Processing and Interpretation phases were carried out under the supervision of Geoffrey Plastow, P. Geo, and Data Processing Manager. The customer relations were looked after by David Hitz.

4. DATA PROCESSING AND PRESENTATION

Data compilation and processing were carried out by the application of Geosoft OASIS Montaj and programs proprietary to Geotech Ltd.

4.1 FLIGHT PATH

The flight path, recorded by the acquisition program as WGS 84 latitude/longitude, was converted into the NAD83 Datum, UTM Zone 9 North coordinate system in Oasis Montaj.

The flight path was drawn using linear interpolation between x, y positions from the navigation system. Positions are updated every second and expressed as UTM easting's (x) and UTM northing's (y).

4.2 ELECTROMAGNETIC DATA

The Full Waveform EM specific data processing operations included:

- Half cycle stacking (performed at time of acquisition);
- System response correction;
- Parasitic and drift removal by deconvolution.

A three stage digital filtering process was used to reject major sferic events and to reduce noise levels. Local sferic activity can produce sharp, large amplitude events that cannot be removed by conventional filtering procedures. Smoothing or stacking will reduce their amplitude but leave a broader residual response that can be confused with geological phenomena. To avoid this possibility, a computer algorithm searches out and rejects the major sferic events.

The signal to noise ratio was further improved by the application of a low pass linear digital filter. This filter has zero phase shift which prevents any lag or peak displacement from occurring, and it suppresses only variations with a wavelength less than about 1 second or 15 metres. This filter is a symmetrical 1 sec linear filter.

The results are presented as stacked profiles of EM voltages for the time gates, in linear - logarithmic scale for the B-field Z component and dB/dt responses in the Z and X components. B-field Z component time channel recorded at 2.021 milliseconds (Kudz Ze Kayah) and at 4.641 milliseconds (Limy and Pelly) after the termination of the impulse is also presented as a colour image. Calculated Time Constant (TAU) with Calculated Vertical Derivative contours is presented in Appendix C and E. Resistivity Depth Image (RDI) is also presented in Appendix F and G.

VTEM has two receiver coil orientations. Z-axis coil is oriented parallel to the transmitter coil axis and both are horizontal to the ground. The X-axis coil is oriented parallel to the ground and along the line-of-flight. This combined two coil configuration provides information on the position, depth, dip and thickness of a conductor. Generalized modeling results of VTEM max data are shown in Appendix D.

In general X-component data produce cross-over type anomalies: from "+ to – "in flight direction of flight for "thin" sub vertical targets and from "- to +" in direction of flight for "thick" targets. Z component data produce double peak type anomalies for "thin" sub vertical targets and single peak for "thick" targets.

The limits and change-over of "thin-thick" depends on dimensions of a TEM system (Appendix D, Figure D-16).

Because of X component polarity is under line-of-flight, convolution Fraser Filter (Figure 8) is applied to X component data to represent axes of conductors in the form of grid map. In this case positive FF anomalies always correspond to "plus-to-minus" X data crossovers independent of the flight direction.

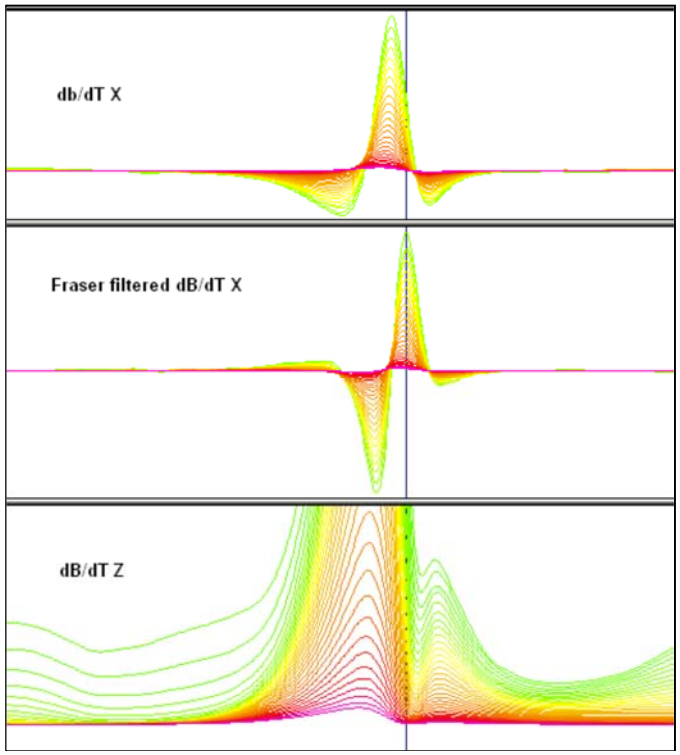

Figure 8: Z, X and Fraser filtered X (FFx) components for "thin" target.

4.3 HORIZONTAL MAGNETIC GRADIOMETER DATA

The horizontal gradients data from the VTEM™Plus are measured by two magnetometers 12.5 m apart on an independent bird mounted10m above the VTEM™ loop. A GPS and a Gyro Inclinometer help to determine the positions and orientations of the magnetometers. The data from the two magnetometers are corrected for position and orientation variations, as well as for the diurnal variations using the base station data.

The position of the centre of the horizontal magnetic gradiometer bird is calculated form the GPS utilizing in-house processing tool in Geosoft. Following that total magnetic intensity is calculated at the center of the bird by calculating the mean values from both sensors. In addition to the total intensity advanced processing is done to calculate the in-line and cross-line (or lateral) horizontal gradient which enhance the understanding of magnetic targets. The in-line (longitudinal) horizontal gradient is calculated from the difference of two consecutive total magnetic field readings divided by the distance along the flight line direction, while the cross-line (lateral) horizontal magnetic gradient is calculated from the difference in the magnetic readings from both magnetic sensors divided by their horizontal separation.

Two advanced magnetic derivative products, the total horizontal derivative (THDR), and tilt angle derivative and are also created. The total horizontal derivative or gradient is defined as:

THDR = sqrt(Hx*Hx+Hy*Hy), where Hx and Hy are cross-line and in-line horizontal gradients.

The tilt angle derivative (TDR) is defined as:

TDR = arctan(Vz/THDR), where THDR is the total horizontal derivative, and Vz is the vertical derivative.

Measured cross-line gradients can help to enhance cross-line linear features during gridding.

5. DELIVERABLES

5.1 SURVEY REPORT

The survey report describes the data acquisition, processing, and final presentation of the survey results. The survey report is provided in two paper copies and digitally in PDF format.

5.2 MAPS

Final maps were produced at scale of 1:10,000 for best representation of the survey size and line spacing. The coordinate/projection system used was NAD83 Datum, UTM Zone 9 North. All maps show the flight path trace and topographic data; latitude and longitude are also noted on maps.

The preliminary and final results of the survey are presented as EM profiles, a late-time gate gridded EM channel, and a colour magnetic TMI contour map.

- Maps at 1:10,000 in Geosoft MAP format, as follows:

GL150055_10k_bb_dBdtz:	dB/dt profiles Z Component, Time Gates 0.220 – 7.036 ms in linear – logarithmic scale.
GL150055_10k_bb_Bfieldz:	B-field profiles Z Component, Time Gates 0.220 – 7.036 ms in linear – logarithmic scale.
GL150055_10k_bb_BFz36:	B-field early time Z Component Channel 36, Time Gate 2.021 ms colour image.
GL150055_10k_bb_BFz42:	B-field early time Z Component Channel 42, Time Gate 4.641 ms colour image.
GL150055_10k_bb_SFxFF24:	dBdt X Component Fraser Filtered Channel 24, Time Gate 0.383 ms colour image.
GL150055_10k_bb_SFxFF26:	dBdt X Component Fraser Filtered Channel 26, Time Gate 0.505 ms colour image.
GL150055_10k_bb_SFxFF30:	dBdt X Component Fraser Filtered Channel 30, Time Gate 0.880 ms colour image.
GL150055_10k_bb_TMI:	Total magnetic intensity (TMI) colour image and contours.
GL150055_10k_bb_TauSF:	dB/dt Calculated Time Constant (Tau) with Calculated Vertical Derivative contours
GL150055_10k_bb_TotHGrad:	Magnetic Total Horizontal Gradient colour image.
GL150055_10k_bb_TiltDrv:	Magnetic Tilt-Angle Derivative colour image.

where bb represents the block name. (i.e. GL150055_10k_Limy_TMI)

- Maps are also presented in PDF format.
- The topographic data base was derived from 1:50,000 NRC (Natural Resources Canada) NTDB data, www.geogratis.ca.
- A Google Earth file *GL150055_bb_FP.kml* showing the flight path of the block is included. Free versions of Google Earth software from: http://earth.google.com/download-earth.html

  where bb represents the block name.

5.3 DIGITAL DATA

Two copies of the data and maps on DVD were prepared to accompany the report. Each DVD contains a digital file of the line data in GDB Geosoft Montaj format as well as the maps in Geosoft Montaj Map and PDF format.

- DVD structure.

Data contains databases, grids and maps, as described below.
Report contains a copy of the report and appendices in PDF format.

Databases in Geosoft GDB format, containing the channels listed in Table 5.

Table 5: Geosoft GDB Data Format

Channel name	Units	Description
X:	metres	UTM Easting NAD83 Zone 9 North
Y:	metres	UTM Northing NAD83 Zone 9 North
Longitude:	Decimal Degrees	WGS 84 Longitude data
Latitude:	Decimal Degrees	WGS 84 Latitude data
Z:	metres	GPS antenna elevation (above Geoid)
Zb:	metres	EM bird elevation (above Geoid)
Radar:	metres	helicopter terrain clearance from radar altimeter
Radarb:	metres	Calculated EM transmitter-receiver loop terrain clearance from radar altimeter
DEM:	metres	Digital Elevation Model
Gtime:	Seconds of the day	GPS time
Mag1L:	nT	Measured Total Magnetic field data (left sensor)
Mag1R:	nT	Measured Total Magnetic field data (right sensor)
Basemag:	nT	Magnetic diurnal variation data
Mag2LZ	nT	Z corrected (w.r.t. loop center) and diurnal corrected magnetic field left mag
Mag2RZ	nT	Z corrected (w.r.t. loop center) and diurnal corrected magnetic field right mag
TMI2	nT	Calculated from diurnal corrected total magnetic field intensity of the centre of the loop
TMI3	nT	Microleveled total magnetic field intensity of the centre of the loop
Hginline		Calculated in-line gradient
Hgcxline		measured cross-line gradient
CVG	nT/m	Calculated Magnetic Vertical Gradient
SFz[4]:	pV/(A*m^4)	Z dB/dt 0.021 millisecond time channel
SFz[5]:	pV/(A*m^4)	Z dB/dt 0.026 millisecond time channel
SFz[6]:	pV/(A*m^4)	Z dB/dt 0.031 millisecond time channel
SFz[7]:	pV/(A*m^4)	Z dB/dt 0.036 millisecond time channel
SFz[8]:	pV/(A*m^4)	Z dB/dt 0.042 millisecond time channel
SFz[9]:	pV/(A*m^4)	Z dB/dt 0.048 millisecond time channel
SFz[10]:	pV/(A*m^4)	Z dB/dt 0.055 millisecond time channel
SFz[11]:	pV/(A*m^4)	Z dB/dt 0.063 millisecond time channel
SFz[12]:	pV/(A*m^4)	Z dB/dt 0.073 millisecond time channel
SFz[13]:	pV/(A*m^4)	Z dB/dt 0.083 millisecond time channel
SFz[14]:	pV/(A*m^4)	Z dB/dt 0.096 millisecond time channel

Channel name	Units	Description
SFz[15]:	pV/(A*m^4)	Z dB/dt 0.110 millisecond time channel
SFz[16]:	pV/(A*m^4)	Z dB/dt 0.126 millisecond time channel
SFz[17]:	pV/(A*m^4)	Z dB/dt 0.145 millisecond time channel
SFz[18]:	pV/(A*m^4)	Z dB/dt 0.167 millisecond time channel
SFz[19]:	pV/(A*m^4)	Z dB/dt 0.192 millisecond time channel
SFz[20]:	pV/(A*m^4)	Z dB/dt 0.220 millisecond time channel
SFz[21]:	pV/(A*m^4)	Z dB/dt 0.253 millisecond time channel
SFz[22]:	pV/(A*m^4)	Z dB/dt 0.290 millisecond time channel
SFz[23]:	pV/(A*m^4)	Z dB/dt 0.333 millisecond time channel
SFz[24]:	pV/(A*m^4)	Z dB/dt 0.383 millisecond time channel
SFz[25]:	pV/(A*m^4)	Z dB/dt 0.440 millisecond time channel
SFz[26]:	pV/(A*m^4)	Z dB/dt 0.505 millisecond time channel
SFz[27]:	pV/(A*m^4)	Z dB/dt 0.580 millisecond time channel
SFz[28]:	pV/(A*m^4)	Z dB/dt 0.667 millisecond time channel
SFz[29]:	pV/(A*m^4)	Z dB/dt 0.766 millisecond time channel
SFz[30]:	pV/(A*m^4)	Z dB/dt 0.880 millisecond time channel
SFz[31]:	pV/(A*m^4)	Z dB/dt 1.010 millisecond time channel
SFz[32]:	pV/(A*m^4)	Z dB/dt 1.161 millisecond time channel
SFz[33]:	pV/(A*m^4)	Z dB/dt 1.333 millisecond time channel
SFz[34]:	pV/(A*m^4)	Z dB/dt 1.531 millisecond time channel
SFz[35]:	pV/(A*m^4)	Z dB/dt 1.760 millisecond time channel
SFz[36]:	pV/(A*m^4)	Z dB/dt 2.021 millisecond time channel
SFz[37]:	pV/(A*m^4)	Z dB/dt 2.323 millisecond time channel
SFz[38]:	pV/(A*m^4)	Z dB/dt 2.667 millisecond time channel
SFz[39]:	pV/(A*m^4)	Z dB/dt 3.063 millisecond time channel
SFz[40]:	pV/(A*m^4)	Z dB/dt 3.521 millisecond time channel
SFz[41]:	pV/(A*m^4)	Z dB/dt 4.042 millisecond time channel
SFz[42]:	pV/(A*m^4)	Z dB/dt 4.641 millisecond time channel
SFz[43]:	pV/(A*m^4)	Z dB/dt 5.333 millisecond time channel
SFz[44]:	pV/(A*m^4)	Z dB/dt 6.125 millisecond time channel
SFz[45]:	pV/(A*m^4)	Z dB/dt 7.036 millisecond time channel
SFz[46]:	pV/(A*m^4)	Z dB/dt 8.083 millisecond time channel
SFx[20]:	pV/(A*m^4)	X dB/dt 0.220 millisecond time channel
SFx[21]:	pV/(A*m^4)	X dB/dt 0.253 millisecond time channel
SFx[22]:	pV/(A*m^4)	X dB/dt 0.290 millisecond time channel
SFx[23]:	pV/(A*m^4)	X dB/dt 0.333 millisecond time channel
SFx[24]:	pV/(A*m^4)	X dB/dt 0.383 millisecond time channel
SFx[25]:	pV/(A*m^4)	X dB/dt 0.440 millisecond time channel
SFx[26]:	pV/(A*m^4)	X dB/dt 0.505 millisecond time channel
SFx[27]:	pV/(A*m^4)	X dB/dt 0.580 millisecond time channel
SFx[28]:	pV/(A*m^4)	X dB/dt 0.667 millisecond time channel
SFx[29]:	pV/(A*m^4)	X dB/dt 0.766 millisecond time channel
SFx[30]:	pV/(A*m^4)	X dB/dt 0.880 millisecond time channel
SFx[31]:	pV/(A*m^4)	X dB/dt 1.010 millisecond time channel
SFx[32]:	pV/(A*m^4)	X dB/dt 1.161 millisecond time channel
SFx[33]:	pV/(A*m^4)	X dB/dt 1.333 millisecond time channel
SFx[34]:	pV/(A*m^4)	X dB/dt 1.531 millisecond time channel
SFx[35]:	pV/(A*m^4)	X dB/dt 1.760 millisecond time channel
SFx[36]:	pV/(A*m^4)	X dB/dt 2.021 millisecond time channel
SFx[37]:	pV/(A*m^4)	X dB/dt 2.323 millisecond time channel

Channel name	Units	Description
SFx[38]:	pV/(A*m^4)	X dB/dt 2.667 millisecond time channel
SFx[39]:	pV/(A*m^4)	X dB/dt 3.063 millisecond time channel
SFx[40]:	pV/(A*m^4)	X dB/dt 3.521 millisecond time channel
SFx[41]:	pV/(A*m^4)	X dB/dt 4.042 millisecond time channel
SFx[42]:	pV/(A*m^4)	X dB/dt 4.641 millisecond time channel
SFx[43]:	pV/(A*m^4)	X dB/dt 5.333 millisecond time channel
SFx[44]:	pV/(A*m^4)	X dB/dt 6.125 millisecond time channel
SFx[45]:	pV/(A*m^4)	X dB/dt 7.036 millisecond time channel
SFx[46]:	pV/(A*m^4)	X dB/dt 8.083 millisecond time channel
BFz	(pV*ms)/(A*m^4)	Z B-Field data for time channels 4 to 46
BFx	(pV*ms)/(A*m^4)	X B-Field data for time channels 20 to 46
SFxFF	pV/(A*m^4)	Fraser Filtered X dB/dt
NchanBF		Latest time channels of TAU calculation
TauBF	ms	Time constant B-Field
NchanSF		Latest time channels of TAU calculation
TauSF	ms	Time constant dB/dt
PLM:		60 Hz power line monitor

Electromagnetic B-field and dB/dt Z component data is found in array channel format between indexes 4 – 46, and X component data from 20 – 46, as described above.

- Database of the Resistivity Depth Images in Geosoft GDB format, containing the following channels:

Table 6: Geosoft Resistivity Depth Image GDB Data Format

Channel name	Units	Description
Xg	metres	UTM Easting NAD83 Zone 9 North
Yg	metres	UTM Northing NAD83 Zone 9 North
Dist:	meters	Distance from the beginning of the line
Depth:	meters	array channel, depth from the surface
Z:	meters	array channel, depth from sea level
AppRes:	Ohm-m	array channel, Apparent Resistivity
TR:	meters	EM system height from sea level
Topo:	meters	digital elevation model
Radarb:	metres	Calculated EM transmitter-receiver loop terrain clearance from radar altimeter
SF:	pV/(A*m^4)	array channel, dB/dT
MAG:	nT	TMI data
CVG:	nT/m	CVG data
DOI:	metres	Depth of Investigation: a measure of VTEM depth effectiveness
PLM:		60Hz Power Line Monitor

- Database of the VTEM Waveform "GL150055_waveform_final.gdb" in Geosoft GDB format, containing the following channels:

Table 7: Geosoft database for the VTEM waveform

Channel name	Units	Description
Time:	milliseconds	Sampling rate interval, 5.2083 microseconds
Tx_Current:	amps	Output current of the transmitter

- Grids in Geosoft GRD and GeoTIFF format, as follows:

bb_BFz36: B-Field Z Component Channel 36 (Time Gate 2.021 ms)
bb_BFz42: B-Field Z Component Channel 42 (Time Gate 4.641 ms)
bb_CVG_TMI: Calculated Vertical Derivative (nT/m)
bb_DEM: Digital Elevation Model (metres)
bb_Hgcxline: Measured Cross-Line Gradient (nT/m)
bb_Hginline: Measured In-Line Gradient (nT/m)
bb_SFxFF24: Fraser Filtered dB/dt X Component Channel 24 (Time Gate 0.383ms)
bb_SFxFF26: Fraser Filtered dB/dt X Component Channel 26 (Time Gate 0.505ms)
bb_SFxFF30: Fraser Filtered dB/dt X Component Channel 30 (Time Gate 0.880ms)
bb_SFz12: dB/dt Z Component Channel 12 (Time Gate 0.073 ms)
bb_SFz30: dB/dt Z Component Channel 30 (Time Gate 0.880 ms)
bb_SFz42: dB/dt Z Component Channel 42 (Time Gate 4.641 ms)
bb_SFz46: dB/dt Z Component Channel 46 (Time Gate 8.083 ms)
bb_TauBF: B-Field Z Component, Calculated Time Constant (ms)
bb_TauSF: dB/dt Z Component, Calculated Time Constant (ms)
bb_Tiltdrv: Magnetic Tilt derivative (radians)
bb_TMI3: Total Magnetic Intensity (nT)
bb_TotHgrad: Magnetic Total Horizontal Gradient (nT/m)

where bb represents block name

A Geosoft .GRD file has a .GI metadata file associated with it, containing grid projection information. A grid cell size of 37.5 metres was used.

6. CONCLUSIONS AND RECOMMENDATIONS

A helicopter-borne versatile time domain electromagnetic (VTEMplus) and horizontal magnetic gradiometer geophysical survey has been completed over Kudz Ze Kayah, Pelly and Limy situated near Wolverine Lake, Yukon.

The total area coverage is 73 km². Total survey line coverage 557 line kilometres. The principal sensors included a Time Domain EM system and a horizontal magnetic gradiometer using two caesium magnetometers. Results have been presented as stacked profiles, and contour colour images at a scale of 1:10,000. A formal Interpretation has not been included or requested.

Based on the geophysical results obtained, a number of TEM anomalous zones are identified across the properties. They can be seen overlapping the TAU decay parameter image presented with the calculated vertical magnetic gradient (CVG) contours (see Appendix C).

If the conductors correspond to an exploration model on the area it is recommended picking EM anomalies with conductance grading and center localization of the targets, detail resistivity depth imaging and plate modeling with test drill hole parameters planning prior to ground follow up and drill testing.

Respectfully submitted[2],

Neil Fiset
Geotech Ltd.

TaiChyi Shei
Geotech Ltd.

Geoffrey Plastow, P. Geo.
Data Processing Manager
Geotech Ltd.

PROFESSIONAL GEOSCIENTIST
GEOFFREY C. PLASTOW
PRACTISING MEMBER
2171
ONTARIO

November, 2015

[2] Final data processing of the EM and magnetic data were carried out by ZiHao Han, from the office of Geotech Ltd. in Aurora, Ontario, under the supervision of Geoffrey Plastow, P.Geo. Data Processing Manager.

APPENDIX A

SURVEY AREA LOCATION MAP

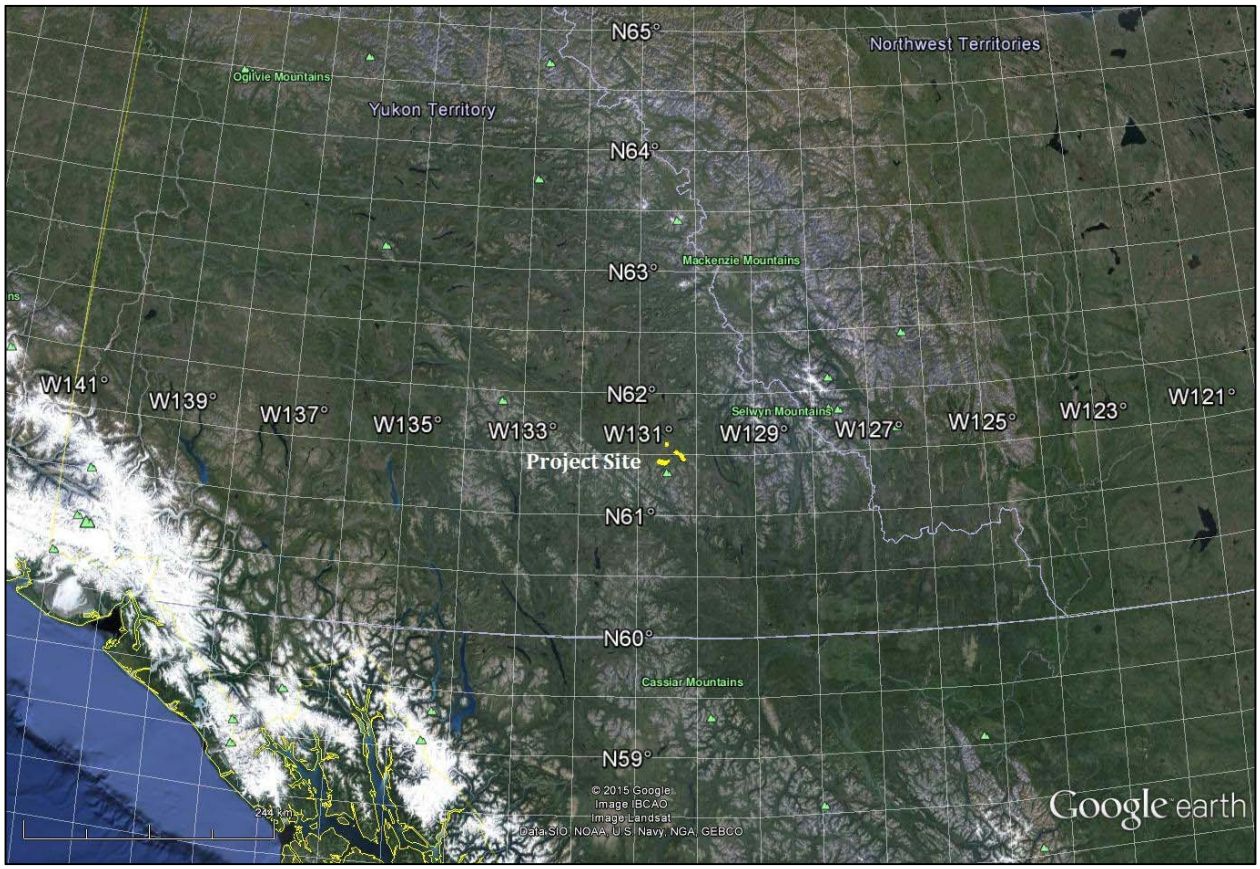

Overview of the Survey Area

APPENDIX B

SURVEY AREA COORDINATES
(WGS 84, UTM Zone 9 North)

Kudz Ze Kayah

X	Y
411912	6816608
410899	6812834
417670	6811469
417915	6811601
418000	6811446
419109	6812060
419254	6812104
420807	6813491
421585	6816389
420031	6815002
419887	6814958
411912	6816608
411912	6816608

Limy

X	Y
419090	6829290
419090	6830665
420490	6830665
420490	6829290

Pelly

X	Y
426041	6822058
428270	6824066
429636	6823115
432388	6822007
433912	6820700
435278	6818265
437147	6816154
434918	6814147
433049	6816258
431683	6818693
430158	6819999
427407	6821108

APPENDIX C

GEOPHYSICAL MAPS[1]

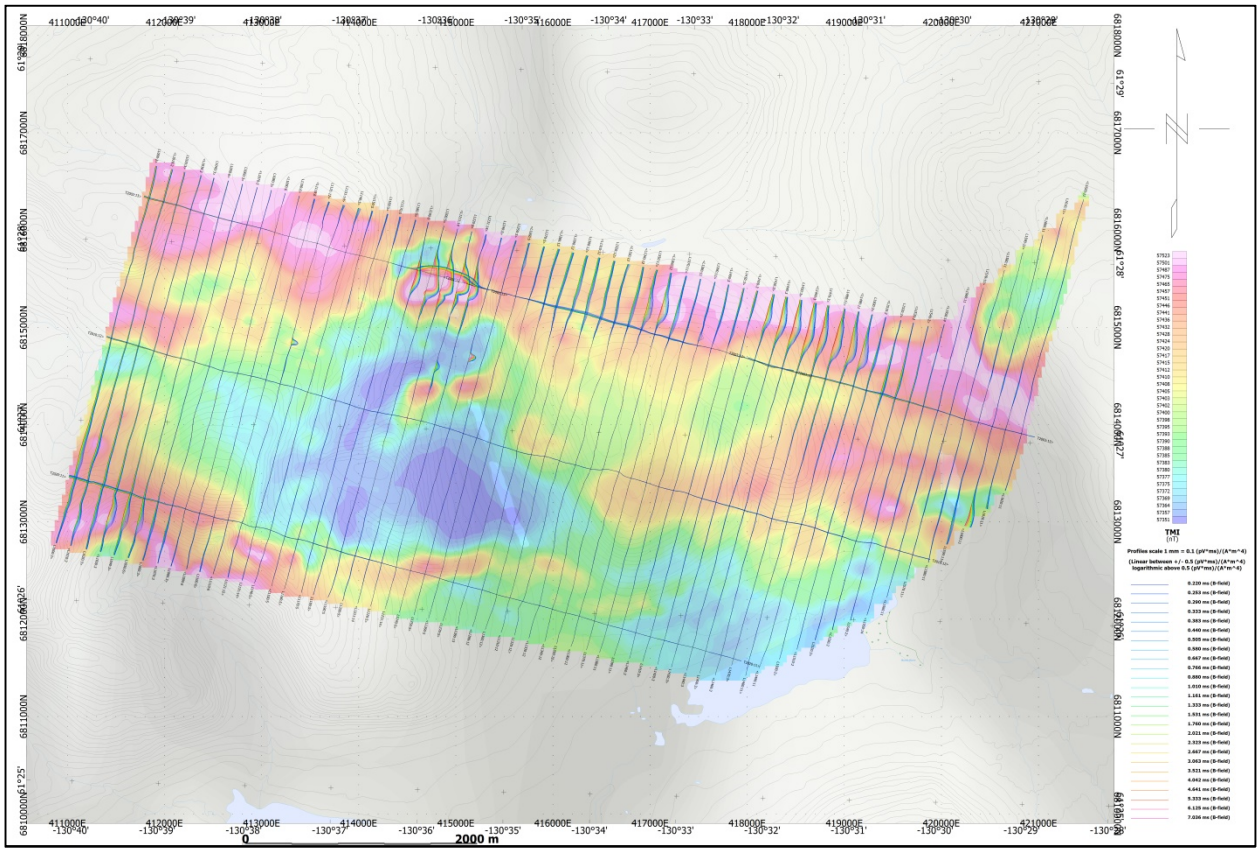

Kudz Ze Kayah - VTEM B-Field Z Component Profiles, Time Gates 0.220 to 7.036 ms

[1] Full size geophysical maps are also available in PDF format on the final DVD

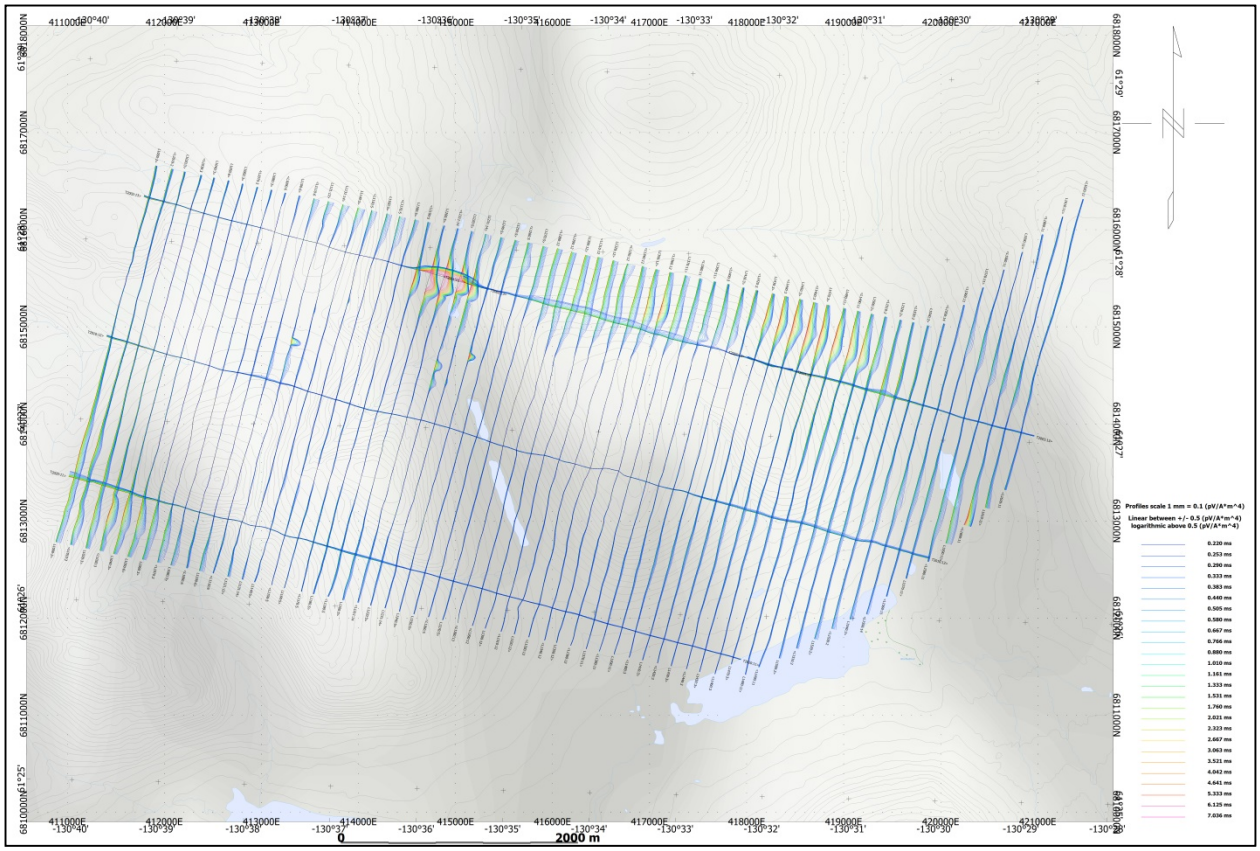

Kudz Ze Kayah - VTEM dB/dt Z Component Profiles, Time Gates 0.220 to 7.036 ms

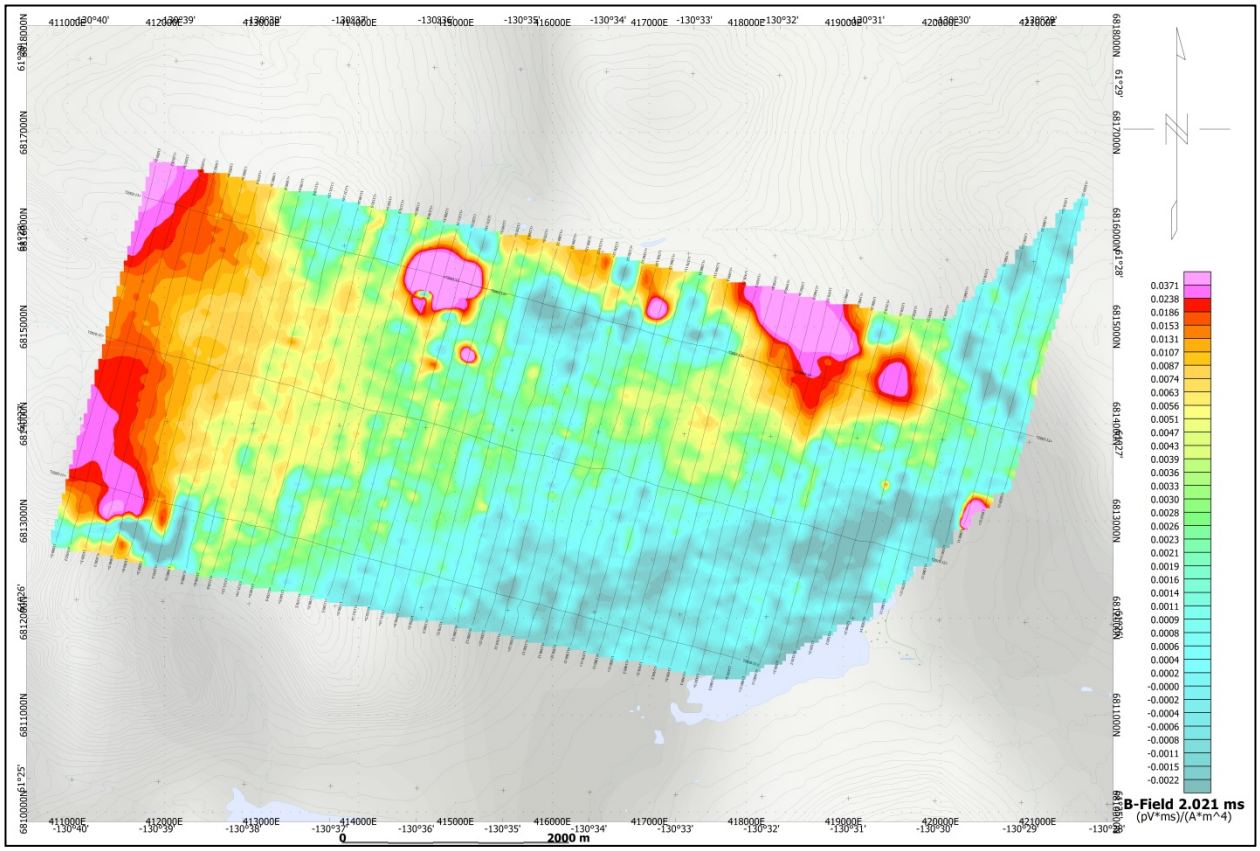

Kudz Ze Kayah - VTEM B-Field Z Component Channel 36, Time Gate 2.021 ms

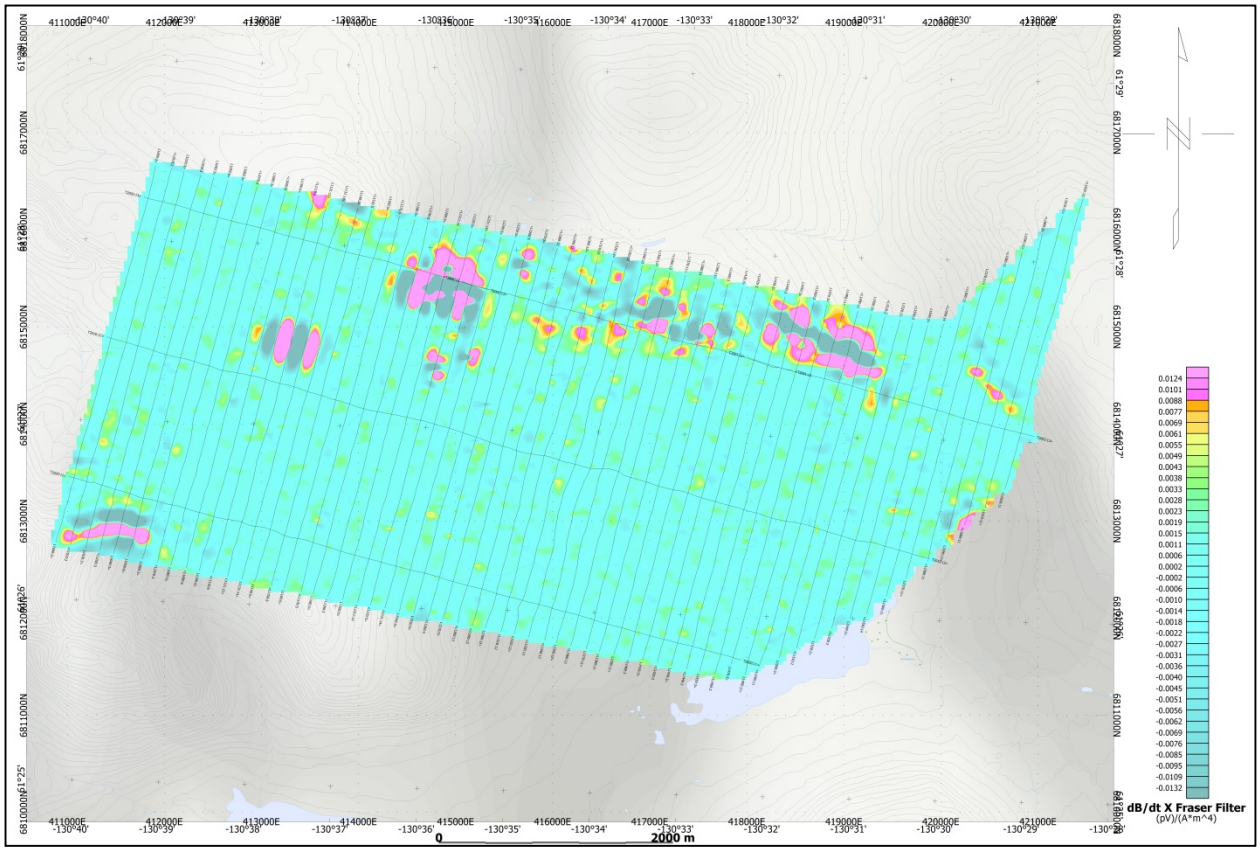

Kudz Ze Kayah - VTEM dB/dt X Component Fraser Filtered Channel 24, Time Gate 0.383 ms

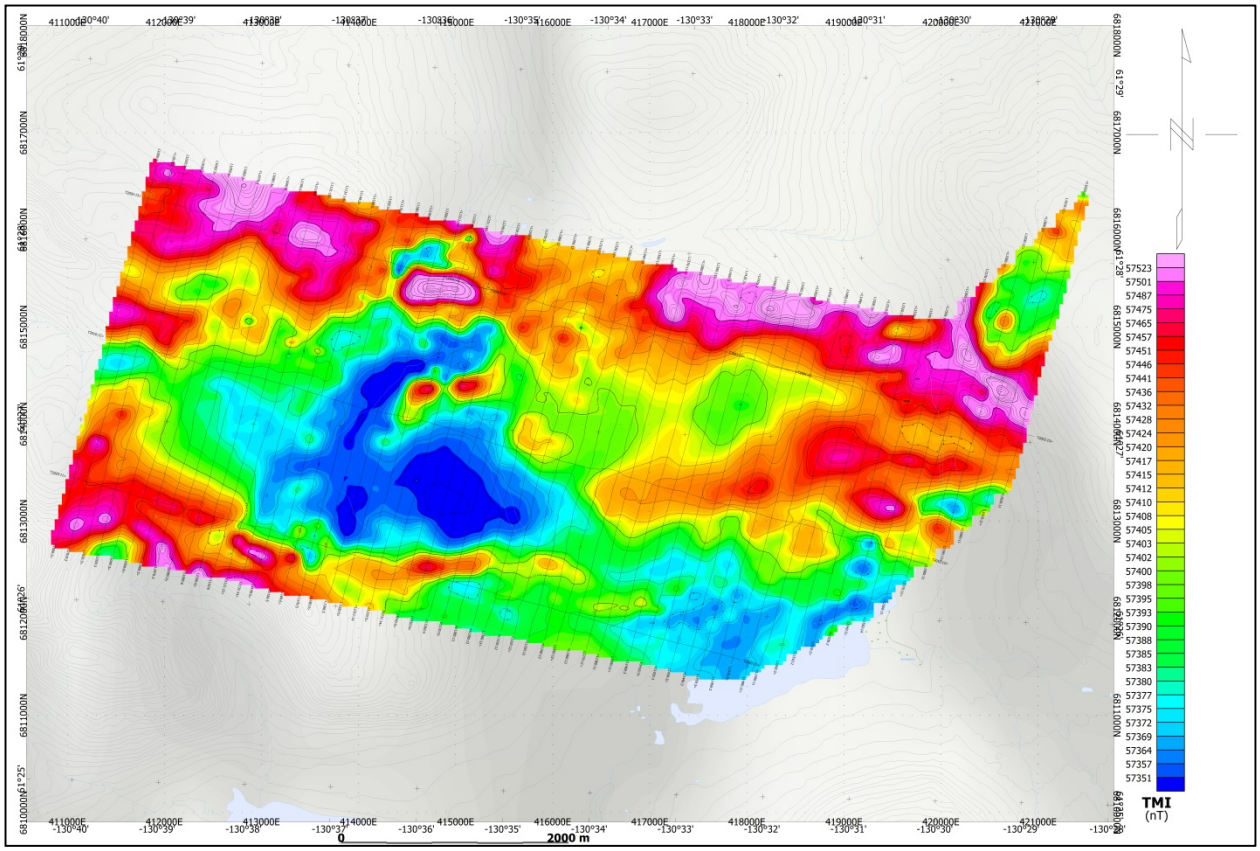

Kudz Ze Kayah - Total Magnetic Intensity (TMI)

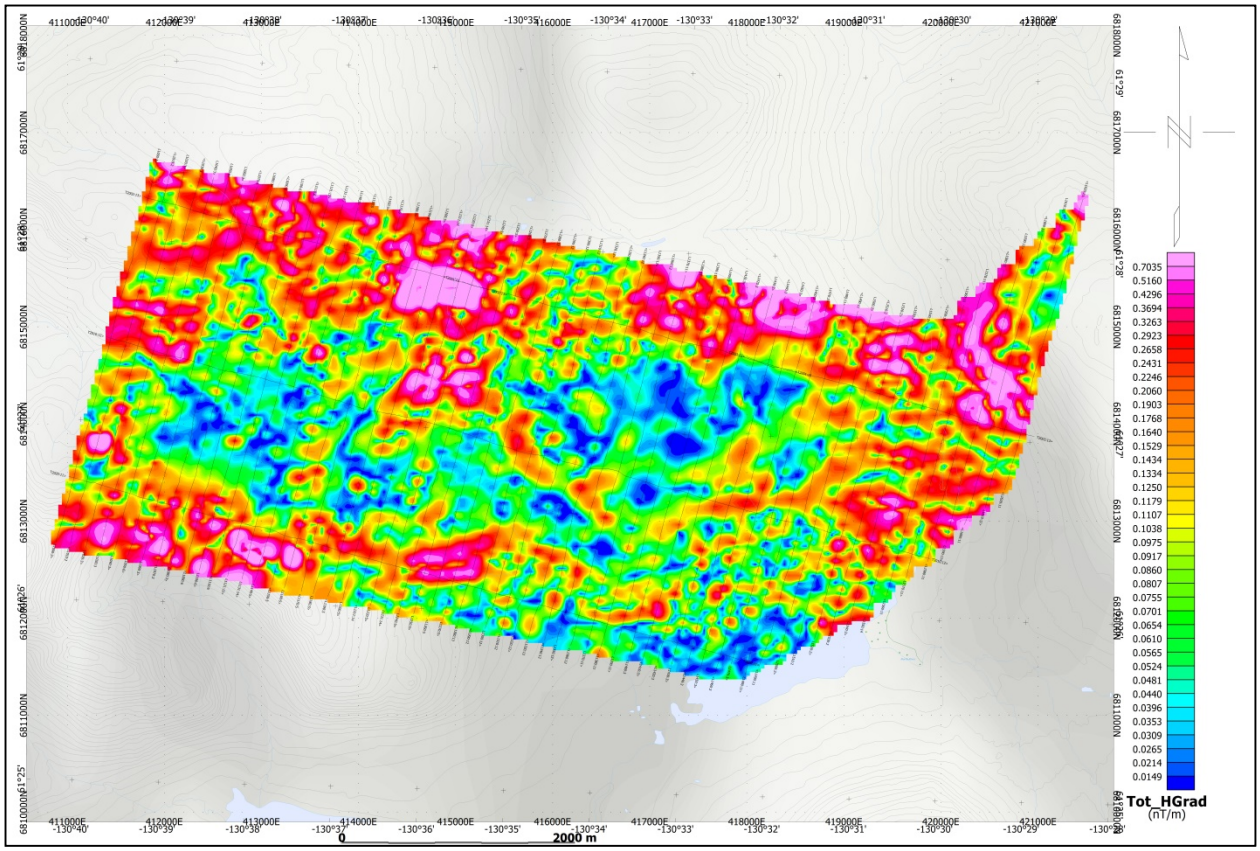

Kudz Ze Kayah - Magnetic Total Horizontal Gradient

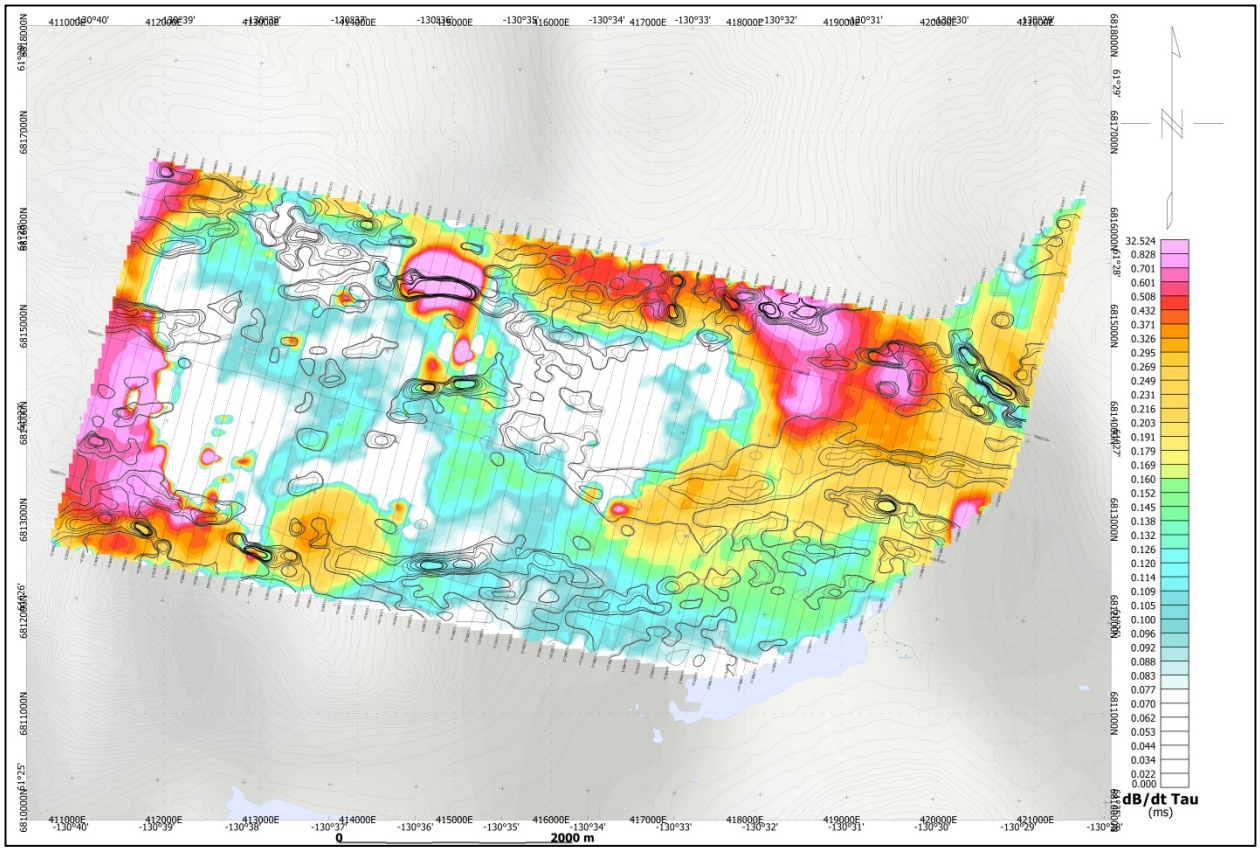

Kudz Ze Kayah - dB/dt Calculated Time Constant (Tau) with Calculated Vertical Derivative contours

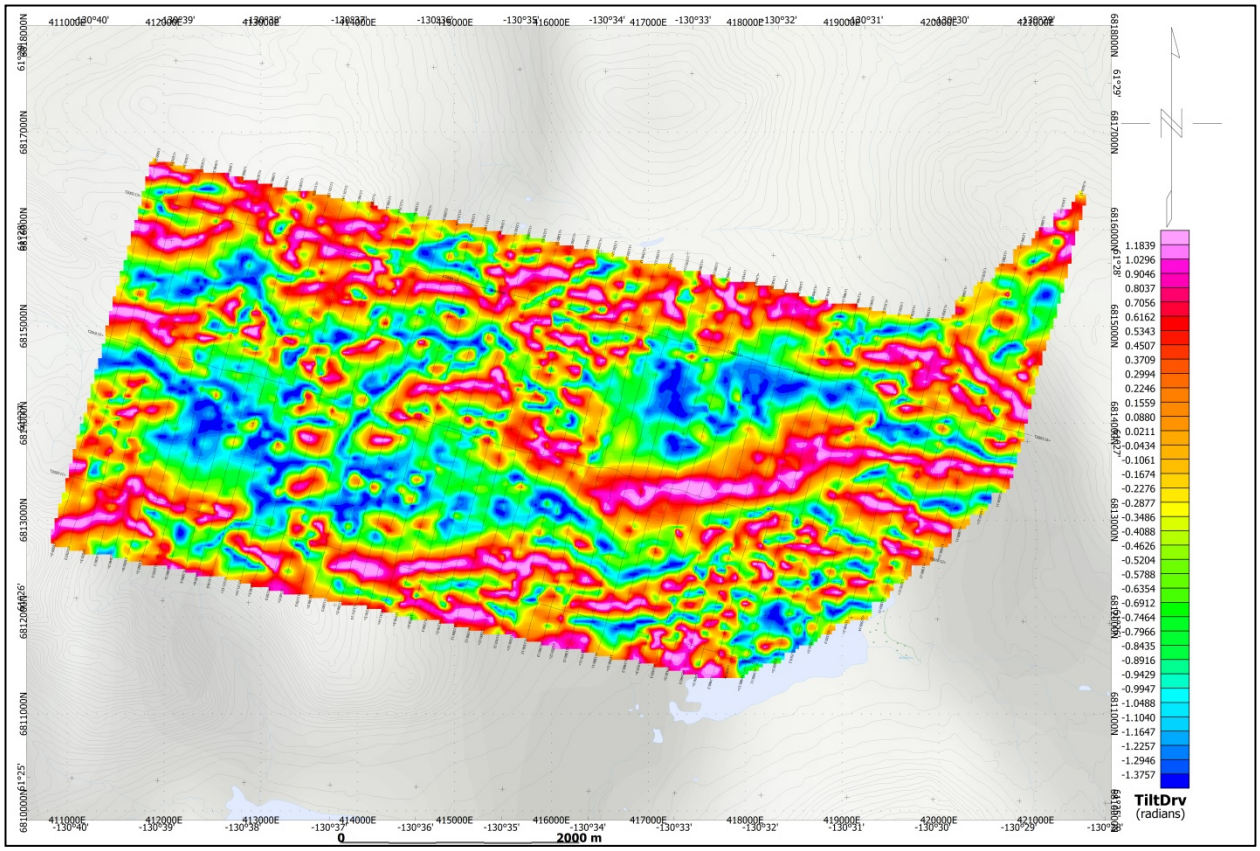

Kudz Ze Kayah - Magnetic Tilt - Angle Derivative

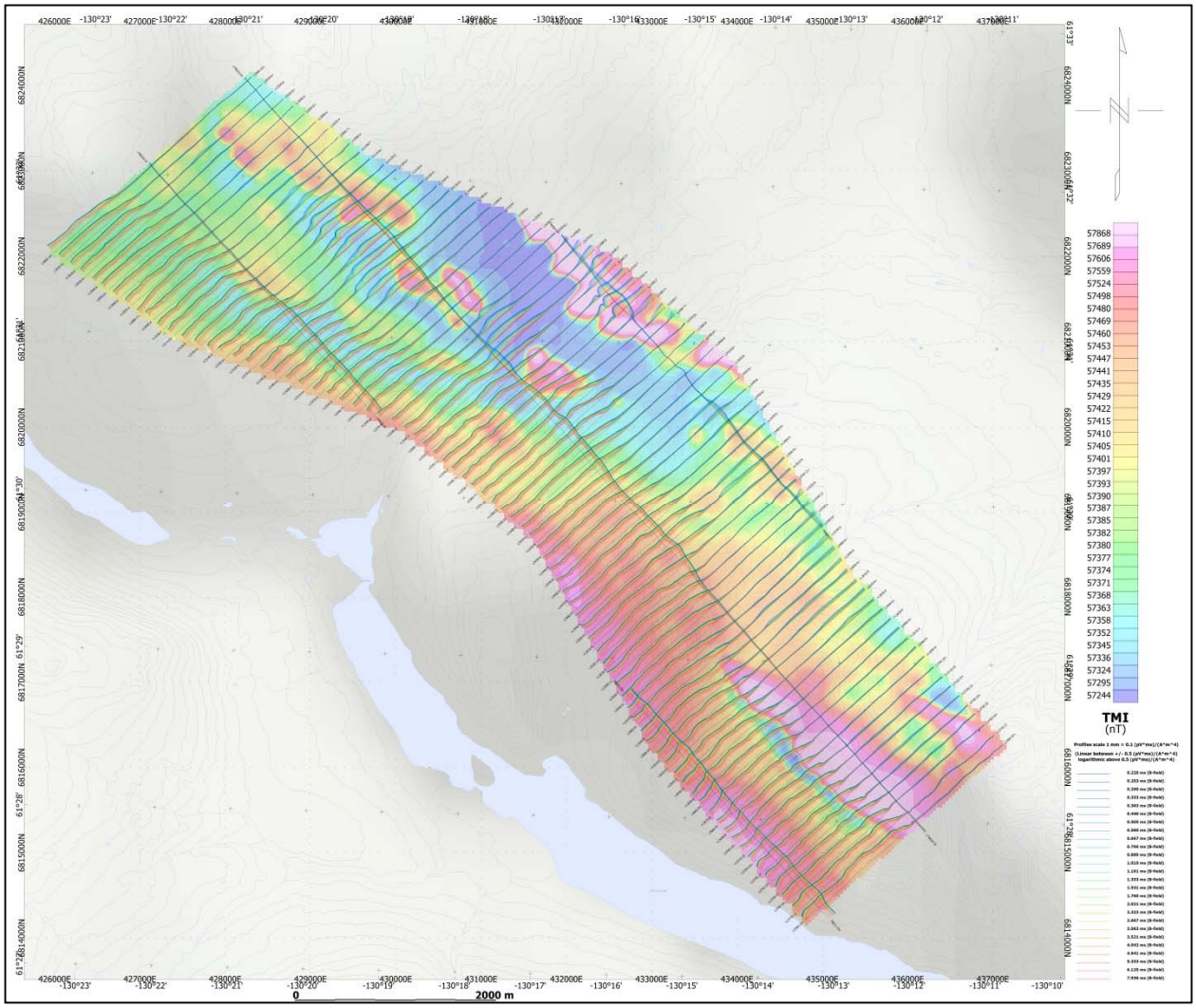

Pelly - VTEM B-Field Z Component Profiles, Time Gates 0.220 to 7.036 ms

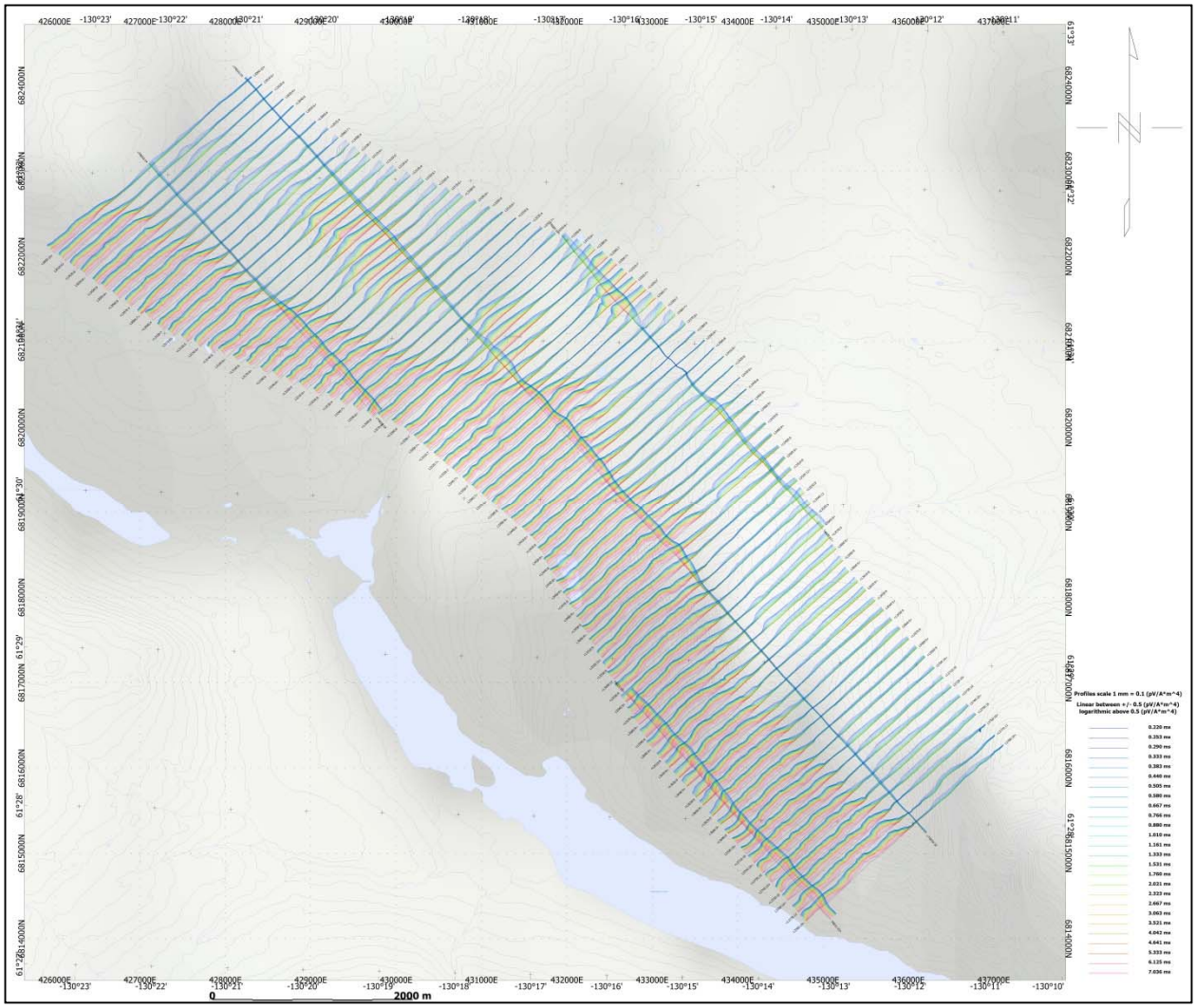

Pelly - VTEM dB/dt Z Component Profiles, Time Gates 0.220 to 7.036 ms

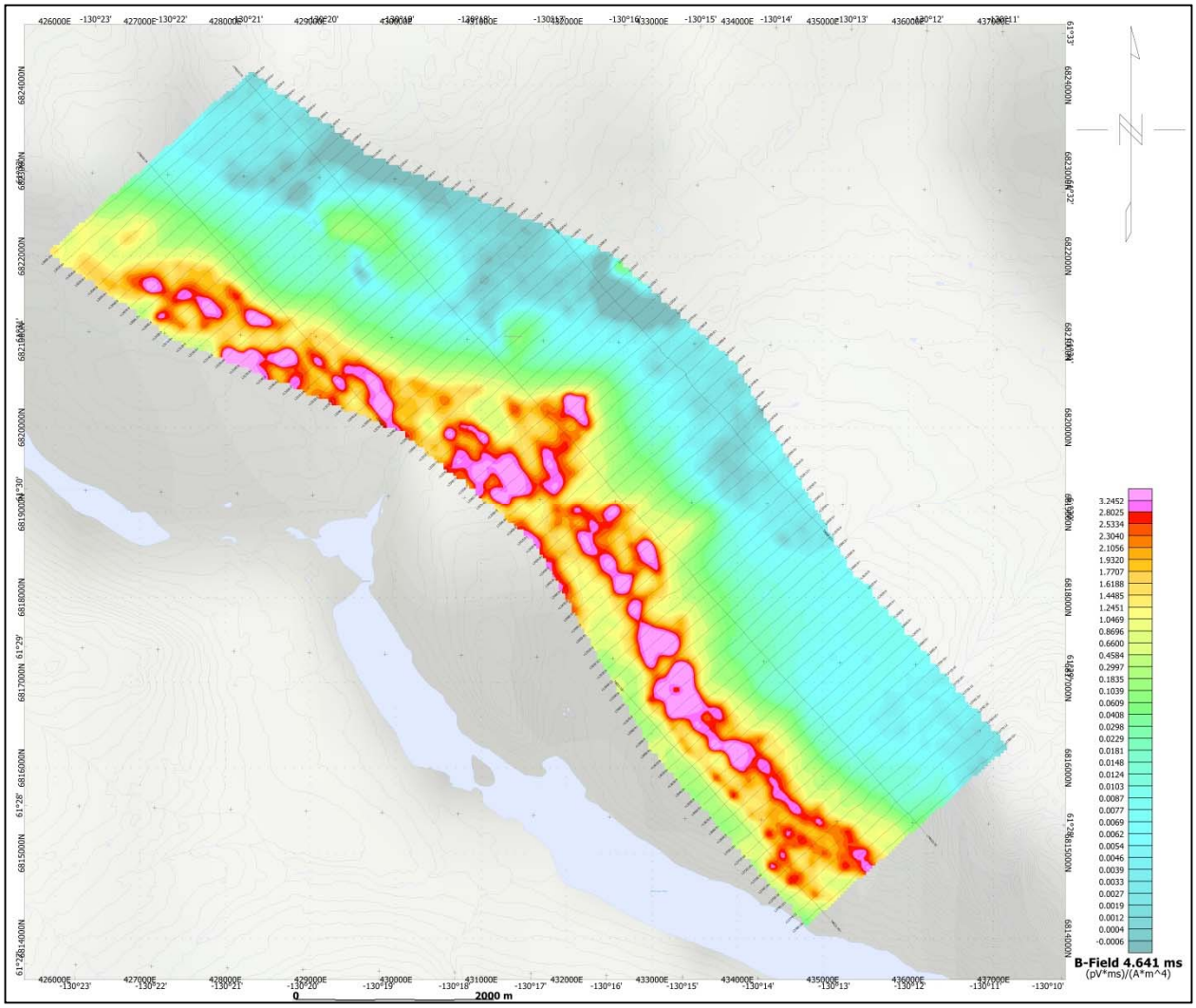

Pelly - VTEM B-Field Z Component Channel 42, Time Gate 4.641 ms

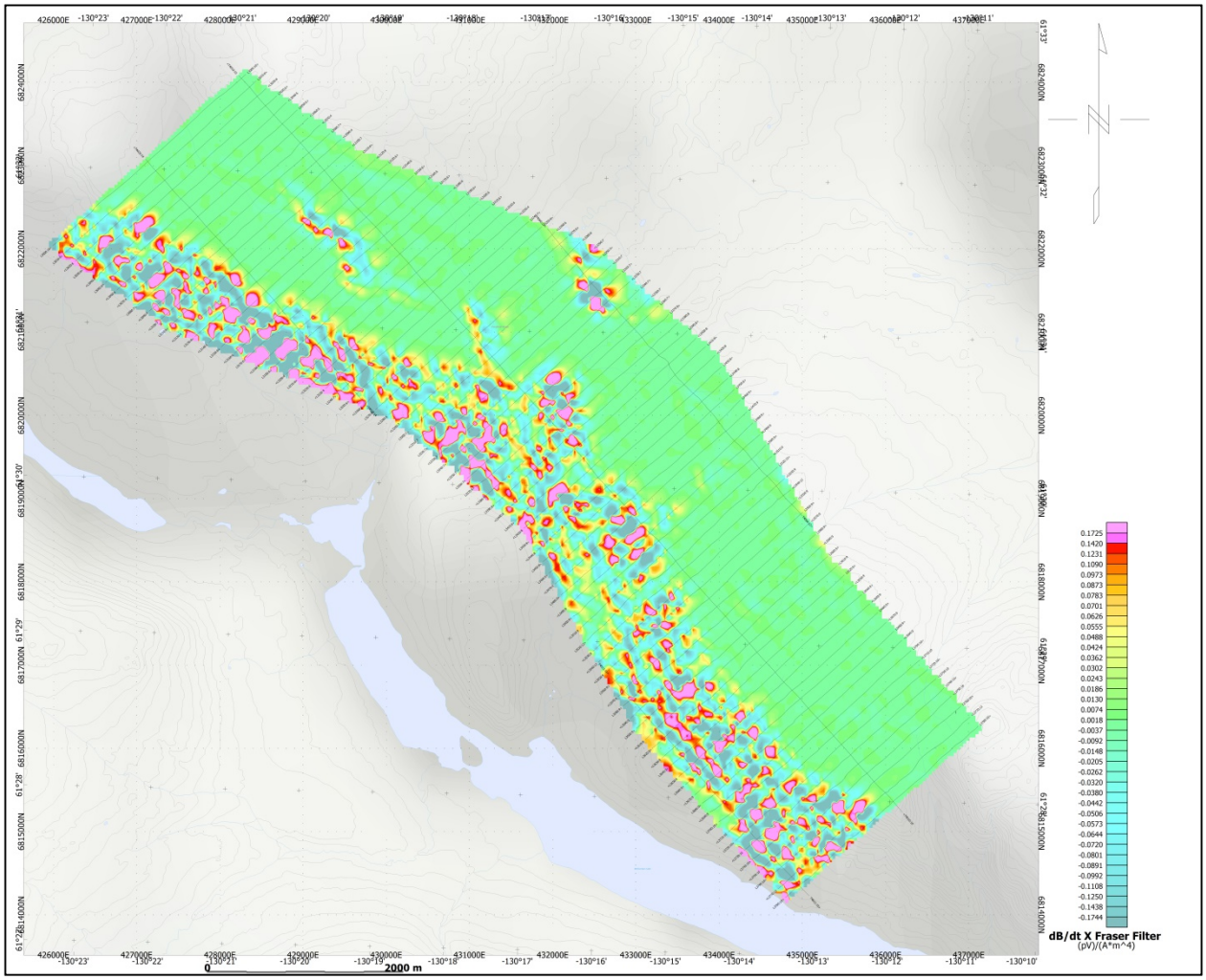

Pelly - VTEM dB/dt X Component Fraser Filtered Channel 26, Time Gate 0.505 ms

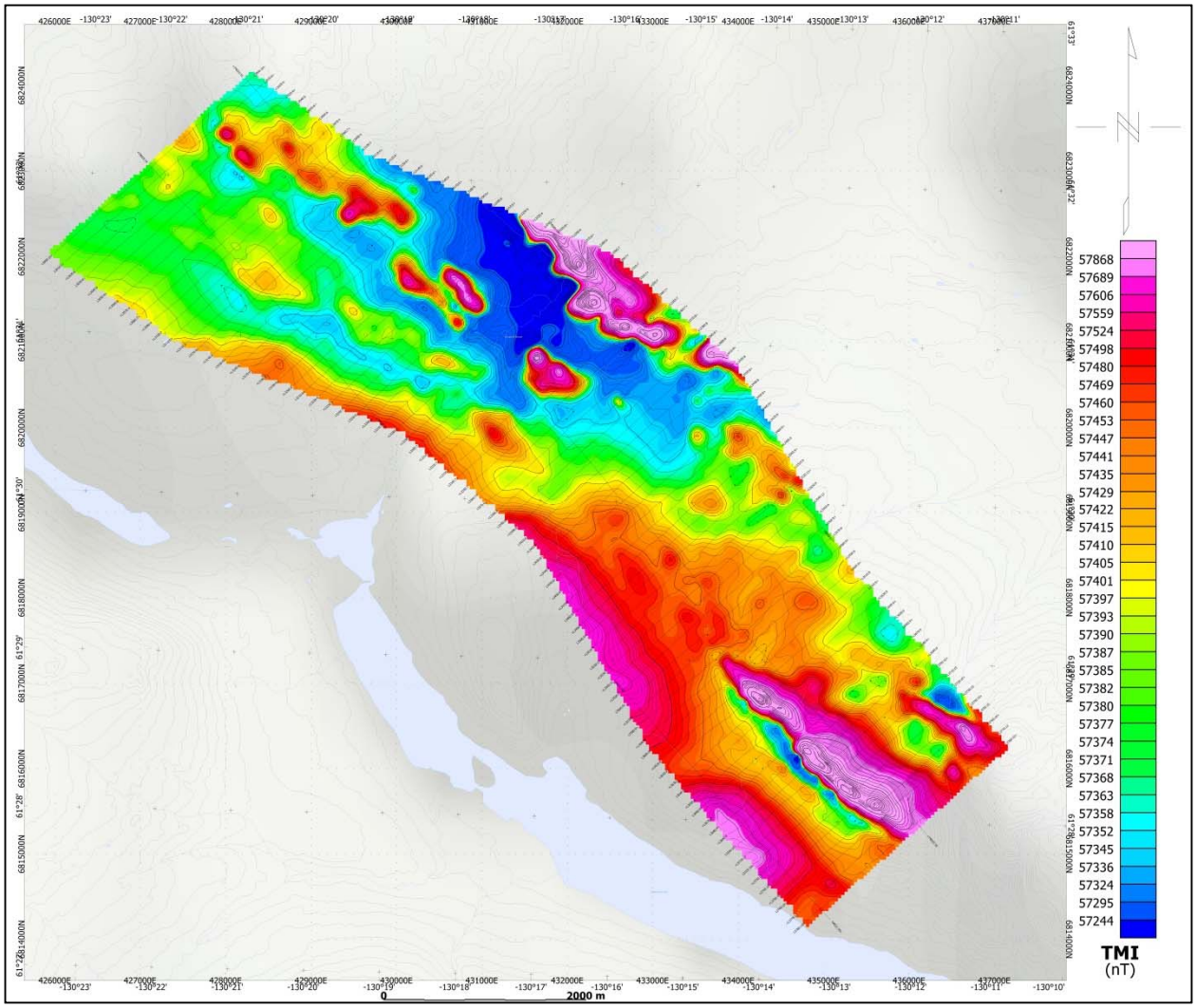

Pelly - Total Magnetic Intensity (TMI)

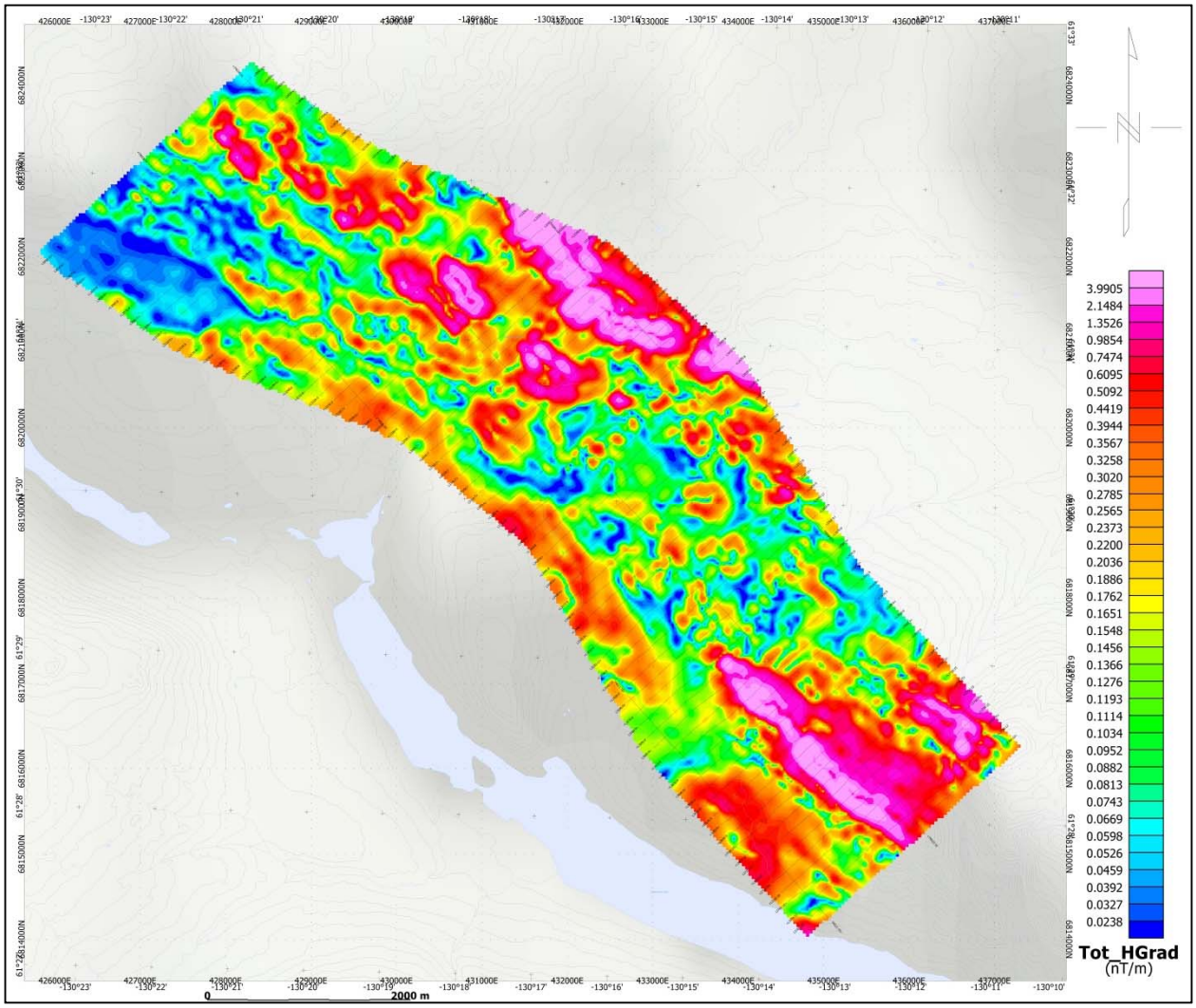

Pelly - Magnetic Total Horizontal Gradient

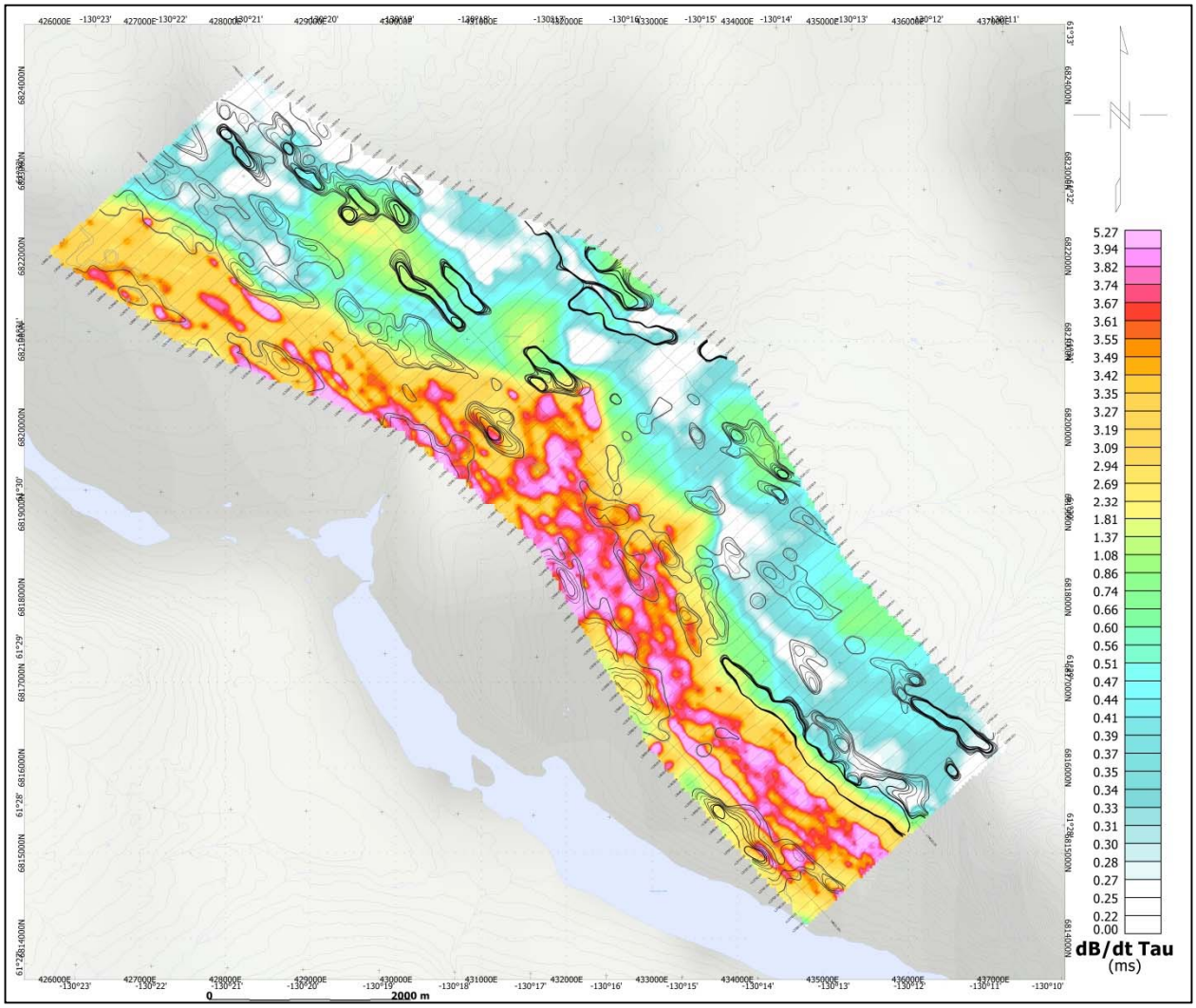

Pelly - dB/dt Calculated Time Constant (Tau) with Calculated Vertical Derivative contours

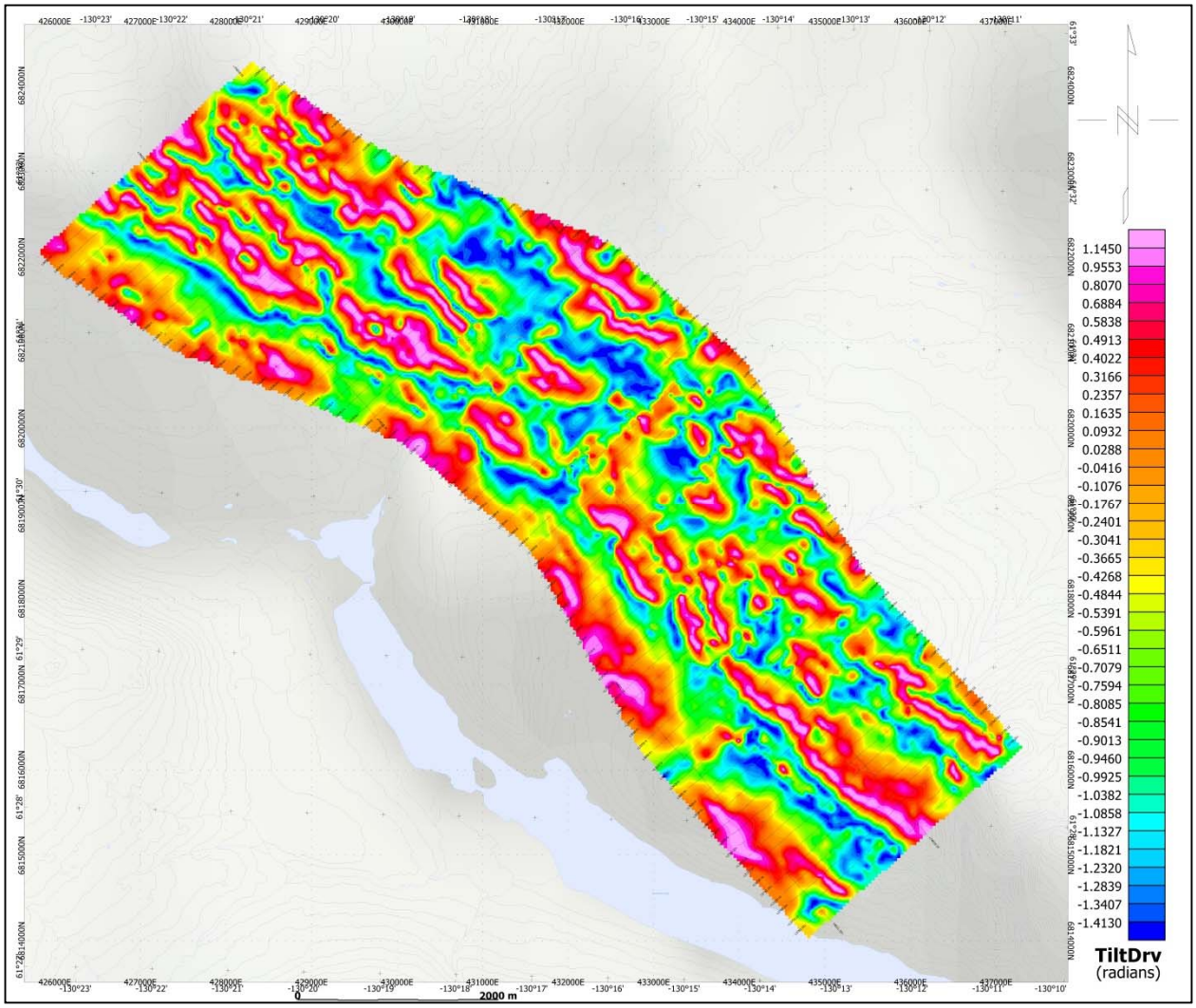

Pelly - Magnetic Tilt - Angle Derivative

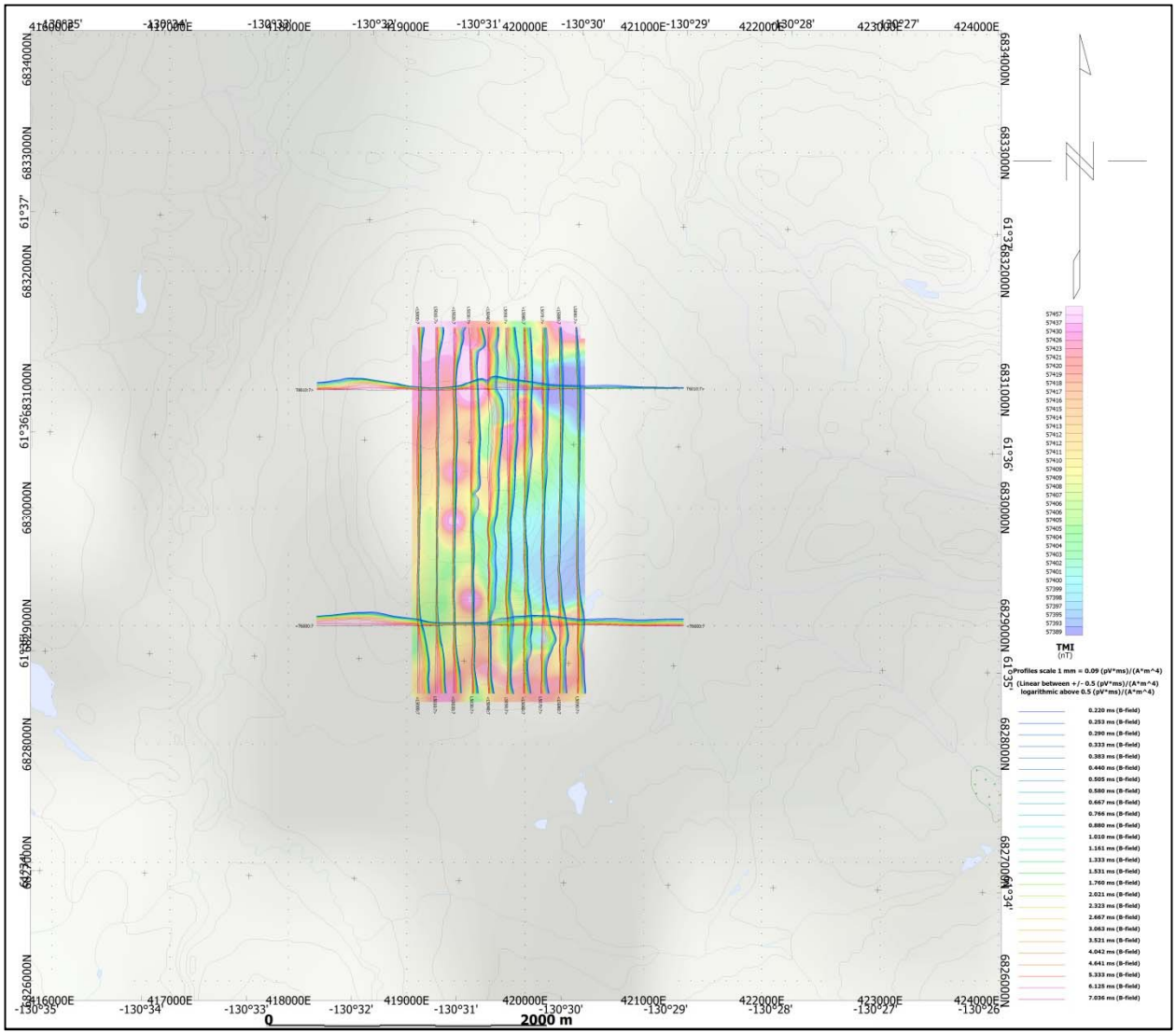

Limy - VTEM B-Field Z Component Profiles, Time Gates 0.220 to 7.036 ms

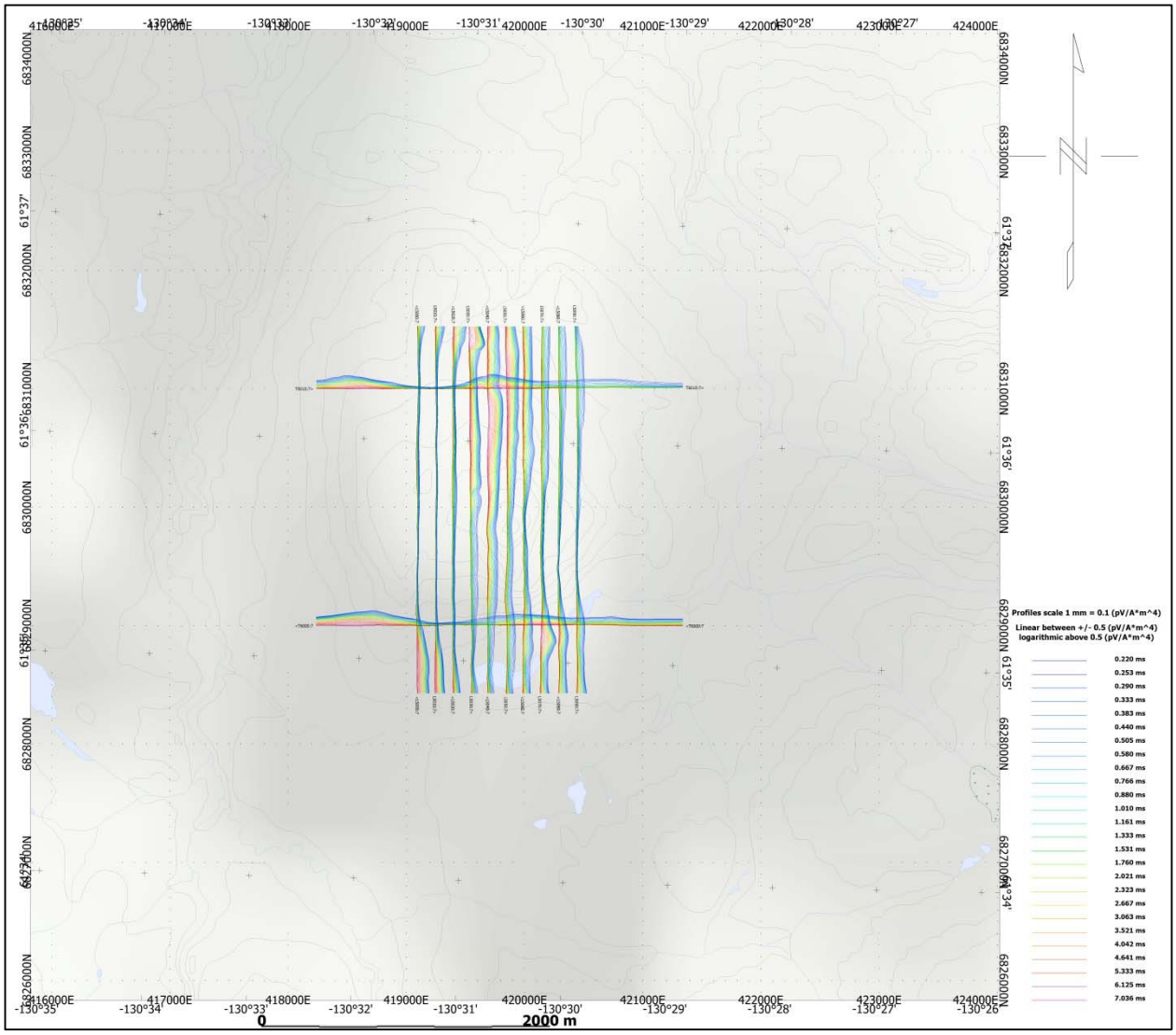

Limy - VTEM dB/dt Z Component Profiles, Time Gates 0.220 to 7.036 ms

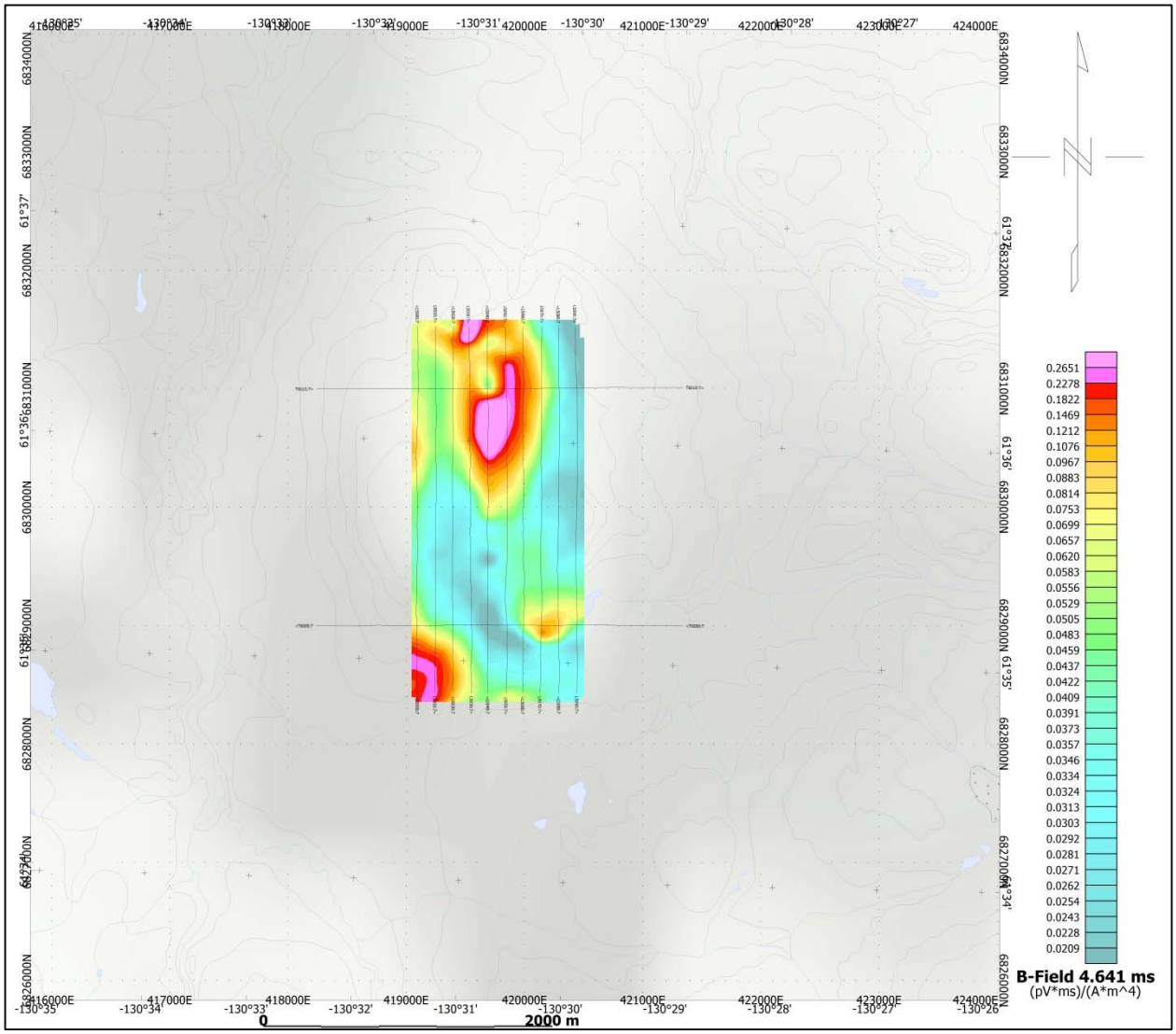

Limy - VTEM B-Field Z Component Channel 42, Time Gate 4.641 ms

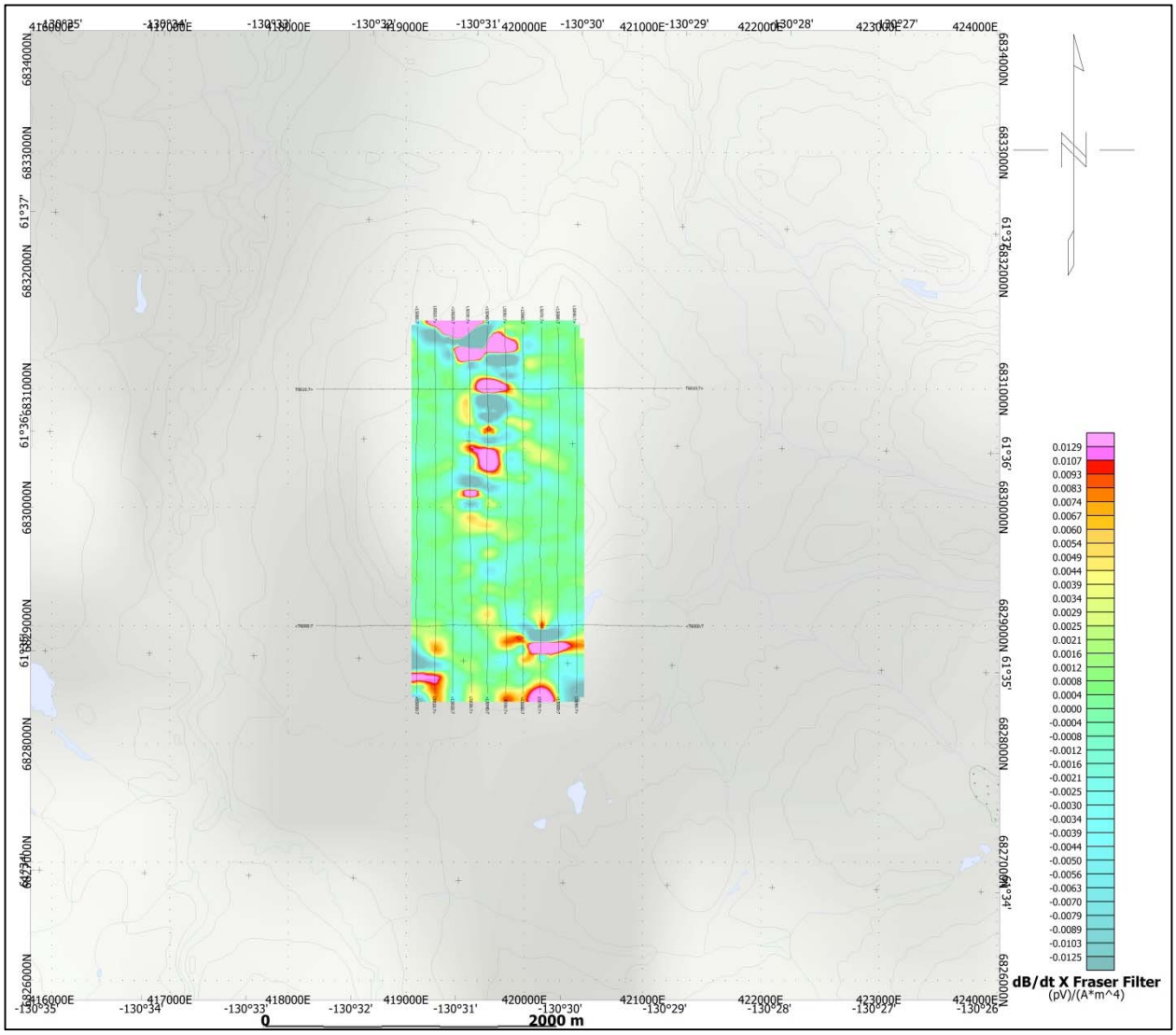

Limy - VTEM dB/dt X Component Fraser Filtered Channel 30, Time Gate 0.880 ms

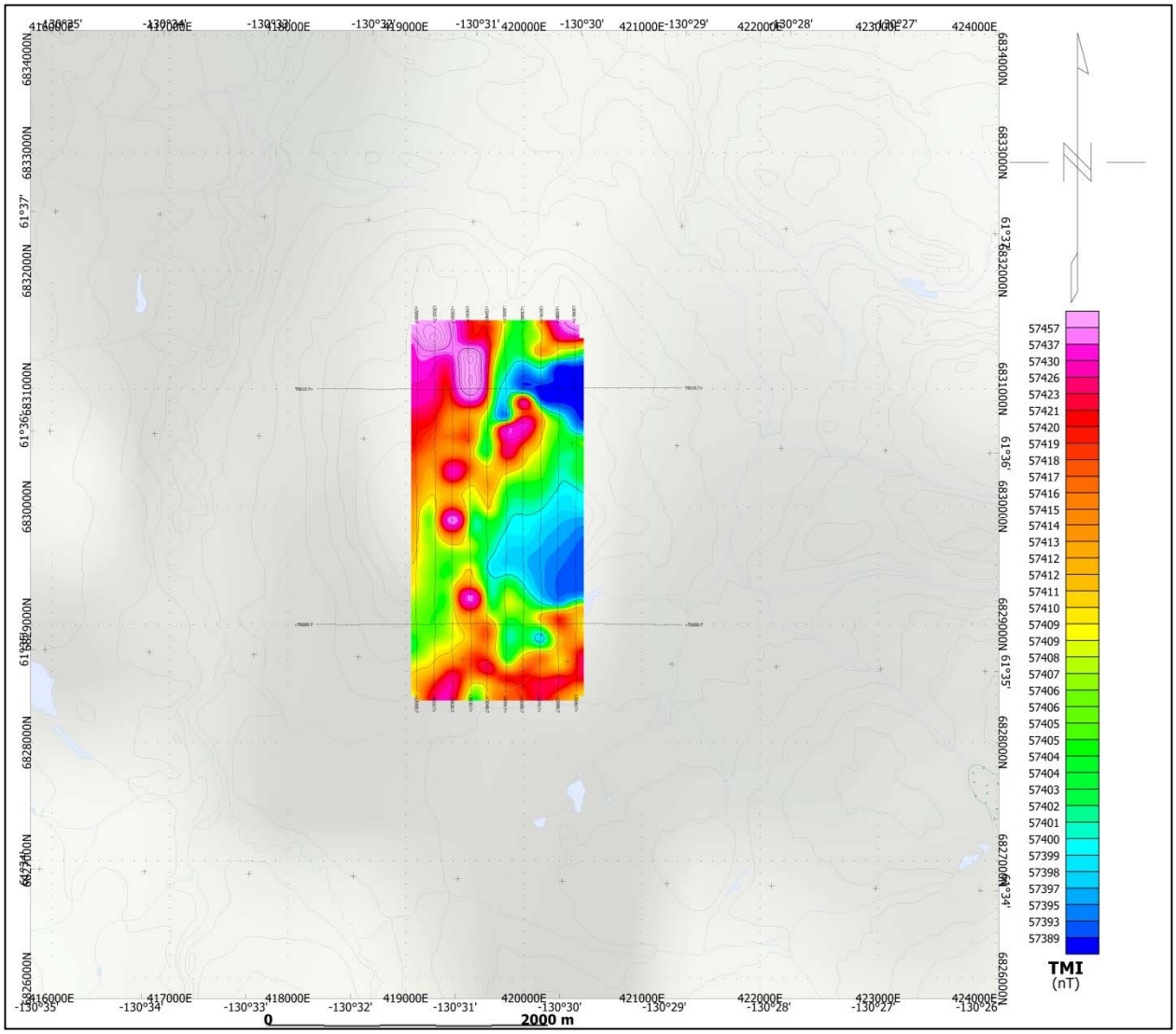

Limy - Total Magnetic Intensity (TMI)

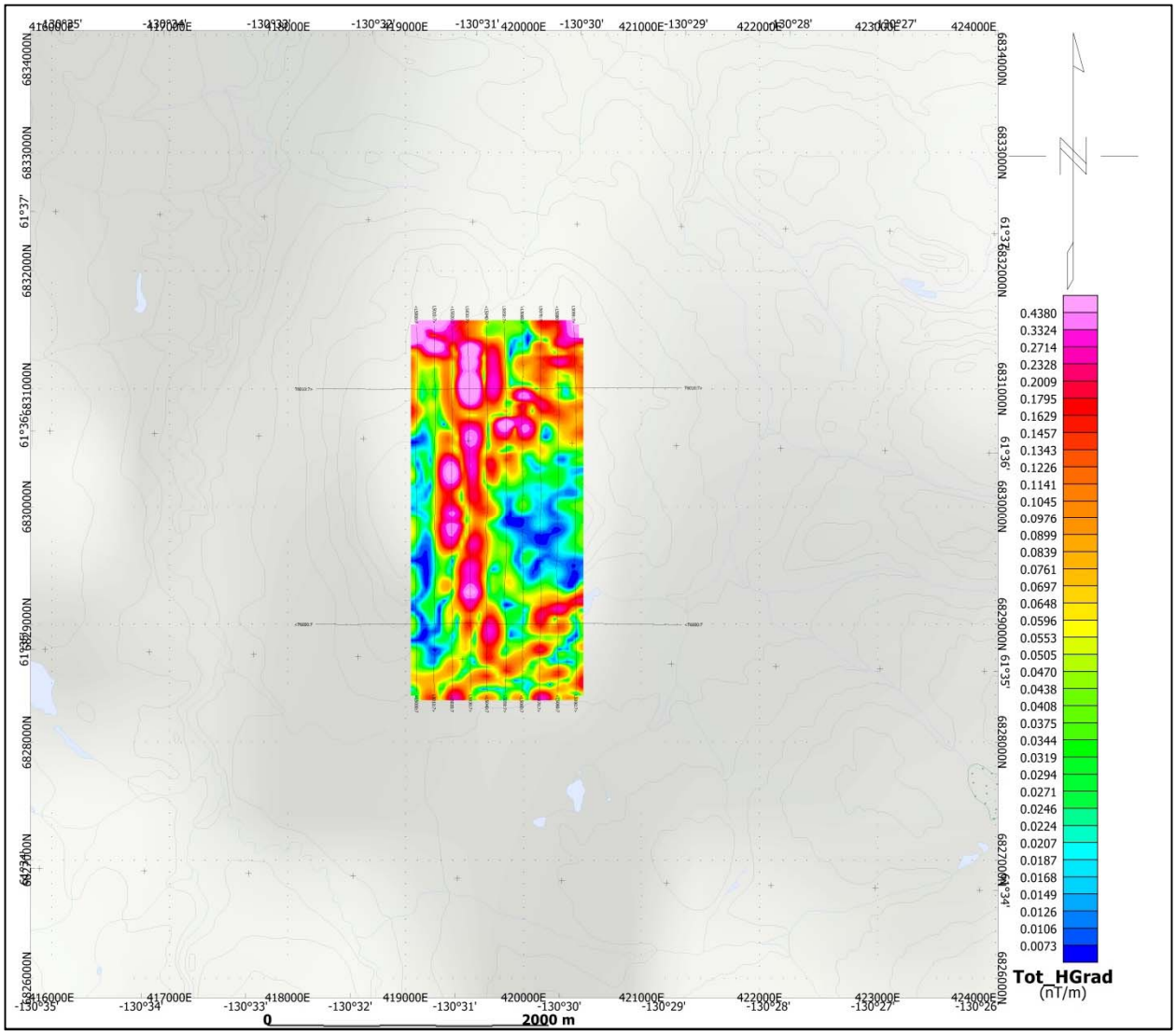

Limy - Magnetic Total Horizontal Gradient

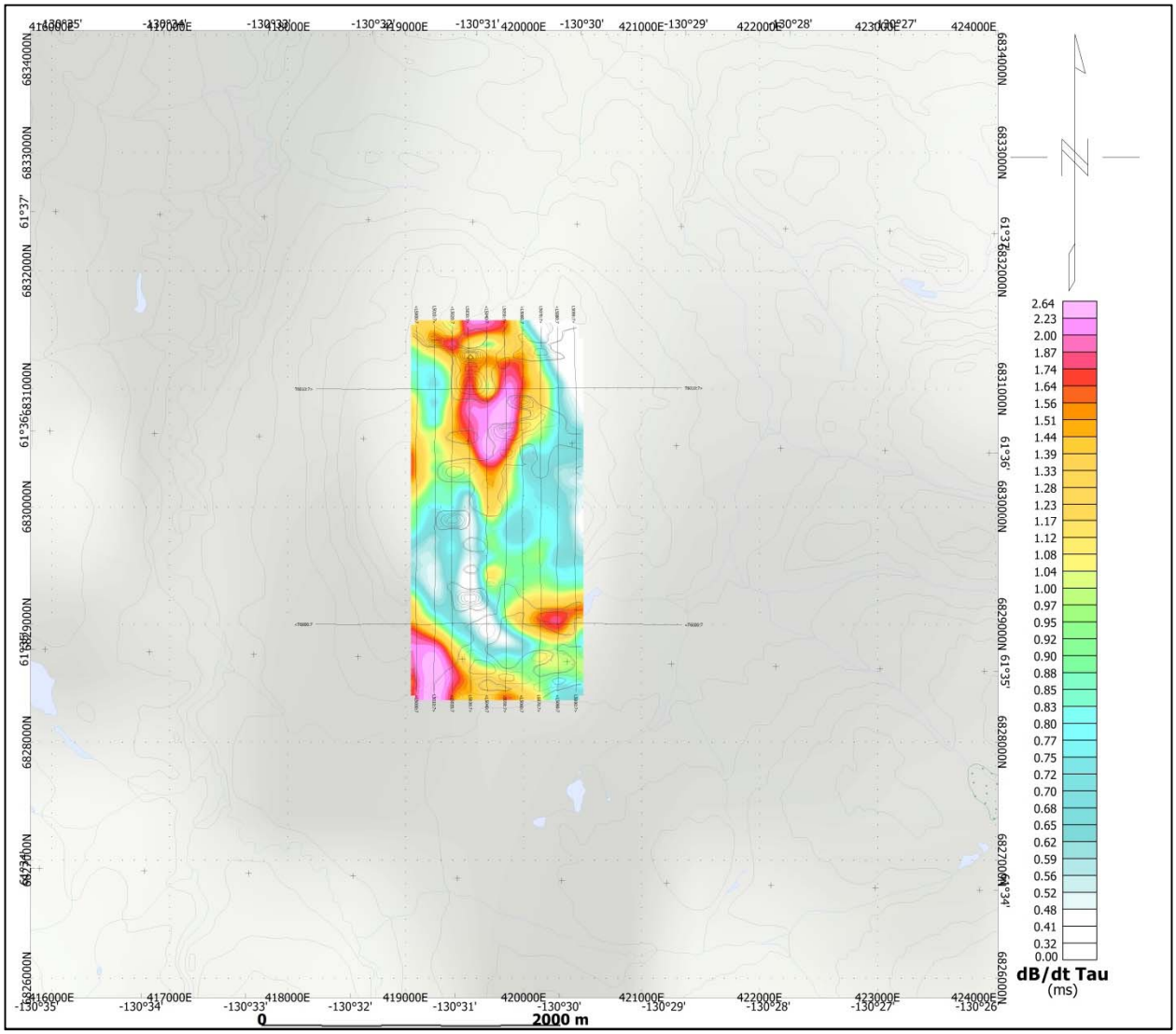

Limy - dB/dt Calculated Time Constant (Tau) with Calculated Vertical Derivative contours

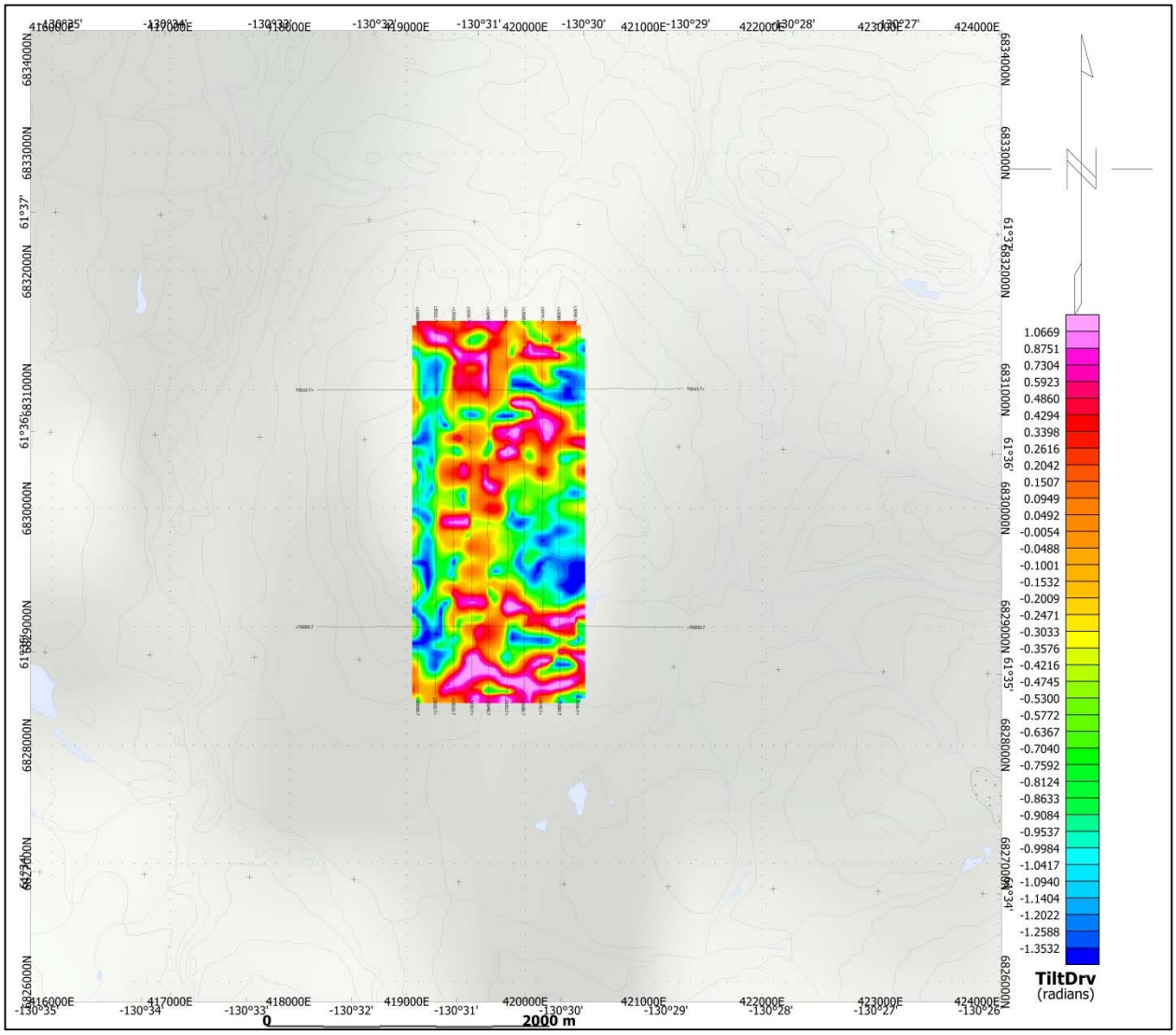

Limy - Magnetic Tilt - Angle Derivative

RESISTIVITY DEPTH IMAGE (RDI) MAPS

3D Resistivity-Depth Image (RDI)

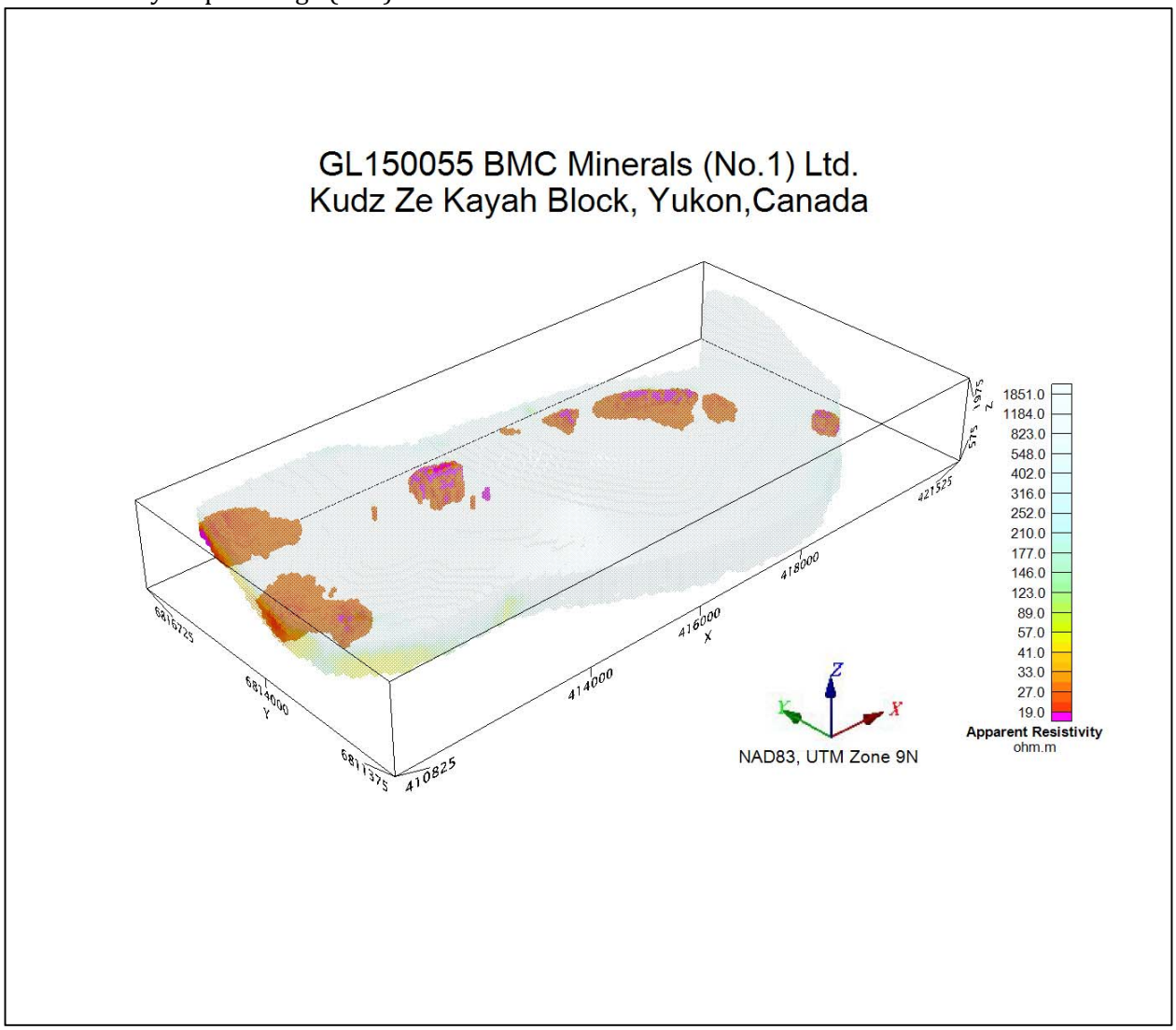

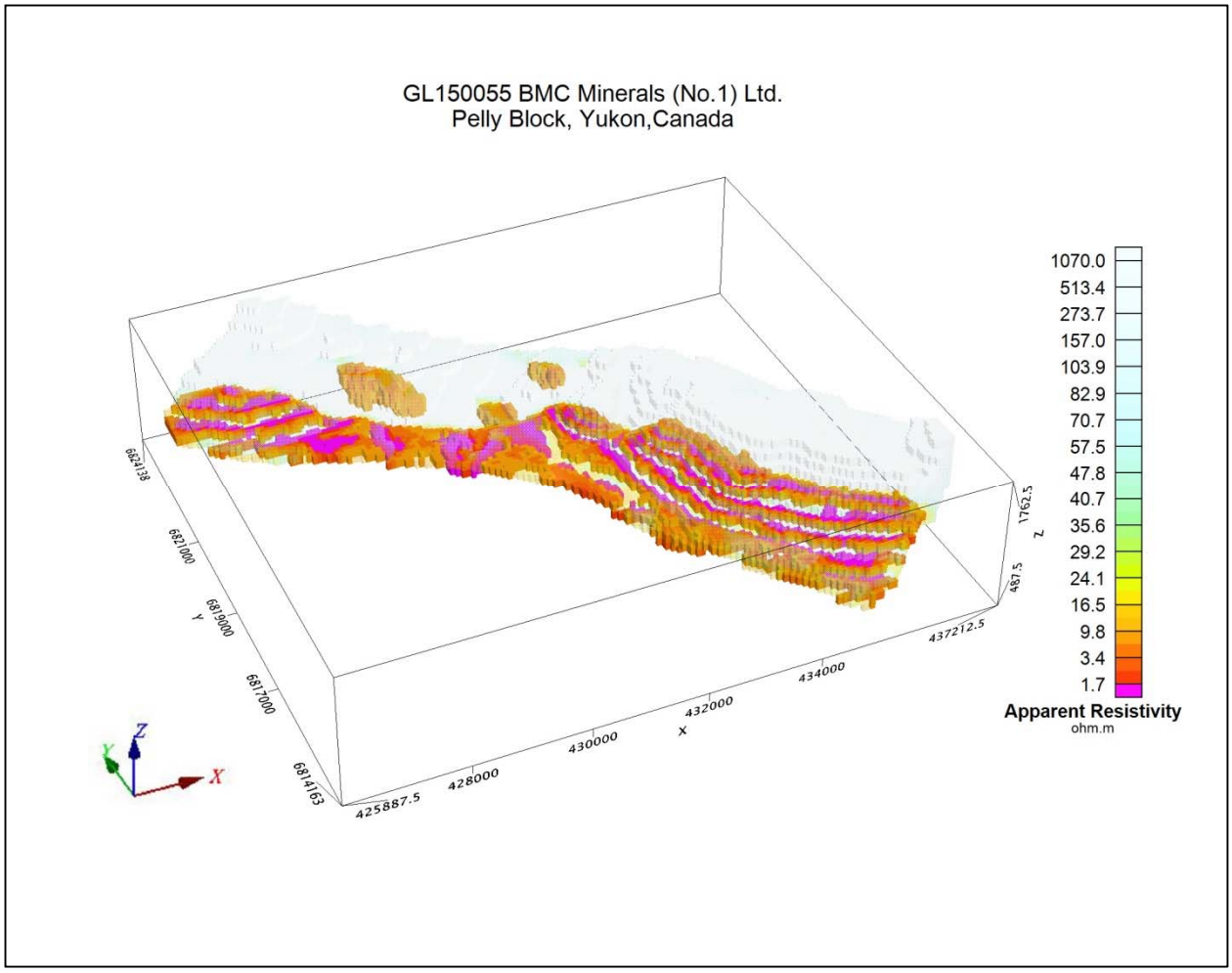
GL150055 BMC Minerals (No.1) Ltd.
Pelly Block, Yukon,Canada
1070.0
513.4
273.7
157.0
103.9
82.9
70.7
57.5
47.8
40.7
35.6
29.2
24.1
16.5
9.8
3.4
1.7
Apparent Resistivity
ohm.m
6824138
6821000
6819000
6817000
6814163
Y
425887.5
428000
430000
432000
434000
437212.5
X
1762.5
487.5
Z
Z
Y
X

GL150055 BMC Minerals (No.1) Ltd.
VTEM_Limy_Block, Yukon,Canada

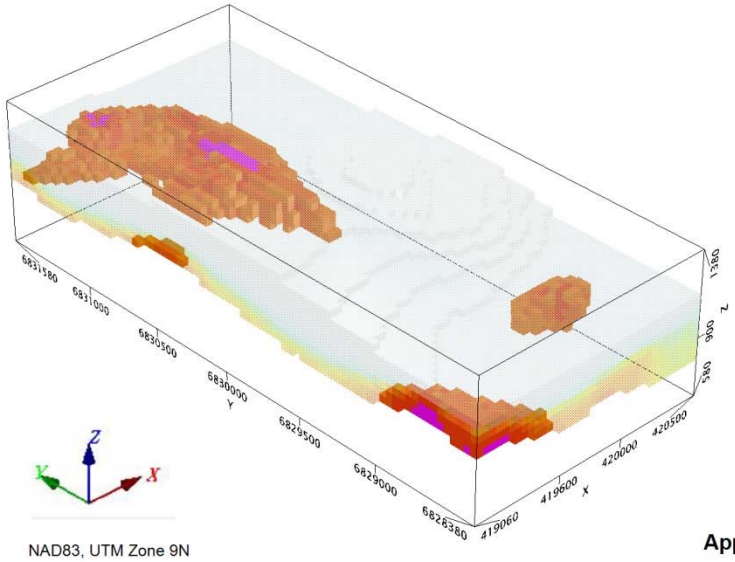

NAD83, UTM Zone 9N

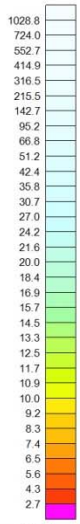

Apparent Resistivity
ohm.m

APPENDIX D

GENERALIZED MODELING RESULTS OF THE VTEM SYSTEM
INTRODUCTION

The VTEM system is based on a concentric or central loop design, whereby, the receiver is positioned at the centre of a transmitter loop that produces a primary field. The wave form is a bi-polar, modified square wave with a turn-on and turn-off at each end.

During turn-on and turn-off, a time varying field is produced (dB/dt) and an electro-motive force (emf) is created as a finite impulse response. A current ring around the transmitter loop moves outward and downward as time progresses. When conductive rocks and mineralization are encountered, a secondary field is created by mutual induction and measured by the receiver at the centre of the transmitter loop.

Efficient modeling of the results can be carried out on regularly shaped geometries, thus yielding close approximations to the parameters of the measured targets. The following is a description of a series of common models made for the purpose of promoting a general understanding of the measured results.

A set of models has been produced for the Geotech VTEM® system dB/dT Z and X components (see models D1 to D15). The Maxwell ™ modeling program (EMIT Technology Pty. Ltd. Midland, WA, AU) used to generate the following responses assumes a resistive half-space. The reader is encouraged to review these models, so as to get a general understanding of the responses as they apply to survey results. While these models do not begin to cover all possibilities, they give a general perspective on the simple and most commonly encountered anomalies.

As the plate dips and departs from the vertical position, the peaks become asymmetrical.

As the dip increases, the aspect ratio (Min/Max) decreases and this aspect ratio can be used as an empirical guide to dip angles from near 90º to about 30º. The method is not sensitive enough where dips are less than about 30º.

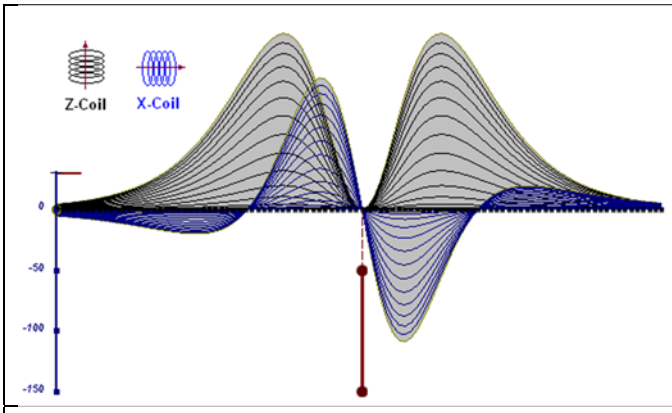

Figure D-1: vertical thin plate

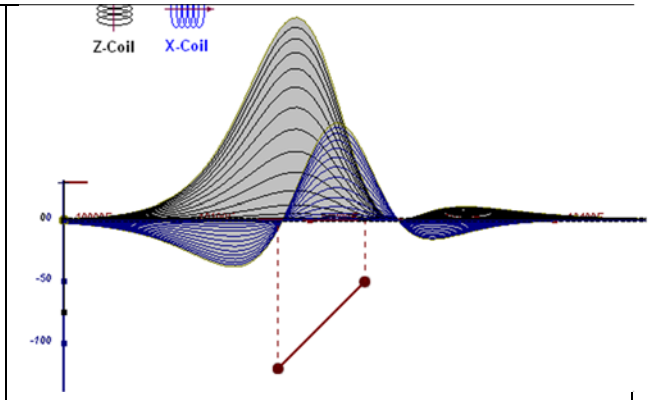

Figure D-2: inclined thin plate

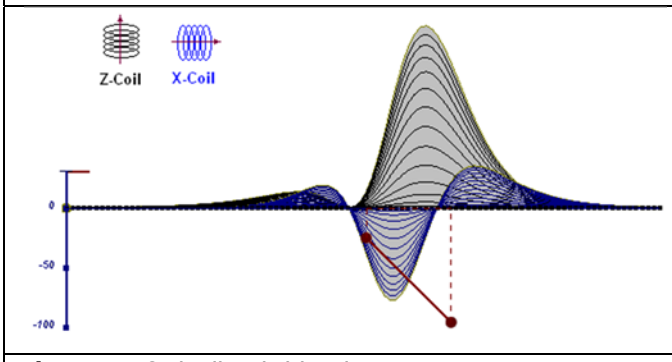

Figure D-3: inclined thin plate

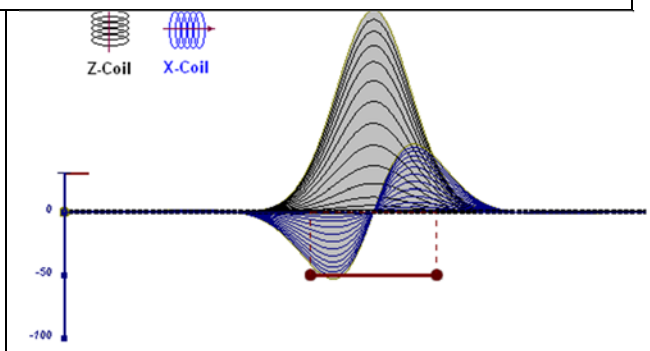

Figure D-4: horizontal thin plate

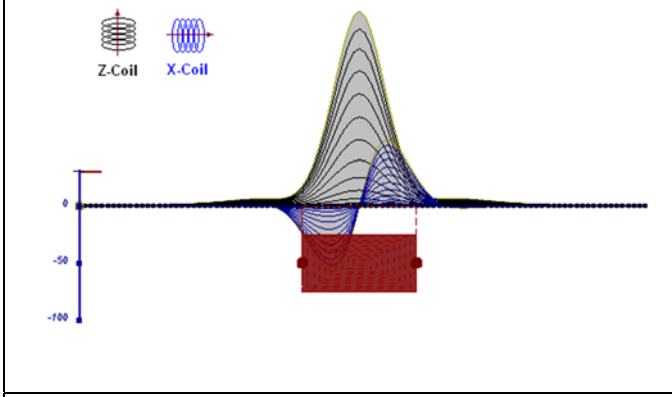

Figure D-5: horizontal thick plate (linear scale of the response)

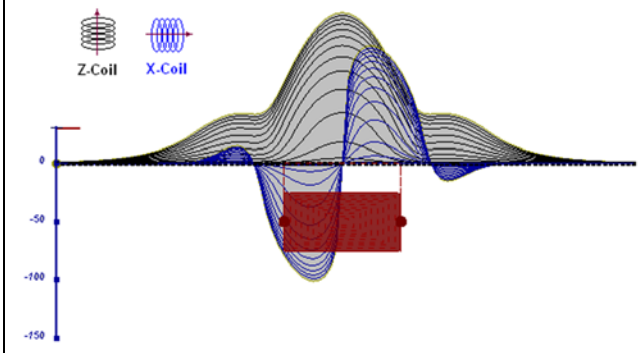

Figure D-6: horizontal thick plate (log scale of the response)

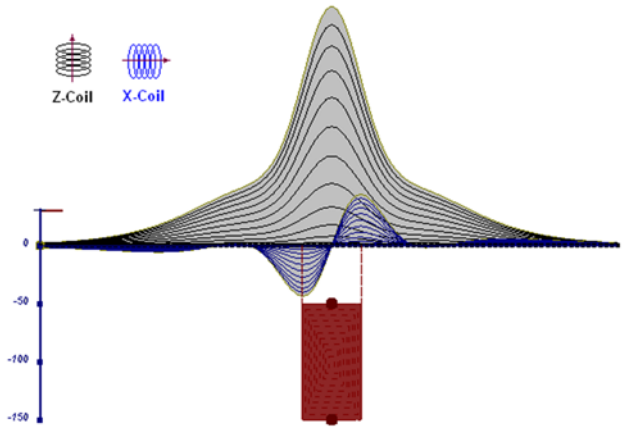

Figure D-7: vertical thick plate (linear scale of the response). 50 m depth

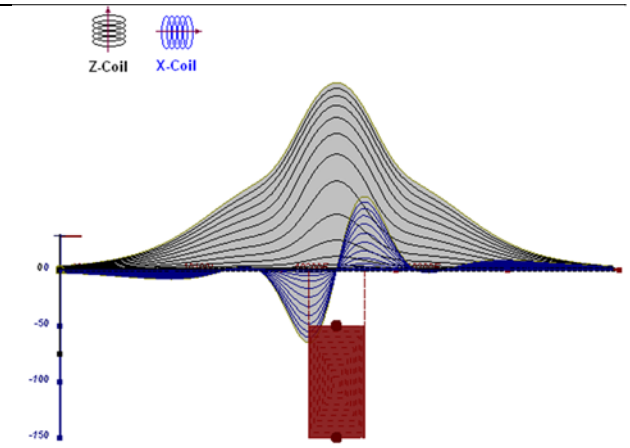

Figure D-8: vertical thick plate (log scale of the response). 50 m depth

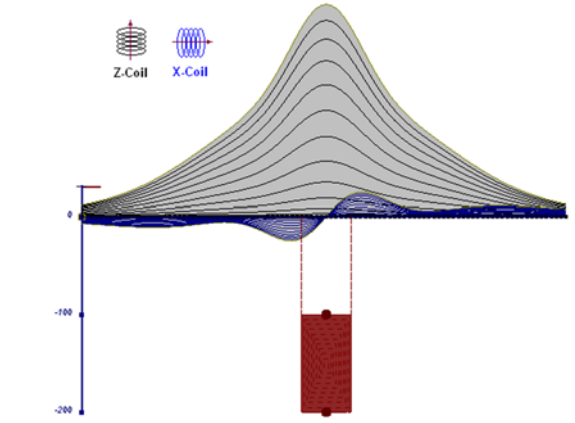

Figure D-9: vertical thick plate (linear scale of the response). 100 m depth

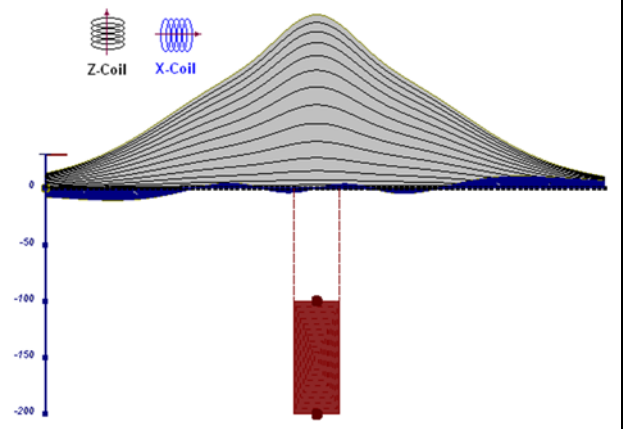

Figure D-10: vertical thick plate (linear scale of the response). Depth / horizontal thickness=2.5

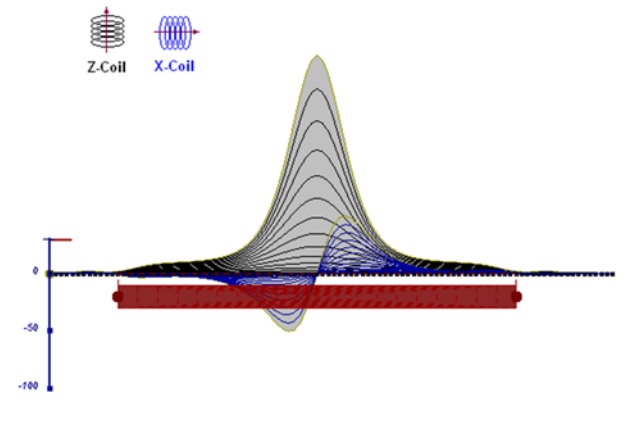

Figure D-11: horizontal thick plate (linear scale of the response)

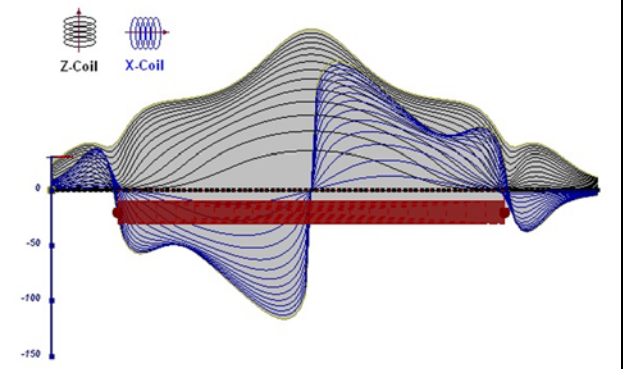

Figure D-12: horizontal thick plate (log scale of the response)

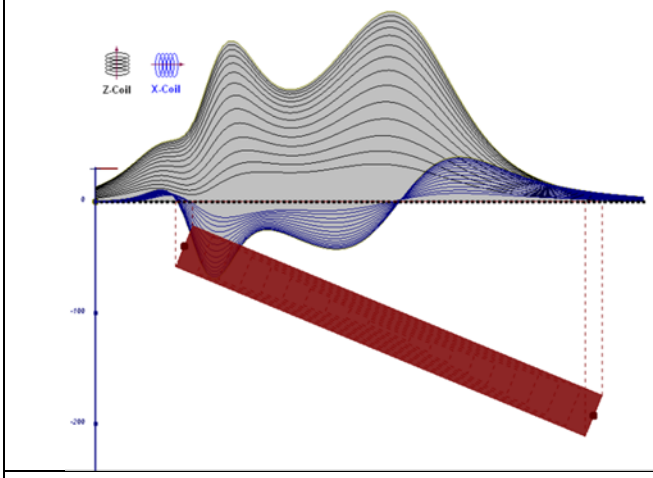

Figure D-13: inclined long thick plate

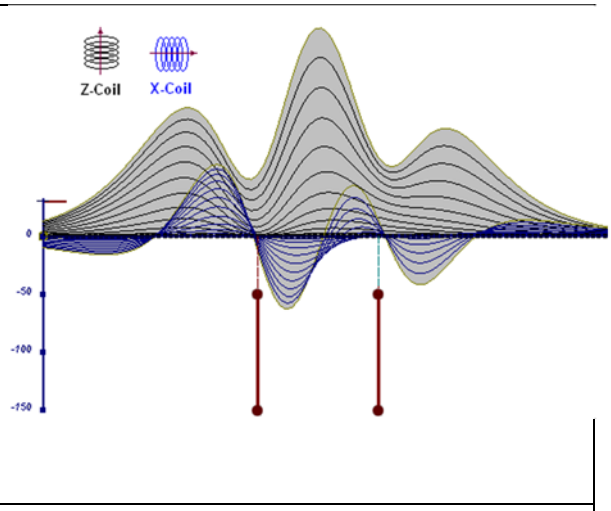

Figure D-14: two vertical thin plates

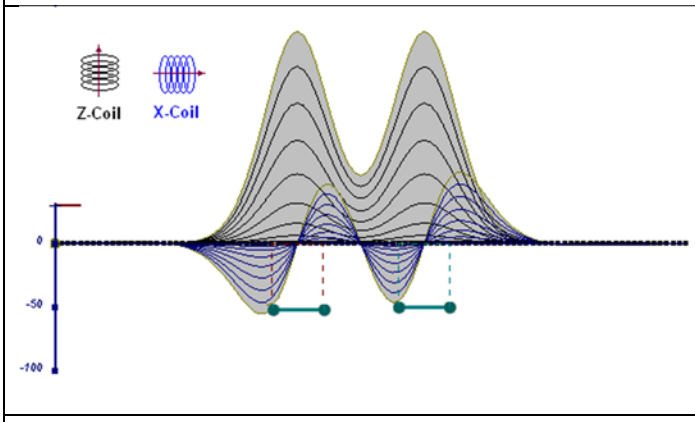

Figure D-15: two horizontal thin plates

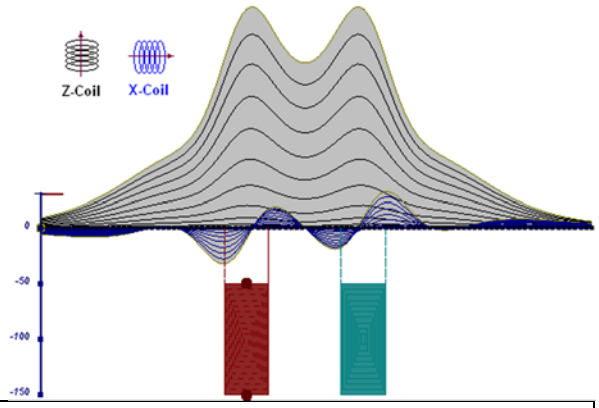

Figure D-16: two vertical thick plates

The same type of target but with different thickness, for example, creates different form of the response:

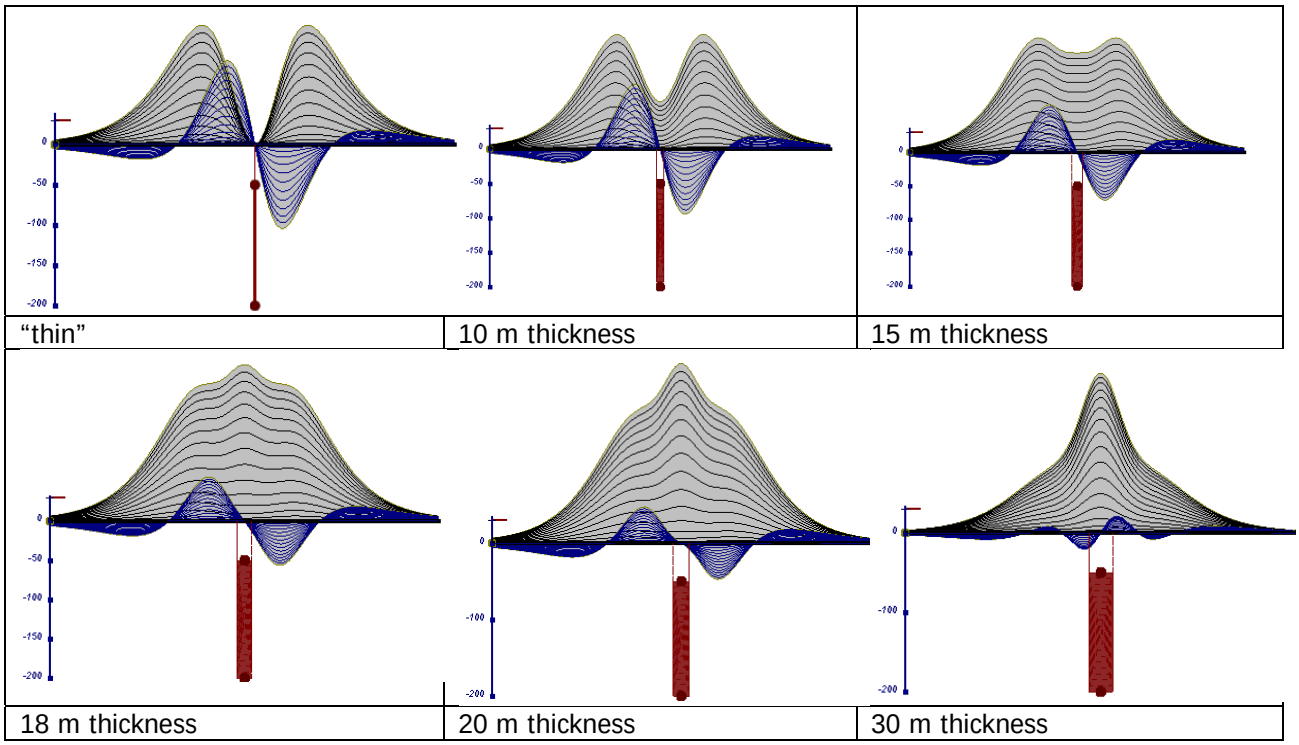

Figure D-17: Conductive vertical plate, depth 50 m, strike length 200 m, depth extends 150 m.

Alexander Prikhodko, PhD, P.Geo
Geotech Ltd.

September 2010

APPENDIX E

EM TIME CONSTANT (TAU) ANALYSIS

Estimation of time constant parameter[1] in transient electromagnetic method is one of the steps toward the extraction of the information about conductances beneath the surface from TEM measurements.

The most reliable method to discriminate or rank conductors from overburden, background or one and other is by calculating the EM field decay time constant (TAU parameter), which directly depends on conductance despite their depth and accordingly amplitude of the response.

THEORY

As established in electromagnetic theory, the magnitude of the electro-motive force (emf) induced is proportional to the time rate of change of primary magnetic field at the conductor. This emf causes eddy currents to flow in the conductor with a characteristic transient decay, whose Time Constant (Tau) is a function of the conductance of the survey target or conductivity and geometry (including dimensions) of the target. The decaying currents generate a proportional secondary magnetic field, the time rate of change of which is measured by the receiver coil as induced voltage during the Off time.

The receiver coil output voltage ($\mathbf{e_0}$) is proportional to the time rate of change of the secondary magnetic field and has the form,

$$e_0 \, \alpha \, (1 / \tau) \, e^{-(t/\tau)}$$

Where,
τ = L/R is the characteristic time constant of the target (TAU)
R = resistance
L = inductance

From the expression, conductive targets that have small value of resistance and hence large value of τ yield signals with small initial amplitude that decays relatively slowly with progress of time. Conversely, signals from poorly conducting targets that have large resistance value and smallτ, have high initial amplitude but decay rapidly with time[1] (Fig. E1).

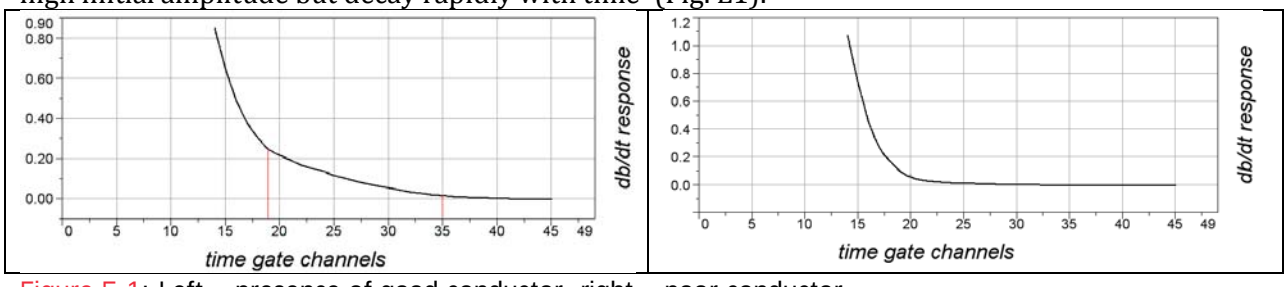

Figure E-1: Left – presence of good conductor, right – poor conductor.

[1] McNeill, JD, 1980, "Applications of Transient Electromagnetic Techniques", Technical Note TN-7 page 5, Geonics Limited, Mississauga, Ontario.

EM Time Constant (Tau) Calculation

The EM Time-Constant (TAU) is a general measure of the speed of decay of the electromagnetic response and indicates the presence of eddy currents in conductive sources as well as reflecting the "conductance quality" of a source. Although TAU can be calculated using either the measured dB/dt decay or the calculated B-field decay, dB/dt is commonly preferred due to better stability (S/N) relating to signal noise. Generally, TAU calculated on base of early time response reflects both near surface overburden and poor conductors whereas, in the late ranges of time, deep and more conductive sources, respectively. For example early time TAU distribution in an area that indicates conductive overburden is shown in Figure 2.

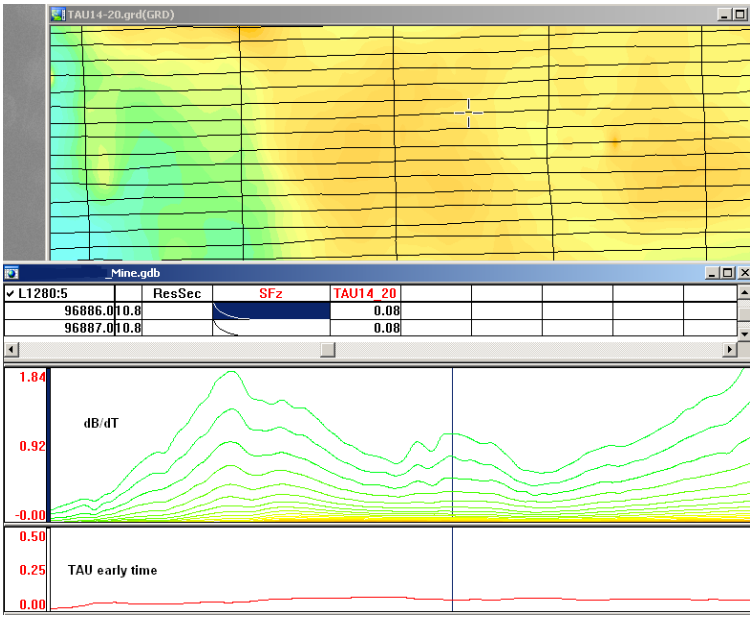

Figure E-2: Map of early time TAU. Area with overburden conductive layer and local sources.

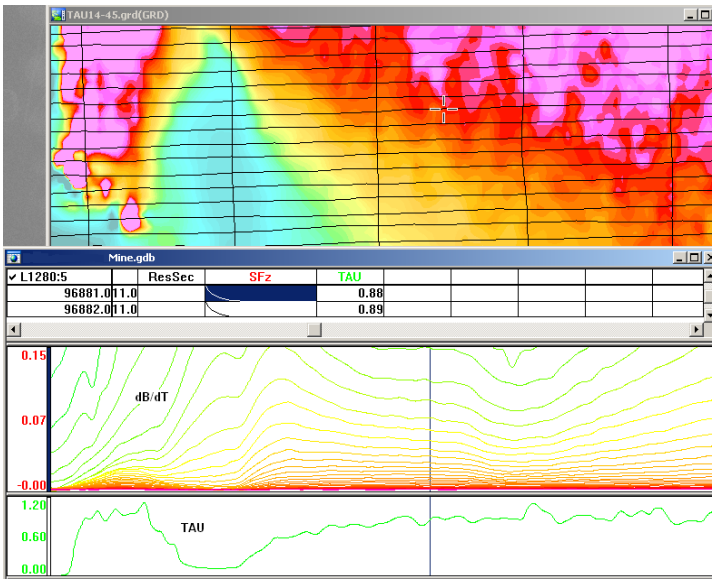

Figure E-3: Map of full time range TAU with EM anomaly due to deep highly conductive target.

There are many advantages of TAU maps:

- TAU depends only on one parameter (conductance) in contrast to response magnitude;
- TAU is integral parameter, which covers time range and all conductive zones and targets are displayed independently of their depth and conductivity on a single map.
- Very good differential resolution in complex conductive places with many sources with different conductivity.
- Signs of the presence of good conductive targets are amplified and emphasized independently of their depth and level of response accordingly.

In the example shown in Figure 4 and 5, three local targets are defined, each of them with a different depth of burial, as indicated on the resistivity depth image (RDI). All are very good conductors but the deeper target (number 2) has a relatively weak dB/dt signal yet also features the strongest total TAU (Figure 4). This example highlights the benefit of TAU analysis in terms of an additional target discrimination tool.

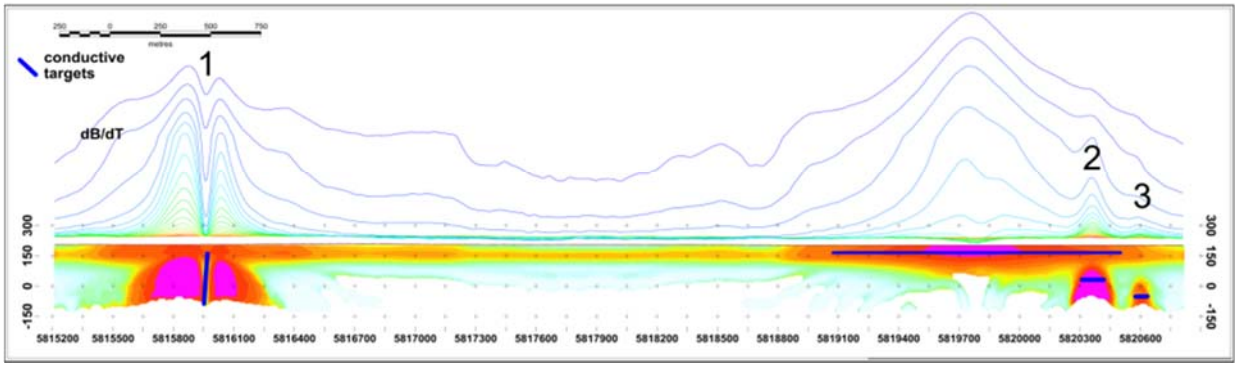

Figure E-4: dB/dt profile and RDI with different depths of targets.

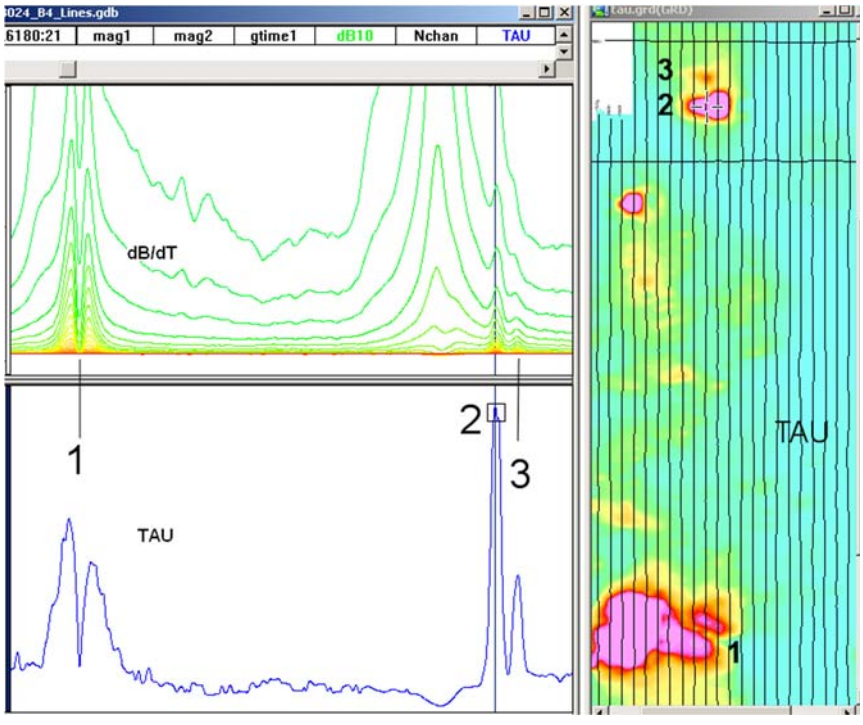

Figure E-5: Map of total TAU and dB/dt profile.

The EM Time Constants for dB/dt and B-field were calculated using the "sliding Tau" in-house program developed at Geotech2. The principle of the calculation is based on using of time window (4 time channels) which is sliding along the curve decay and looking for latest time channels which have a response above the level of noise and decay. The EM decays are obtained from all available decay channels, starting at the latest channel. Time constants are taken from a least square fit of a straight-line (log/linear space) over the last 4 gates above a pre-set signal threshold level (Figure F6). Threshold settings are pointed in the "label" property of TAU database channels. The sliding Tau method determines that, as the amplitudes increase, the time-constant is taken at progressively later times in the EM decay. Conversely, as the amplitudes decrease, Tau is taken at progressively earlier times in the decay. If the maximum signal amplitude falls below the threshold, or becomes negative for any of the 4 time gates, then Tau is not calculated and is assigned a value of "dummy" by default.

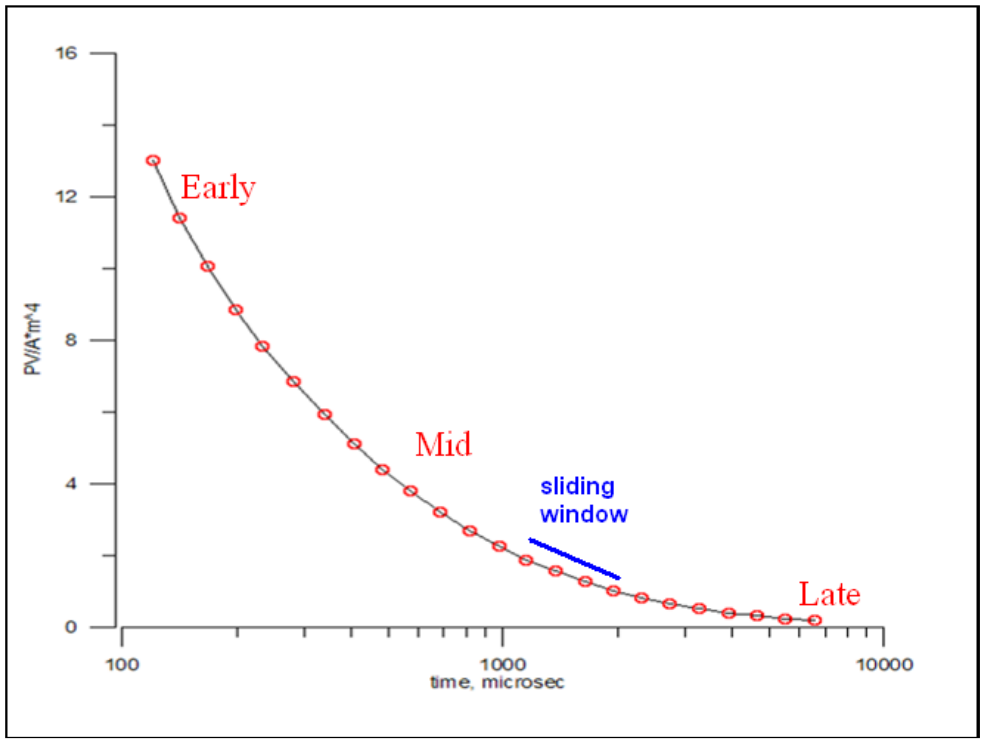

Figure E-6: Typical dB/dt decays of Vtem data

Alexander Prikhodko, PhD, P.Geo
Geotech Ltd.

September 2010

[2] by A.Prikhodko

APPENDIX F

TEM RESISTIVITY DEPTH IMAGING (RDI)

Resistivity depth imaging (RDI) is technique used to rapidly convert EM profile decay data into an equivalent resistivity versus depth cross-section, by deconvolving the measured TEM data.
The used RDI algorithm of Resistivity-Depth transformation is based on scheme of the apparent resistivity transform of Maxwell A.Meju (1998)[1] and TEM response from conductive half-space. The program is developed by Alexander Prikhodko and depth calibrated based on forward plate modeling for VTEM system configuration (Fig. 1-10).

RDIs provide reasonable indications of conductor relative depth and vertical extent, as well as accurate 1D layered-earth apparent conductivity/resistivity structure across VTEM flight lines. Approximate depth of investigation of a TEM system, image of secondary field distribution in half space, effective resistivity, initial geometry and position of conductive targets is the information obtained on base of the RDIs.

Maxwell forward modeling with RDI sections from the synthetic responses (VTEM system).

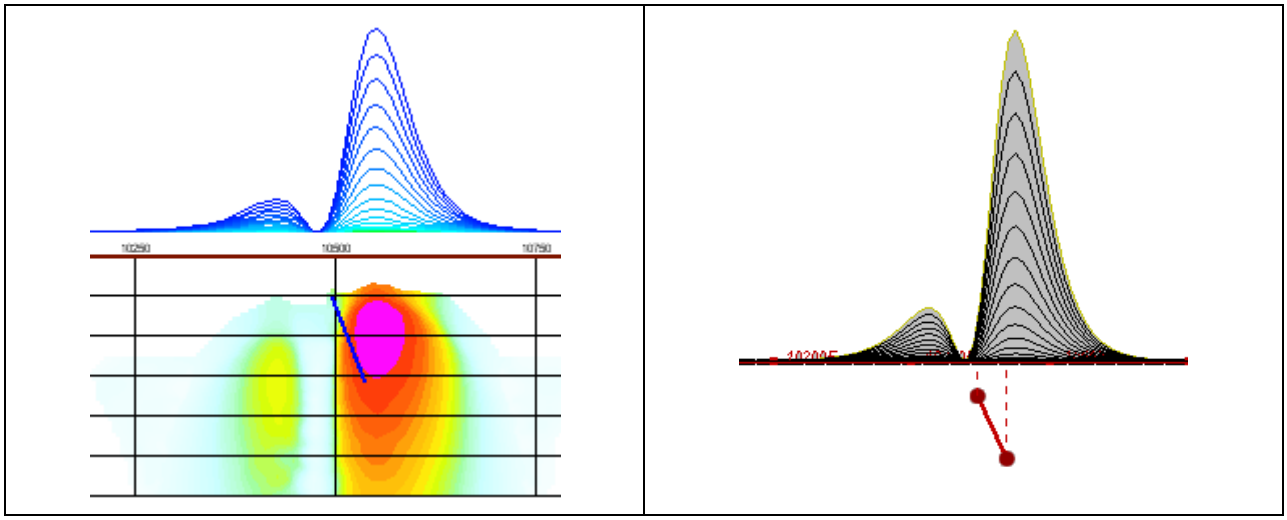

Figure F-1: Maxwell plate model and RDI from the calculated response for conductive “thin” plate (depth 50 m, dip 65 degree, depth extend 100 m).

[1] Maxwell A.Meju, 1998, Short Note: A simple method of transient electromagnetic data analysis, Geophysics, **63**, 405–410.

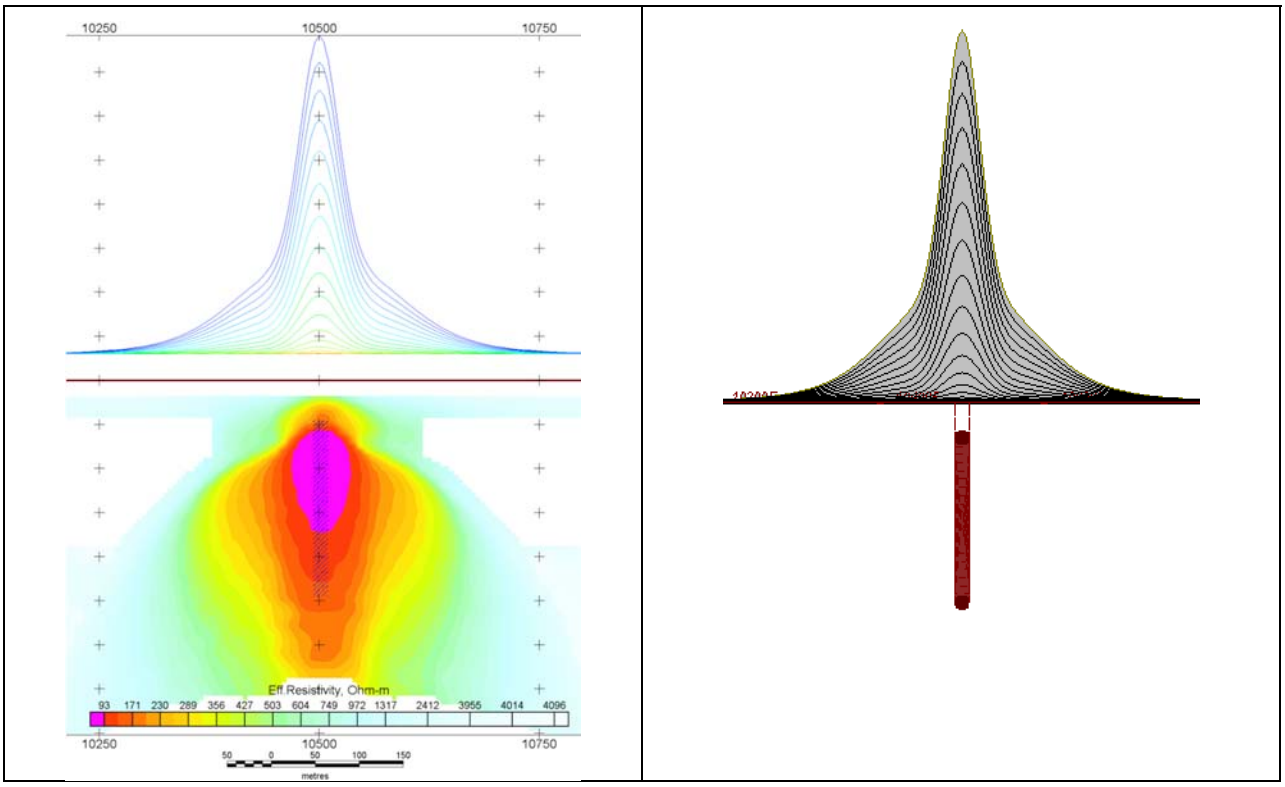

Figure F-2: Maxwell plate model and RDI from the calculated response for “thick” plate 18 m thickness, depth 50 m, depth extend 200 m).

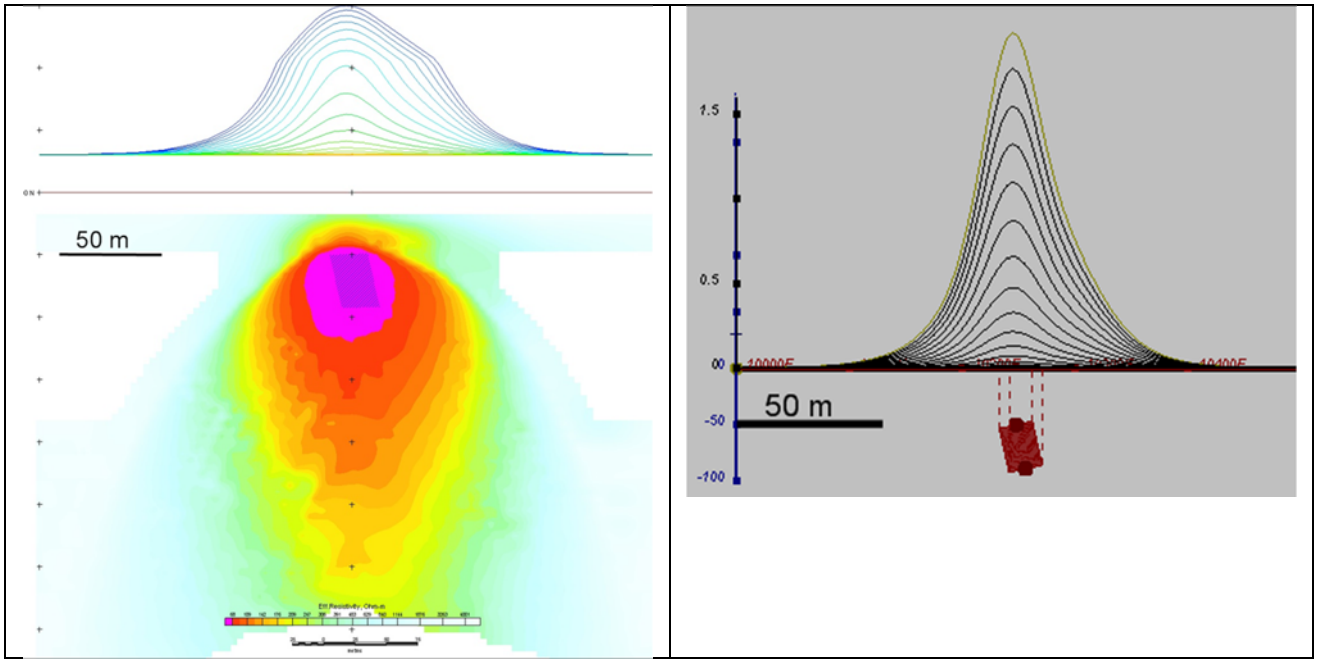

Figure F-3: Maxwell plate model and RDI from the calculated response for bulk (“thick”) 100 m length, 40 m depth extend, 30 m thickness

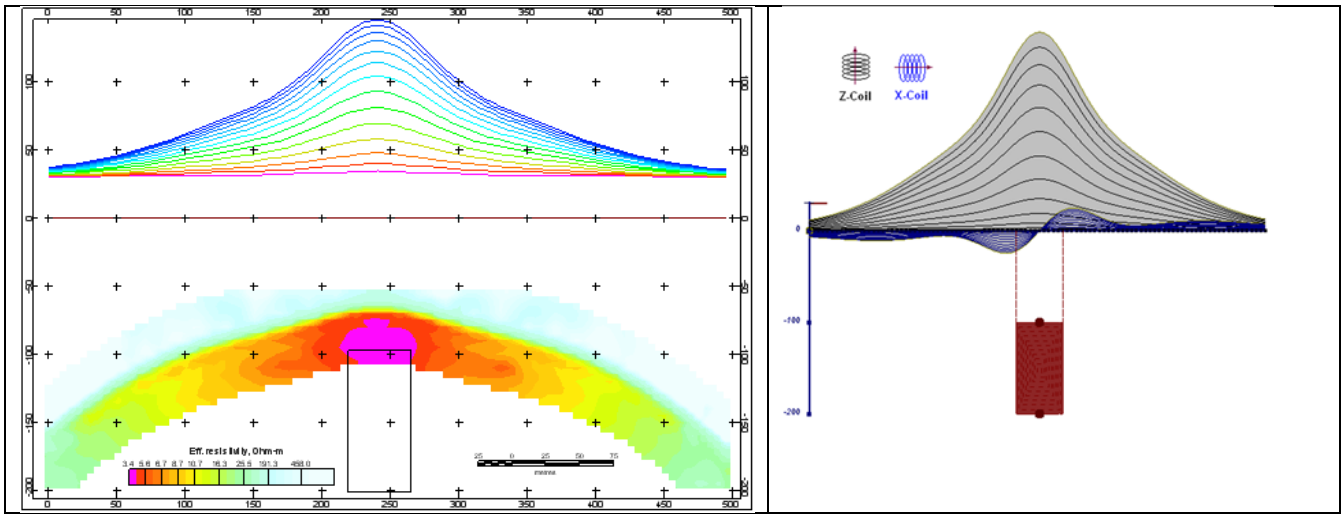

Figure F-4: Maxwell plate model and RDI from the calculated response for “thick” vertical target (depth 100 m, depth extend 100 m). 19-44 chan.

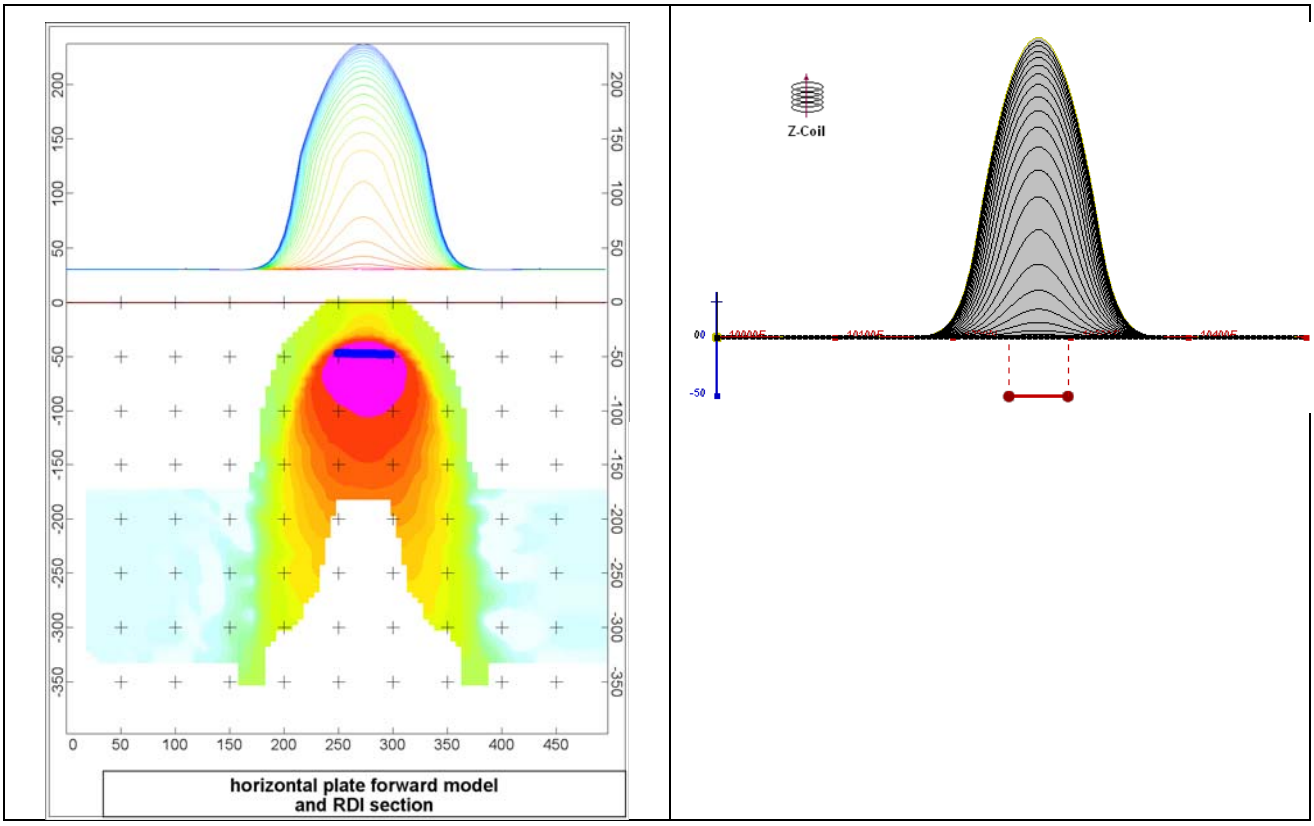

Figure F-5: Maxwell plate model and RDI from the calculated response for horizontal thin plate (depth 50 m, dim 50x100 m). 15-44 chan.

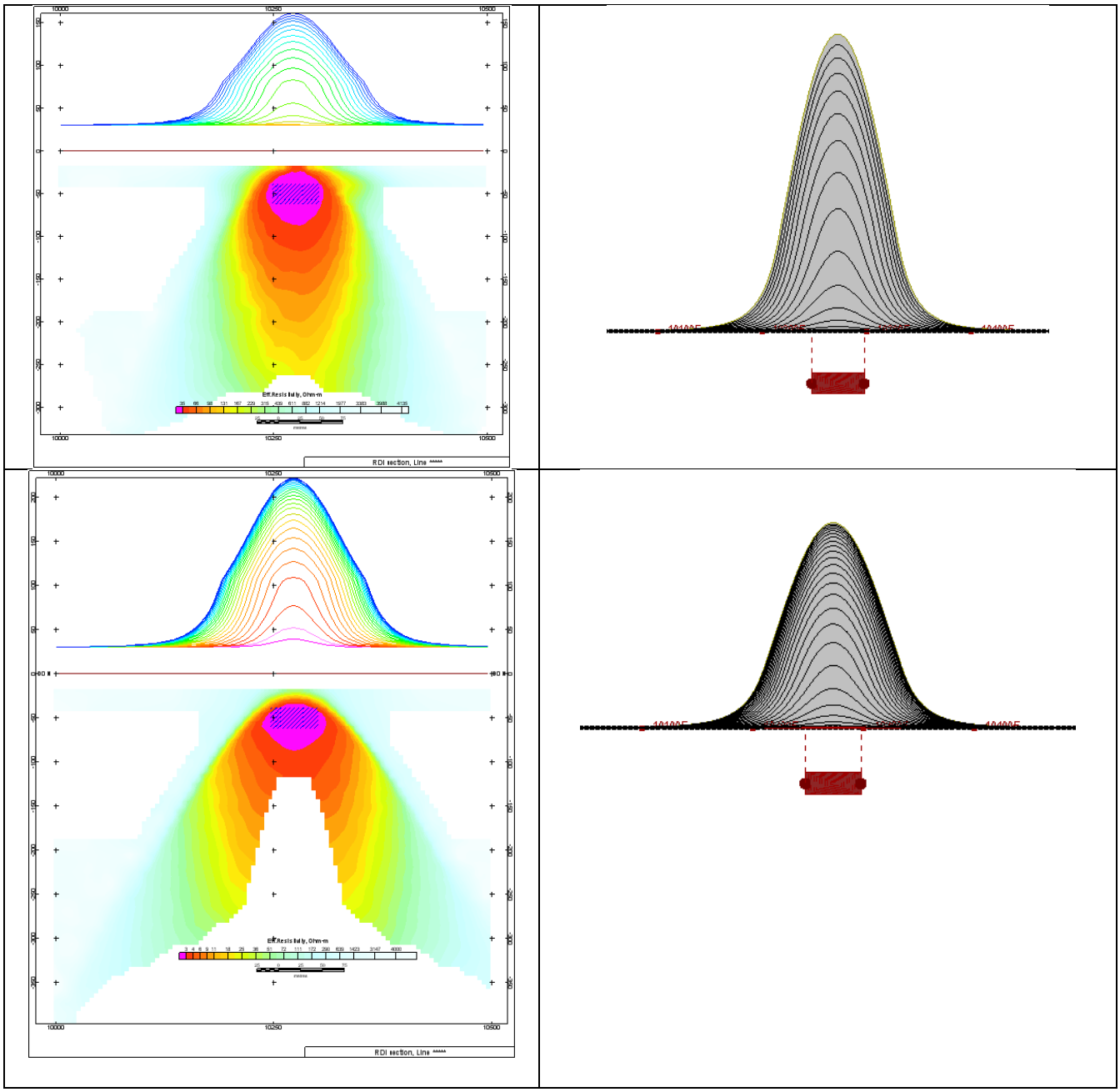

Figure F-6: Maxwell plate model and RDI from the calculated response for horizontal thick (20m) plate – less conductive (on the top), more conductive (below).

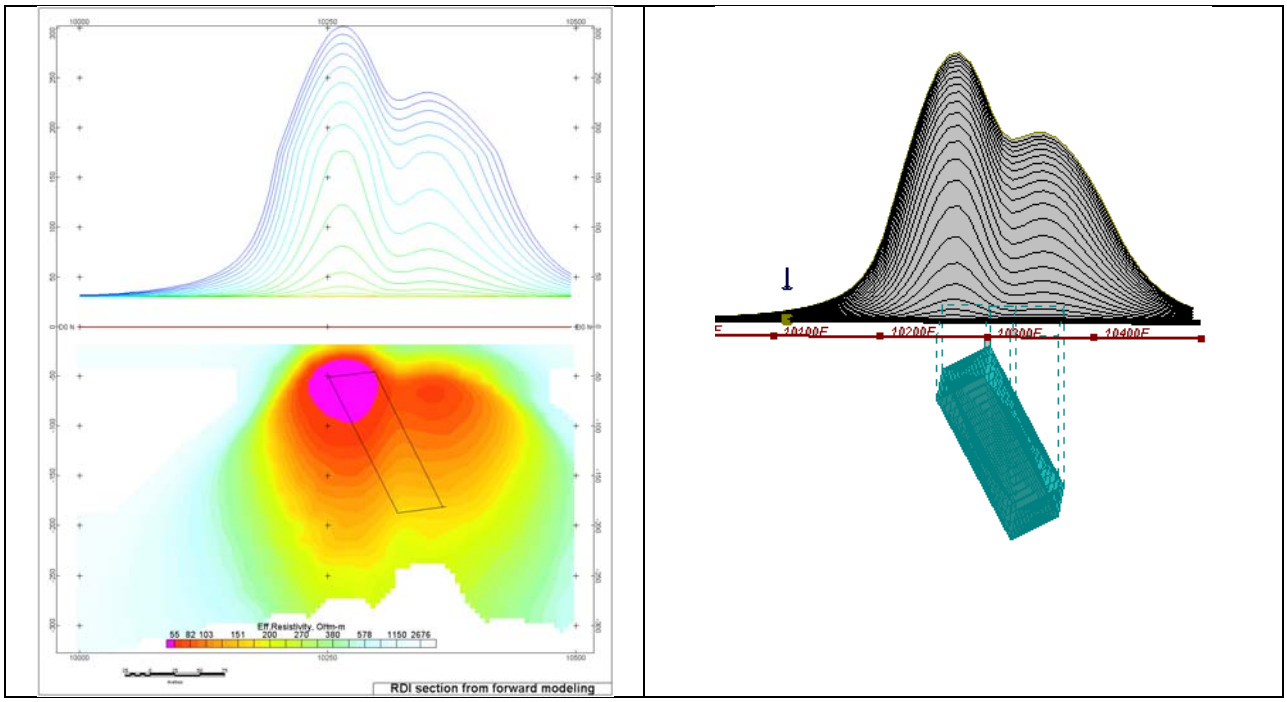

Figure F-7: Maxwell plate model and RDI from the calculated response for inclined thick (50m) plate. Depth extends 150 m, depth to the target 50 m.

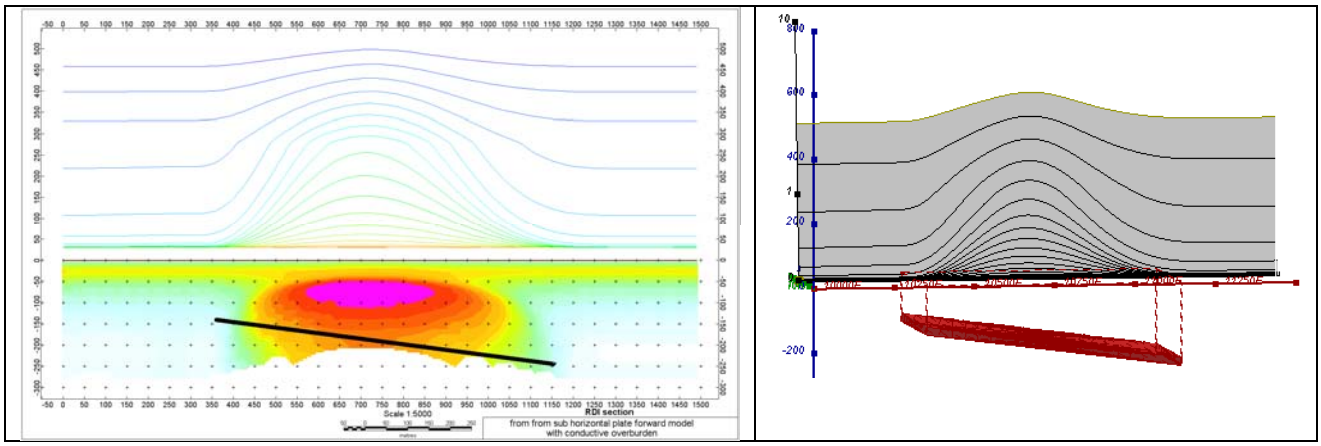

Figure F-8: Maxwell plate model and RDI from the calculated response for the long, wide and deep subhorizontal plate (depth 140 m, dim 25x500x800 m) with conductive overburden.

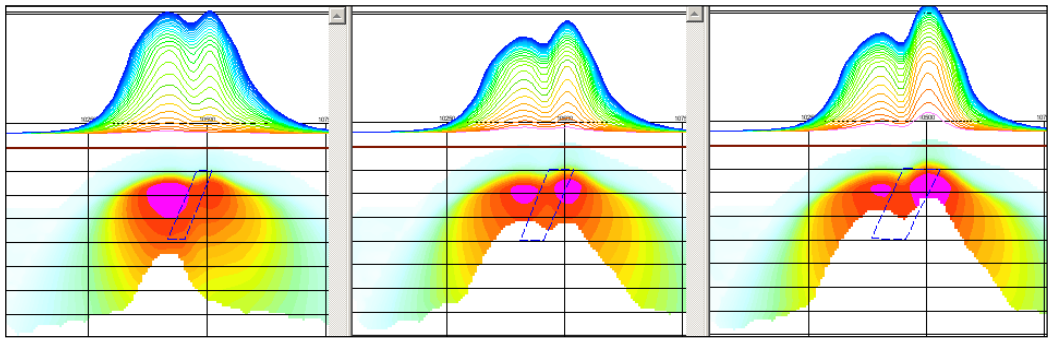

Figure F-9: Maxwell plate models and RDIs from the calculated response for “thick” dipping plates (35, 50, 75 m thickness), depth 50 m, conductivity 2.5 S/m.

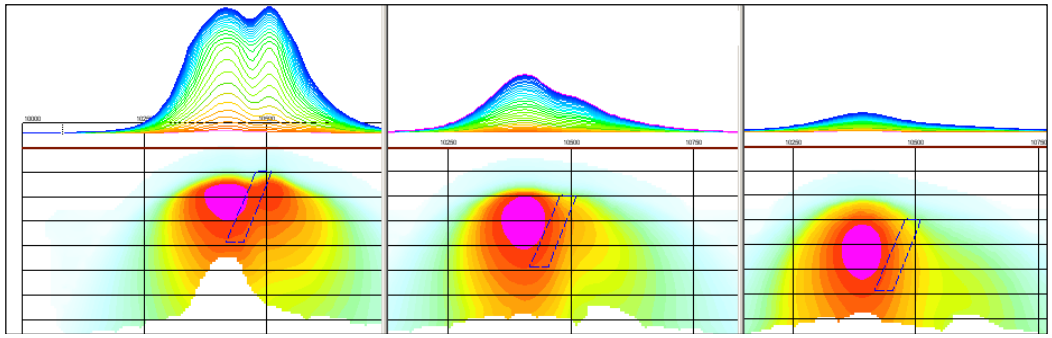

Figure F-10: Maxwell plate models and RDIs from the calculated response for “thick” (35 m thickness) dipping plate on different depth (50, 100, 150 m), conductivity 2.5 S/m.

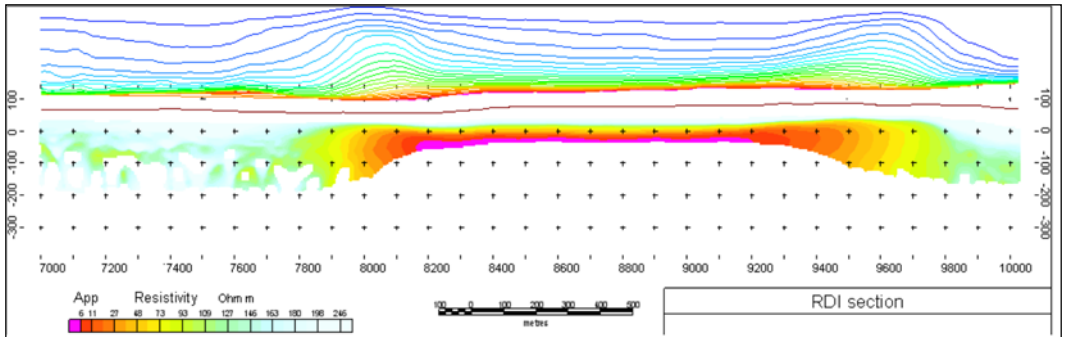

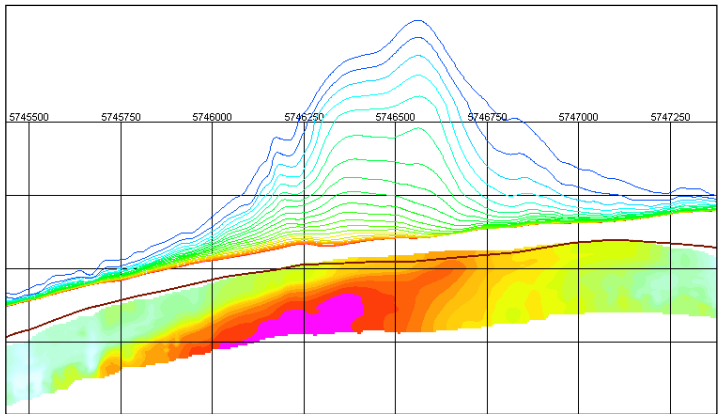

Figure F-11: RDI section for the real horizontal and slightly dipping conductive layers

FORMS OF RDI PRESENTATION

PRESENTATION OF SERIES OF LINES

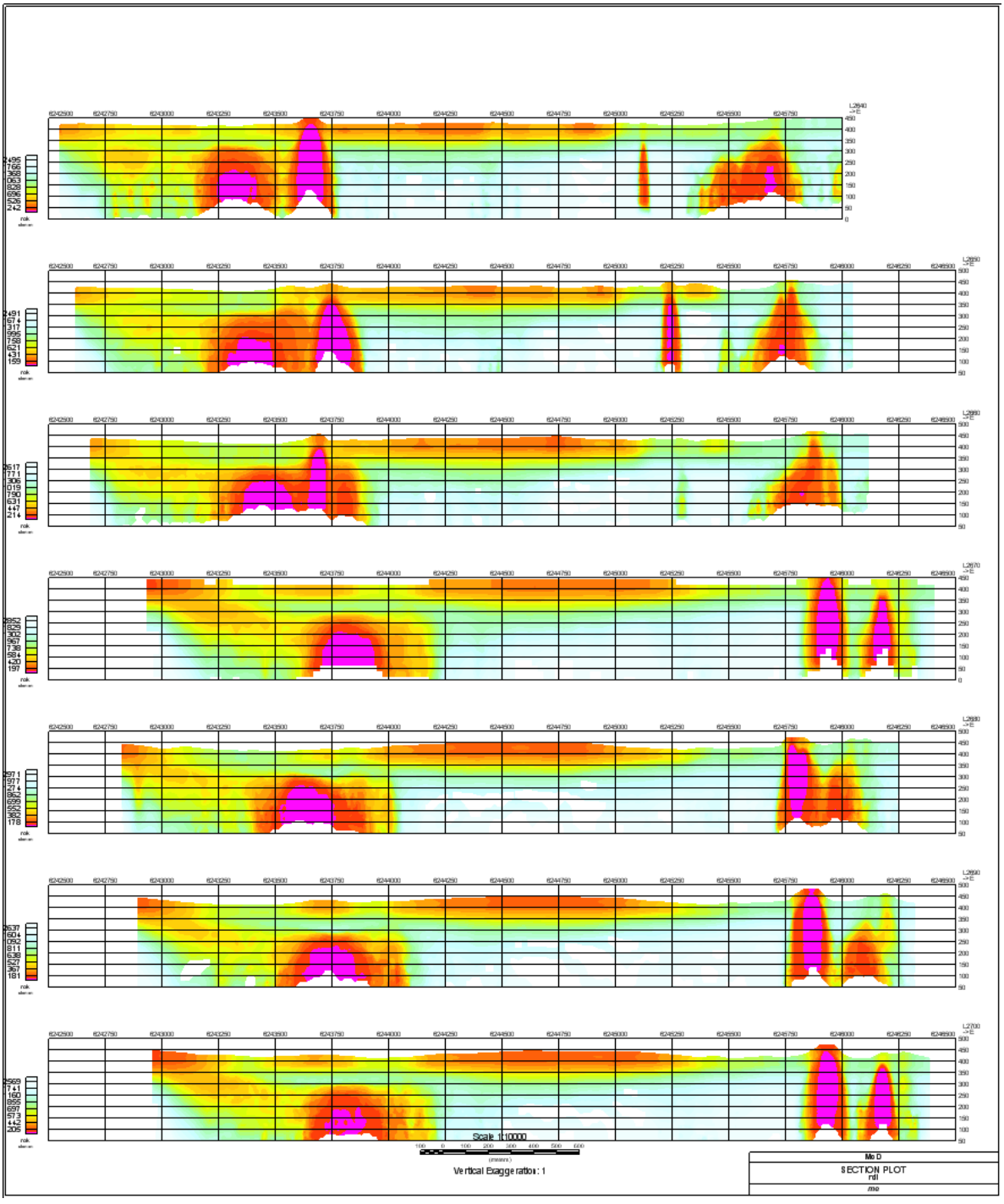

3D PRESENTATION OF RDIS

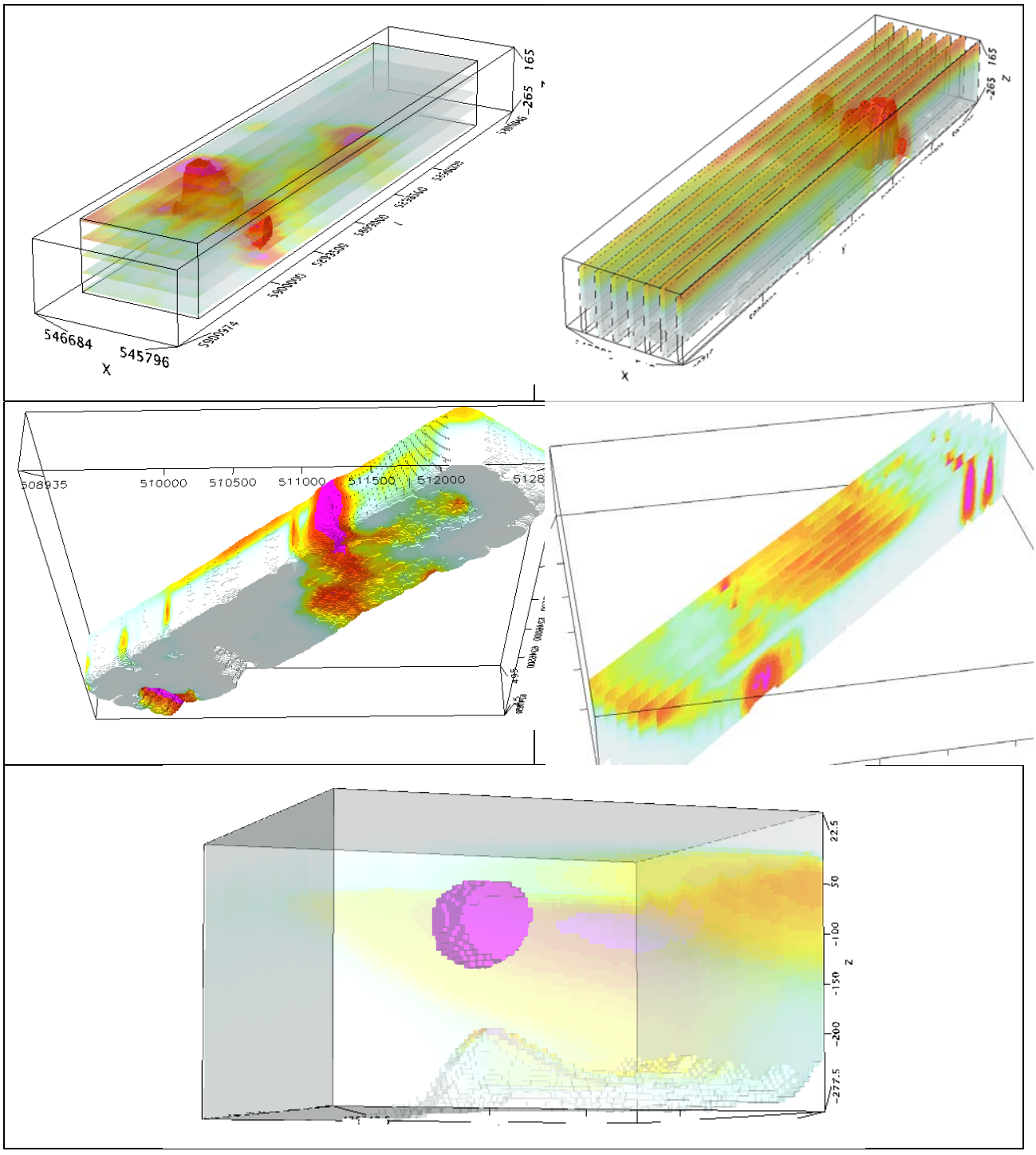

APPARENT RESISTIVITY DEPTH SLICES PLANS:

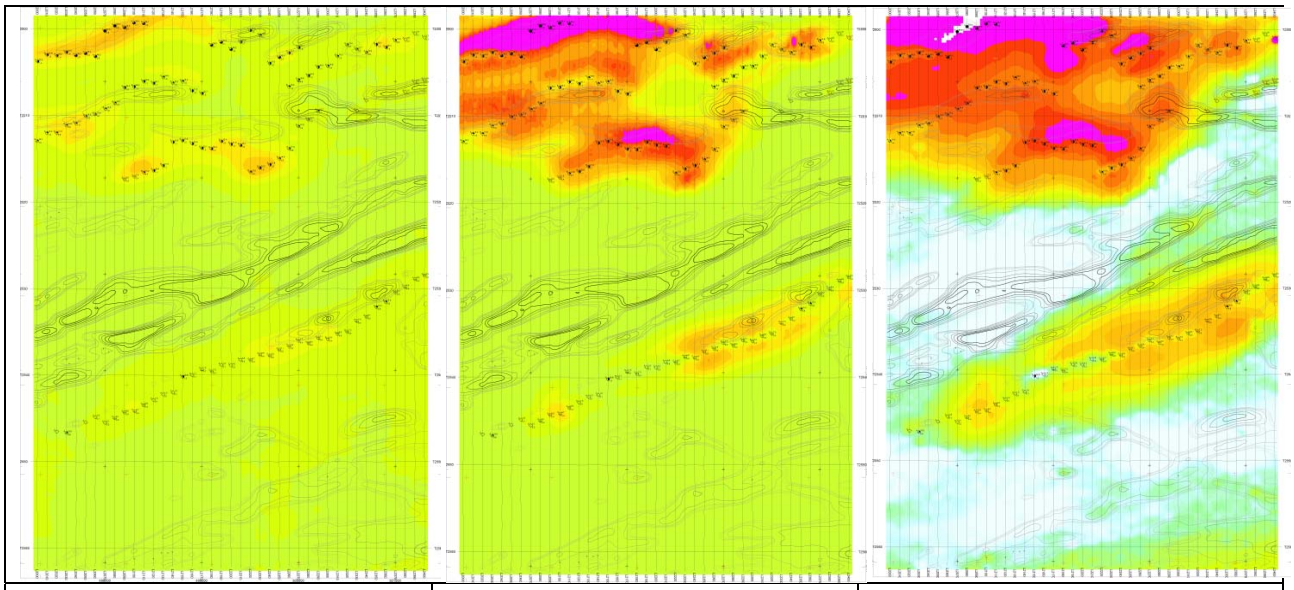

0 m (surface)	-100 m	-200 m

3D VIEWS OF APPARENT RESISTIVITY DEPTH SLICES:

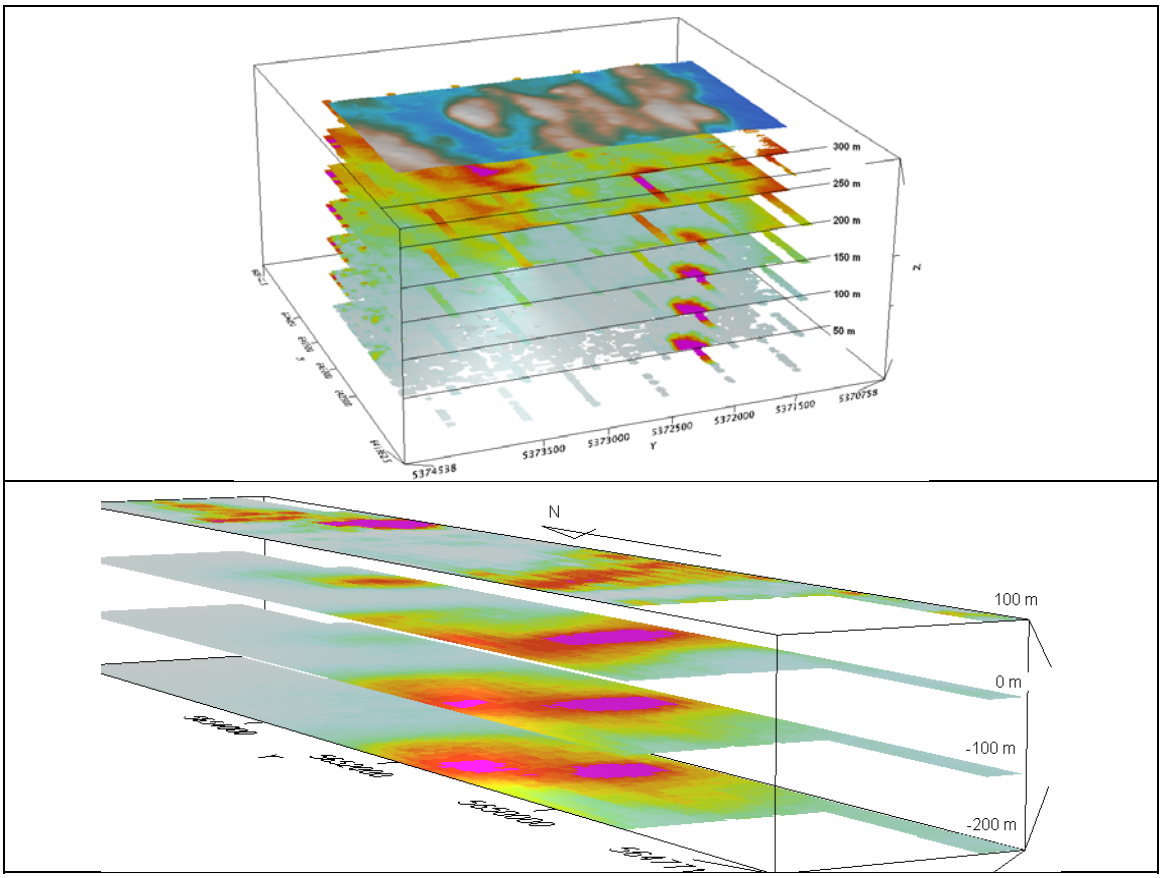

REAL BASE METAL TARGETS IN COMPARISON WITH RDIS:

RDI section of the line over Caber deposit ("thin" subvertical plate target and conductive overburden.

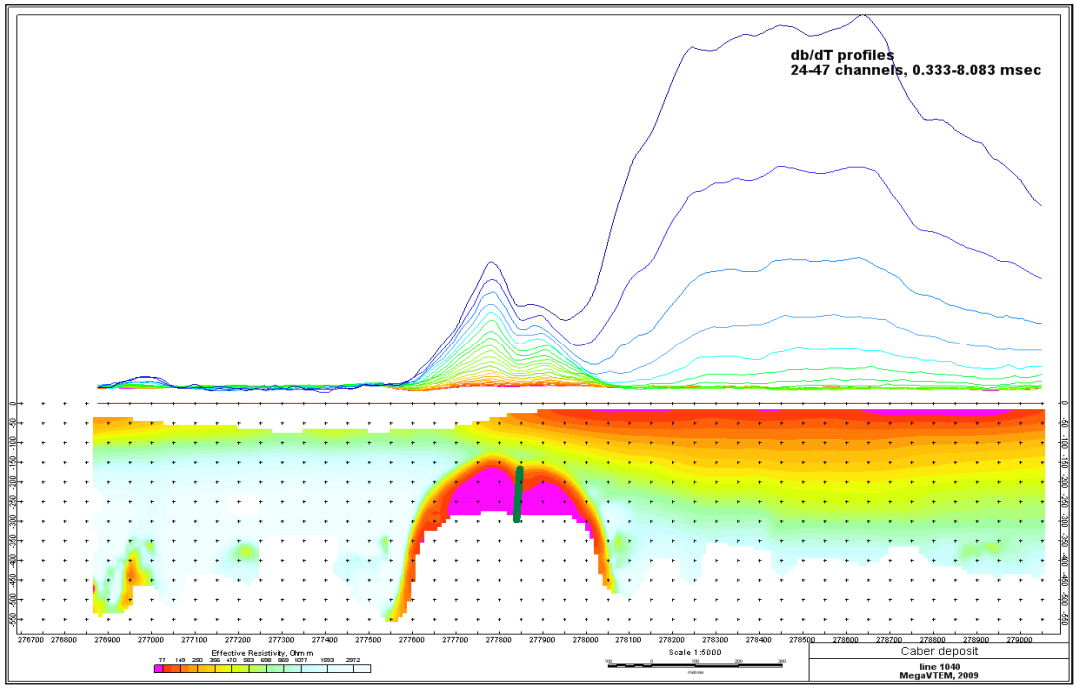

3D RDI VOXELS WITH BASE METALS ORE BODIES (MIDDLE EAST):

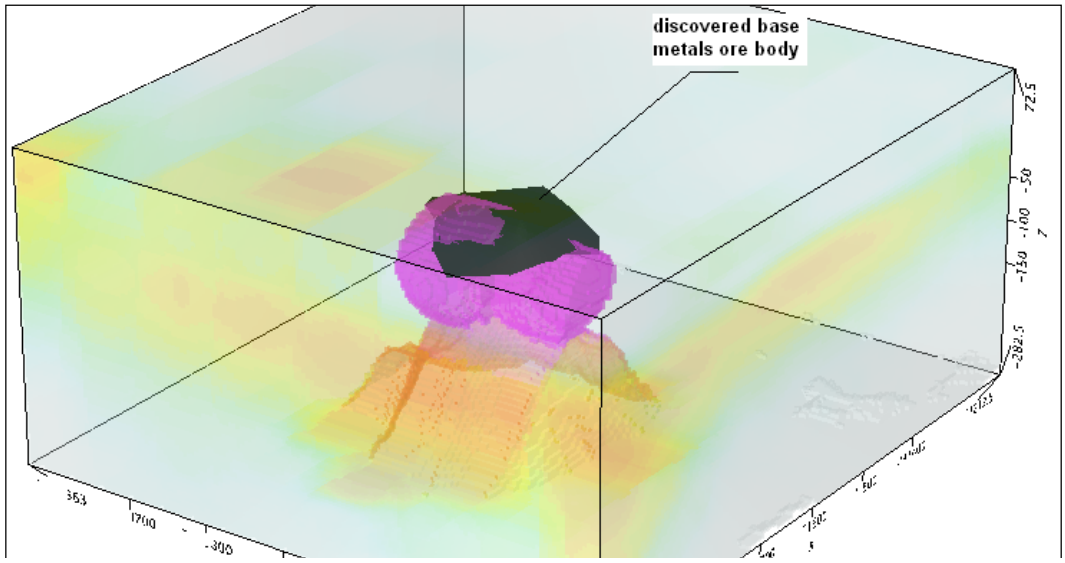

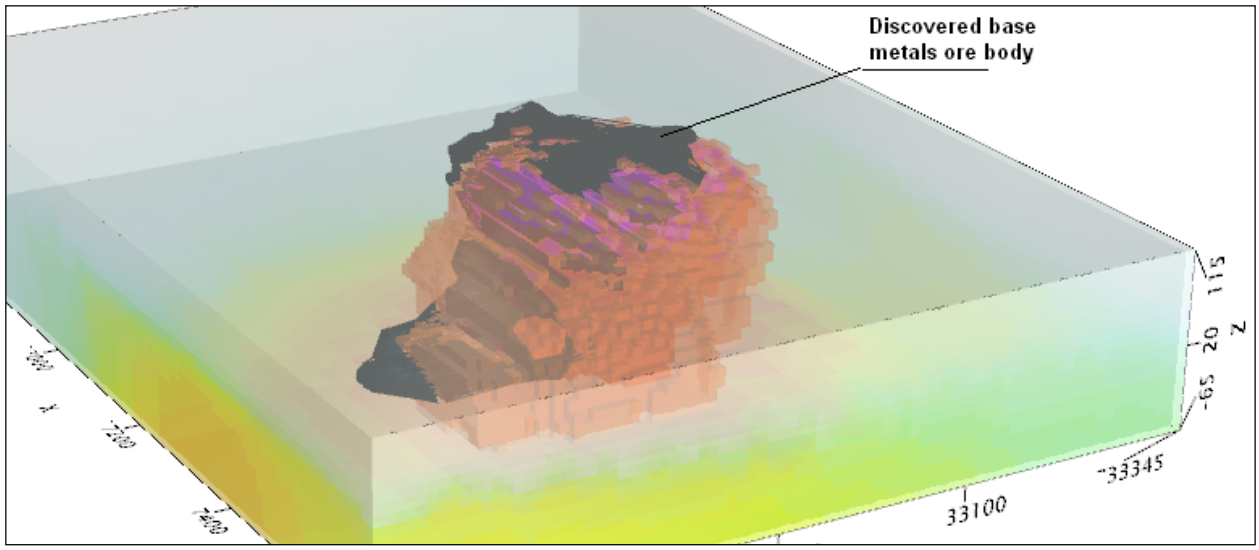

Alexander Prikhodko, PhD, P.Geo
Geotech Ltd.
April 2011

APPENDIX G

RESISTIVITY DEPTH IMAGES (RDI)

Please see attached DVD for the PDF.